UNIVERSITY OF CALIFORNIA
SANTA CRUZ

EFFECTS OF ANTIBIOTICS AND SMALL MOLECULES ON *WOLBACHIA* ENDOSYMBIONTS OF FILARIAL NEMATODES

A dissertation submitted in partial satisfaction
of the requirements for the degree of

DOCTOR OF PHILOSOPHY

in

MOLECULAR, CELL AND DEVELOPMENTAL BIOLOGY

by

Laura C. Chappell

March 2024

The Dissertation of Laura C. Chappell
is approved by:

_____
Professor William Sullivan, Chair

_____
Professor John Tamkun

_____
Professor Jordan Ward

_____
Peter Biehl
Vice Provost and Dean of Graduate Studies

Table of Contents

List of Figures ……v

List of Tables ……vii

Abstract ……viii

Dedication ……x

Acknowledgements ……xi

Chapters

1 Introduction ……1
Endosymbiosis ……1
Wolbachia as a model endosymbiont……2
The biomedical relevance of *Wolbachia*……3
Filarial diseases……4
Preventative measures for filarial disease……5
Targeting *Wolbachia* as a strategy to cure filarial diseases……7
Drug screening……8
References……11

2 Discovery of short-course antiwolbachial quinazolines for elimination of filarial worm infections……15
Abstract……17
Introduction……17
Results……20
Discussion……41
Materials and Methods……45
References……48

3 The Eagle effect in the *Wolbachia*-worm symbiosis……54
Abstract……55
Introduction……56
Results……58
Discussion……70
Materials and Methods……72
References……76

4 The endosymbiont *Wolbachia* rebounds following antibiotic treatment……82
Abstract……84
Introduction……85
Results……87
Discussion……93
Materials and Methods……96
References……102

5 Fexinidazole and Corallopyronin A target antibiotic resistant *Wolbachia* bacteriocytes present in filarial nematodes……109
Abstract……109
Introduction……109
Results……111

Discussion……..……..……..131
Materials and Methods……..……..……..136
References……..……..……..140

6 A novel "lasso" assay reveals *Brugia pahangi* is capable of both ingestion of drugs and absorption through their cuticle……..……144
Abstract……..……..144
Introduction……..……..……..144
Results……..……..……..147
Discussion……..……..……..151
Materials and Methods……..……..……..152
References……..……..……..153

7 Unpublished Screening Data……..……...155

8 Discussion ……..……157
References ……..……..……..164

List of Figures

2.1 A primary cell-based high-throughput phenotypic screen identifies compounds with potent and selective antiwolbachial activity ……..……...22

2.2 Novel small molecules with antiwolbachial activity have a narrow antibacterial spectrum ……..……25

2.3 *Wolbachia* populations in *B. pahangi* adult female worms demonstrate differential susceptibility to antiwolbachial treatment ……..……27

2.4 An *ex vivo* worm-based validation assay rapidly identifies compounds with antifilarial *Wolbachia* activity ……..……..……29

2.5 Optimized quinazoline antiwolbachials demonstrate superior pharmacokinetic profiles...……34

2.6 Quinazolines demonstrate antiwolbachial efficacy in mouse model of *L. sigmodontis* filarial infection ……..……..……...35

2.7 Quinazoline CBR715 demonstrates antiwolbachial efficacy in mouse models of *B. malayi* and *O. ochengi* filarial infection ……..……40

3.1 *Brugia pahangi* worms exposed to higher concentrations of antibiotics maintained higher *Wolbachia* titers……..……..……...61

3.2 Time course experiment reveals antibiotics stop worm motility without a corresponding decrease in *Wolbachia* and *vice versa* ……..……64

3.3 Illustration summarizing the Eagle effect on the endosymbiont *Wolbachia* in its worm host……..……65

3.4 Quinazolines CBR417 and CBR490 are effective in killing worms at high concentrations and reduce *Wolbachia* numbers at low concentrations ……..……67

3.5 *Wolbachia* are depleted in the distal tip region of worm ovaries following antibiotic treatments ……..……..……69

4.1 *Wolbachia* titers return to control levels 8 months after rifampicin treatment ..……..87

4.2 Rifampicin decreases mf shedding from female worms up to 6 weeks, followed by a return to normal by 17 weeks ..……..89

4.3 Rifampicin treatment leads to impaired embryogenesis by the 6-week timepoint but normal developmental stages return by 17 weeks ..……90

4.4 Rebound of *Wolbachia* at later timepoints may be driven by clusters ..……...92

5.1 *Wolbachia* form dense clusters within and dramatically enlarge sheath cells ……113

5.2 The integrity of the plasma membrane is not disrupted in infected sheath cells …….116

5.3 *Wolbachia* bacteriocytes are present in *Brugia malayi* germline tissue ……118

5.4 Nascent bacteriocytes are located near the Distal Tip Cell ……119

5.5 No replicating *Wolbachia* are detected in enlarged infected sheath cells ……121

5.6 Identification of small molecules that target sheath cell *Wolbachia* ……...125

Supplemental 5.1 EM analysis identifies host membrane surrounding *Wolbachia* clusters in *B. pahangi* germline tissue ……...127

Supplemental 5.2 Nascent bacteriocytes are located near the Distal Tip Cell ……...128

Supplemental 5.3 Replicating bacteria are detected hypodermal chords after 3 days …….129

Supplemental 5.4 No replicating bacteria are detected in infected sheath cells after 3 days ……..130

6.1 *Brugia pahangi* heads were suspended above fluorescently-labeled media using a novel lasso procedure ……148

6.2 Rhodamine incorporation of *Brugia pahangi* tissues is independent of the head being submerged in media ……150

7.1 Unpublished secondary and tertiary screening data ……156

List of Tables

2.1 Structures and activities of quinazoline antiwolbachials ……...23

2.2 *Wolbachia* elimination from female adult worms achieved after quinazoline treatment in the mouse/*L. sigmodontis* in vivo model of filarial infection ..……..……...36

2.3 *In vitro* ADME and safety profiling data for optimized leads ..……37

3.1 Viability of female worms treated with doxycycline was highly correlated with worm motility ……58

5.1 List of small molecules screened for anti-bacteriocyte activity in *Brugia pahangi* ……...124

Abstract

EFFECTS OF ANTIBIOTICS AND SMALL MOLECULES ON *WOLBACHIA* ENDOSYMBIONTS OF FILARIAL NEMATODES

Laura Chappell

Filarial nematodes are human parasites that infect millions of people across the globe and cause debilitating diseases such as Elephantiasis and African River Blindness. These worms share a symbiotic relationship with *Wolbachia,* an obligate, alpha-proteobacteria endosymbiont, and rely on these bacteria for survival and proper embryogenesis. Taking advantage of this crucial symbiosis, efforts to identify drugs that kill the adult worm by targeting *Wolbachia* have proven to be promising. Here, I describe the discovery and optimization of quinazolines CBR417 and CBR490 that, with a single dose, achieve >99% elimination of *Wolbachia* in the *in vivo Litomosoides sigmodontis* filarial infection model. These potent quinazolines were identified by pairing a primary cell-based high-throughput imaging screen with a secondary *ex vivo* validation assay to rapidly quantify *Wolbachia* elimination in *Brugia pahangi* filarial ovaries. To better understand the relationship between *Wolbachia* and its worm host, adult *Brugia pahangi* were exposed to varying concentrations of common antibiotics *in vitro* and assessed for *Wolbachia* numbers in the germline tissue. Surprisingly, we found that worms treated with higher concentrations of antibiotics had higher *Wolbachia* titers, and antibiotics given at low concentrations reduced *Wolbachia* titers. This counterintuitive dose response is known as the “Eagle effect” and the presence of this effect in *Wolbachia* suggests a common underlying mechanism that allows diverse bacterial and fungal species to persist despite exposure to high concentrations of antimicrobial compounds. To our knowledge this is the first report of this phenomenon occurring in an intracellular endosymbiont, *Wolbachia*, in its filarial host. While several studies have shown that novel and FDA-approved antibiotics are efficacious at depleting the filarial nematodes of their endosymbiont, thus reducing female fecundity, it remains unclear if antibiotics can

permanently deplete *Wolbachia* and cause sterility for the lifespan of the adult worms. We investigated the long-term effects of the antibiotic, rifampicin, in the *Brugia pahangi* jird model of infection. Initially, rifampicin treatment depleted *Wolbachia* in adult worms and simultaneously impaired female worm fecundity. However, during an 8-month washout period, *Wolbachia* titers rebounded and embryogenesis returned to normal. Clusters of densely packed *Wolbachia* within the worm's ovarian tissues were observed by confocal microscopy. The number, size, and *Wolbachia* density of these clusters were not diminished despite large doses of rifampicin antibiotic. This finding suggests that these clusters may serve as privileged sites that allow *Wolbachia* to persist in worms while treated with antibiotic. Lastly, I define the cellular characteristics of these clusters, which fit the definition of endosymbiont bacteriocytes, and I identify drugs that target them. Nascent bacteriocytes arise in newly formed sheath cells adjacent to the distal tip cell of the *Brugia pahangi* germline. They dramatically enlarge but do not appear to disrupt the integrity of the sheath cells. We determined that the *Wolbachia* within bacteriocytes are either in a quiescent form or replicating at a very low rate. These *Wolbachia*-based bacteriocytes are present in *Brugia malayi*, one of the nematode species which cause human filariasis, as well as *B. pahangi*. Screens of known antibiotics and other drugs revealed two drugs, Fexinidazole and Corallopyronin A, have strong anti-bacteriocyte efficacy.

Dedication

I dedicate this dissertation to my younger self.

You have been through so much to get to this point. I am incredibly proud of you.

Acknowledgements

I would like to thank my advisor Bill Sullivan for his mentorship and guidance throughout these years, without which this work would not have been possible. Bill's curious nature and creative approach to science inspires and motivates me to expand my research endeavors. I would also like to thank my thesis committee members, John Tamkun and Jordan Ward, for their time, feedback, and discussions regarding my work. Their support has made me a better scientist.

I would like to thank John Tamkun for his guidance and mentorship with my teaching career. I have greatly enjoyed my time spent as his teaching assistant for Cell and Molecular Biology, as well as Human Genetics. He has helped me become a better educator. I would also like to thank him for his guidance and lively discussions about backpacking. His advice and expertise have helped create some of my most memorable adventures.

I would like to thank my mentor and good friend Pam White for her guidance, advice, and encouragement along the way. She saw potential in me when I did not see it in myself, and she is the reason I began my work on this project. Her understanding and caring nature have helped me grow into the scientist I am today. I could not have done this without her.

I would like to thank my lab mates for their never-ending support. I have been truly blessed with a lab full of kind and caring people who allow space for me to be myself while also offering help and feedback on my work. I want to especially thank Jillian Porter and Sommer Fowler for their friendship. They are both caring, supportive, smart, funny, emotionally intelligent, inspiring, and a joy to work with.

I would like to thank my therapist, Heather, for her unwavering support throughout this process. She has been my number one cheerleader and has helped me cultivate a strong sense of self compassion and personal pride.

I would like to thank Kate Schubert for her support during the writing of my dissertation. It has been so nice to lean on someone who is going through the same process at the same time. Thank you for teaching me that "I am the Parents now."

I would like to thank my amazing housemates, past and present, for their love and support throughout the years: Anna Tucci, Ashley Brumbaugh, Derek Martin, Giselle Plascencia, Gordon Keller, Tiffany Isaak, and Zionne Lee. We have been through so much together. Thank you for your help in creating a loving and welcoming environment in which I feel safe to be myself. I especially want to thank Ashely Brumbaugh, my work session accountability buddy, for helping me stay motivated during those long hours of writing. Thank you for your love and support throughout this process.

I would like to thank Brandt Warecki and Anna Russo for their advice, guidance, support, and friendship throughout my graduate career. They are two of the smartest people I know, and they inspire me to push myself to see how much I can achieve. Thank you for keeping me company and entertained during our Zoom sessions throughout the height of the pandemic. I know we will be lifelong friends.

I would like to thank Megan Durham for always being there to provide emotional support when things got rough. I deeply appreciate our long walks in the upper campus trails when I needed a friend to lend an ear. Your friendship is one of the greatest outcomes of my graduate career. You are loyal, kind, intelligent, hilarious, and my ultimate adventure buddy. I look forward to future trips with you out on the trails.

I would like to thank my oldest and closest friend, Mickie Tang, for the tremendous amount of love and support you have shown me throughout the years. You have been there for me through quite literally everything. I treasure how deeply we connect with each other and how safe and nurtured I feel whenever we talk. I am so grateful for the ways in which we have grown together, and I will value our friendship for the rest of my life.

Lastly, I would like to acknowledge the hard work I put in to my personal growth and healing journey. I fought many battles, internal and external, throughout my graduate career at a time when multiple labor strikes, a global pandemic, national civil unrest, and wildfires threatened my progress and my mental peace. Thank you for always fighting for me.

The text of this dissertation includes reprints of the following previously published material:

[Chapter 2] Bakowski MA, Shiroodi RK, Liu R, Olejniczak J, Yang B, Gagaring K, Guo H, White PM, Chappell L, Debec A, Landmann F, Sullivan W, et al., 2019. Discovery of short-course antiwolbachial quinazolines for elimination of filarial worm infections. Sci Transl Med. 11(491): eaav3523.

[Chapter 3] Bulman CA, Chappell L, Gunderson E, Vogel I, Beerntsen B, Slatko BE, Sullivan W, Sakanari JA, 2021. The Eagle effect in the Wolbachia-worm symbiosis. Parasit Vectors. 14(1):118.

[Chapter 4] Gunderson EL, Vogel I, Chappell L, Bulman CA, Lim KC, Luo M, Whitman JD, Franklin C, Choi YJ, Lefoulon E, Clark T, Beerntsen B, Slatko B, Mitreva M, Sullivan W, Sakanari JA, 2020. The endosymbiont Wolbachia rebounds following antibiotic treatment. PLoS Pathog. 16(7): e1008623.

William Sullivan listed in these publications directed and supervised the research which forms the basis for this dissertation.

Chapter 1: Introduction

ENDOSYMBIOSIS

Endosymbionts are widespread across all kingdoms of life and are crucial for the survival of many organisms and the successful functioning of many ecosystems. The term endosymbiont describes any organism that lives within the tissues or cells and shares a symbiotic relationship with its host. Often this relationship is mutualistic, in which both organisms benefit from the presence of the other, but it can also be commensal (one organism benefits while the other gains no benefit or detriment) or parasitic (one organism benefits while the other is harmed). One example of a mutualistic endosymbiont is the intracellular algae Zooxanthella, which photosynthesizes to provide sugars to their coral reef hosts while obtaining inorganic nutrients from their host [1]. Many plant species harbor nitrogen-fixing bacteria, called rhizobia, in specialized compartments of their host to aid in the harvesting of atmospheric nitrogen [2]. The human microbiome alone consists of trillions of microbes representing up to 400 different species of bacteria in our intestinal tract, without which we would not be able to process and digest many of the foods in our diet [3].

One of the most successful endosymbionts on the planet is the bacterium *Wolbachia*, infecting an estimated 66% of all arthropod species, in addition to several species of filarial nematodes [4, 5]. *Wolbachia* is a Gram-negative alpha-proteobacteria obligate endosymbiont. Facultative endosymbionts do not rely on their host for survival and are capable of living outside of their hosts. The bacteria rhizobia mentioned earlier are an example of facultative endosymbionts, as they can also live freely within the soil and do not need their plant host to survive [2]. In fact, the legume plant must secrete flavonoid molecules into the soil in order to attract and recruit rhizobia to their roots systems [6]. Obligate endosymbionts, however, rely on their host for survival and cannot live outside of the host organism. Due to this reliance on their host, obligate endosymbionts must strike a delicate balance between utilizing host nutrients and/or cellular mechanisms to maintain their

survival, while not depleting the host organism of its own necessities for life. This requirement often forces obligate endosymbionts to evolve clever ways to maintain their intracellular, or intra-organismal, lifestyle. This is most easily demonstrated in the relationship between *Wolbachia* and one of its natural hosts, filarial nematodes.

The basis for the obligate symbiosis between *Wolbachia* and its nematode host is unclear. *Wolbachia* rely on their nematode host to provide nutrients, such as essential amino acids, and an environment in which to replicate [7]. The nematode relies on *Wolbachia* for survival and proper larval development, but the basis of this dependency remains unknown [8-11]. When treated with the antibiotic tetracycline, Landmann et al. discovered a disruption of the anterior-posterior polarity axis in the four-cell stage of developing embryos in the filarial nematode *Brugia malayi* [10]. It has also been shown that depletion of *Wolbachia* in the filarial nematode results in extensive apoptosis of both germline, embryonic, and somatic cells of the worm [11]. Given that both these processes, A-P establishment and apoptosis, are rooted deep in evolution and prior to the presence of *Wolbachia*, it is likely the endosymbionts coevolved with their filarial nematode hosts in such a way that the host became dependent on the *Wolbachia* for these processes. This leads one to argue that the symbiotic relationship of *Wolbachia* and filarial nematodes is one of an addictive symbiosis rather than a mutualism [12].

WOLBACHIA AS A MODEL ENDOSYMBIONT

Wolbachia is an attractive model organism for the study of endosymbiosis for several reasons. It is a natural endosymbiont of the model organism *Drosophila melanogaster*, for which we have ample genetic tools available. Many labs have taken advantage of the powerful *Drosophila* genetic techniques to identify host factors required for *Wolbachia*'s survival, replication, and transmission within its host. For example, these studies revealed *Wolbachia* relies on plus- and minus-directed host microtubule motor proteins in order to localize to the posterior germplasm in the mature *Drosophila* embryo [13]. This co-opting and

utilization of host motor proteins is seen in many other endosymbionts and intracellular pathogens [13].

In addition to the convenience of studying *Wolbachia* within a model organism, it has been suggested that *Wolbachia* may be a perfect model for studying the ancestral mechanisms by which mitochondria evolved to become a critical organelle within eukaryotic cells. Due to the similarities between *Wolbachia* and mitochondria (both are intracellular, reside within a host membrane, provide benefits to their host, and are vertically transmitted through the maternal germline) researchers have suggested using *Wolbachia* as a model for studying the Endosymbiont Theory and the evolution of mitochondria from an ancient prokaryote to a critical eukaryotic organelle [14].

Wolbachia prove to be a particularly important endosymbiont for research regarding pathogen manipulations of host reproduction strategies. *Wolbachia* naturally infect a vast array of arthropod species and exhibit multiple different strategies to manipulate host reproduction. *Wolbachia* are transmitted exclusively via the insect maternal germline. Due to strict transmission via the female germline, the bacteria have evolved several mechanisms to increase the prevalence of infected females of an insect population, thereby enhancing its transmission to the next generation. Depending on the insect host species, these strategies include parthenogenesis, male-killing, feminization, and cytoplasmic incompatibility [15]. Much remains unknown regarding the molecular and cellular basis of these reproductive manipulations.

THE BIOMEDICAL RELEVANCE OF *WOLBACHIA*

Wolbachia are crucial to study for their significant role in preventing the transmission of human diseases. Arthropod-borne viruses, such as Dengue fever, Chikungunya, Yellow fever, and Zika, are transmitted to humans through the bites of mosquitoes [16]. *Wolbachia* co-infection of mosquitoes carrying these viruses inhibits viral replication within the biting insect, preventing transmission of the virus [17]. Several mosquito release programs have

been implemented across the globe with promising results seen in Singapore, Colombia, and Australia [18-20]. Gaining insight into the factors that control *Wolbachia* titers can help improve the success rates of these mosquito release programs and reduce the spread of arboviruses among the global population.

Finally, and most instrumental to my dissertation project, *Wolbachia* share a mutualistic symbiosis with several species of filarial nematodes, the causative agent of filarial diseases. These parasitic worms are known to infect human hosts, causing the neglected tropical diseases Elephantiasis and African River Blindness. Other species of filarial nematodes infect horses, cattle, and other livestock, considerably impacting the beef and farming industries [21]. Even our pets are not safe from *Wolbachia*-harboring filarial nematodes, with an estimated 1.1 million dogs in the U.S. infected with *Dirofilaria immitis*, or heartworm, in 2019 [22]. Due to the symbiotic relationship of *Wolbachia* and its filarial nematode host, targeting *Wolbachia* has long been considered a promising strategy to kill these parasitic worms in both humans and animals, and cure the world of filarial disease. For my dissertation, I explore the effects of common antibiotics and small molecule compounds on *Wolbachia* titer in the filarial nematodes *Brugia pahangi* and *Brugia malayi* as a means to find cures for filarial disease.

FILARIAL DISEASES

Filarial diseases such as Lymphatic filariasis (Elephantiasis) and Onchocerciasis (African River Blindness) are Neglected Tropical Diseases (NTDs) that cause debilitating symptoms for those infected by these parasitic nematodes. Three species of filarial nematodes cause Elephantiasis in humans: *Brugia malayi*, *Brugia timori*, and *Wuchereria bancrofti*. The adult worms of these species reside within the lymphatic system of their human host and have a lifespan of 6-8 years. Due to this longstanding blockage of the lymphatic system, improper drainage of lymphatic and interstitial fluids can lead to painful swelling of the extremities known as lymphedema, thickening of the skin known as

elephantiasis, and scrotal swelling known as hydrocele. In severe cases, people with these disfiguring symptoms cannot walk and may not be able to work and provide for their families, or may be socially outcast within their communities [23]. The latest Global Burden of Disease report by the Institute for Health Metrics and Evaluation in 2019 estimated that 51 million people are currently infected with these parasites, with 46 million of those exhibiting the most severe chronic symptoms of hydrocele and lymphedema [24].

African River Blindness is caused by a single species of filarial nematode, *Onchocerca ochengi*, which has a lifespan of 12-15 years. The larval stages of this species reside in and move throughout the subcutaneous tissues of the skin. This causes intense and often painful itching in people infected by these parasites. Constant scratching to alleviate itching causes continual reopening of wounds and puts sufferers at risk of skin infections. In many cases, the larval worms move into the tissues of the eyes causing inflammation and irreversible damage, leaving individuals permanently blind. According to the 2019 Global Burden of Disease report, an estimated 14.6 million people are currently infected with this filarial nematode, and 1.15 million suffer from vision loss due to this parasite [24, 25].

Together, these two NTDs affect over 65 million people in tropical areas of the world. Over 1 billion people are at risk of infection and require preventative chemotherapy in the form of mass drug administration (MDA) programs [23, 25]. Currently, there are no cures for these diseases, only treatment of symptoms and preventative measures such as MDAs and vector control strategies.

PREVENTATIVE MEASURES FOR FILARIAL DISEASE

Filarial nematodes are transferred to human hosts by way of biting insects. In Lymphatic filariasis, several different mosquito species can transmit the parasite, including those of the genus *Anopheles, Aedes, Culex,* and *Mansonia* [26]. The insect vector responsible for spreading African River Blindness is the biting black fly of the *Simulium* genus

[27]. When the nematode-infected insect vector bites a human, they transfer the third larval stage (L3) of the parasite into the bloodstream of the human host. The L3 larvae then undergo two molting stages until they mature into the adult form. Adult nematodes reproduce within the human body and release the first larval stage, called microfilariae, into the bloodstream. Another bite from an insect vector allows ingestion of the larvae and infection of the vector. Within the insect host, the microfilariae undergo three molts until they reach the L3 larval stage, the infectious stage for humans. The larvae migrate from the stomach to the salivary glands of the insect vector to facilitate transmission to the next host. When the infected insect bites another person, they transfer the L3 larval nematodes into the bloodstream of that human host, completing the transmission cycle [23-27].

Many different strategies have been implemented in countries endemic to filarial parasites as a means to prevent transmission of these diseases, including control of the insect vectors that harbor these worms. Programs such as the Onchocerciasis Control Programme in West Africa utilize the largescale spraying of insecticides to kill insect larvae within the environment [25]. Other programs have implemented the mass distribution of mosquito nets to prevent insects from biting people when they sleep at night [26].

One of the most successful preventative measures for reducing the spread of filarial diseases has been the implementation of mass drug administration programs. Largescale annual and biannual distributions of the drugs Ivermectin, Albendazole, and Diethylcarbamazine (DEC) have proven to successfully reduce the infection status of people in affected countries. Between 1995 and 2015, the African Programme for Onchocerciasis Control (APOC) successfully treated nearly 120 million people with Ivermectin, relieving an estimated 920,000 people in the countries of Uganda and Sudan from requiring preventative chemotherapy measures [25].

While these drugs have proven successful at reducing the spread of filarial diseases, none of these drugs are capable of curing an individual of the parasitic infection. These drugs only target the microfilarial stage of the nematodes and do not affect the adult stages of

these worms [8, 28]. A single female nematode is capable of producing one thousand microfilariae in a day, translating to millions throughout her lifetime [23-28]. Because the adult stages of these worms can live inside the human host for up to 8 to 15 years, massive efforts to continually distribute these microfilaricidal drugs must be maintained each year. In order to rid worms from an infected patient and cure these filarial diseases, the world needs drugs that can specifically target the adult nematodes.

In addition to their absence of macrofilaricidal abilities, current drugs used in MDA programs encounter another problematic situation with the co-endemicity of the filarial parasite *Loa loa*. Certain regions in central Africa are endemic to both *Onchocerca volvulus* and *Loa loa*. When given Ivermectin, individuals who are coinfected with both parasites experience severe adverse side effects. Ivermectin kills off the *Loa loa* parasite at a rate that is too fast for the body's immune system to respond, and *Loa loa* microfilariae infiltrate the brain stem and cerebrospinal fluids of the patient, causing encephalopathy, coma, and eventual death [29, 30]. For these reasons, it has become crucial to find macrofilaricidal drugs that specifically target the adult parasites but do not affect *Loa loa* species in order to cure filarial diseases without these adverse side effects. Fortunately, the natural endosymbiont of filarial nematodes, *Wolbachia*, as proven to be a useful tool in the search for macrofilaricidal drugs.

TARGETING *WOLBACHIA* AS A STRATEGY TO CURE FILARIAL DISEASES

Wolbachia were first discovered in the filarial nematode species *Brugia malayi* and *Onchocerca volvulus* in the 1970's [31, 32]. Shortly after this discovery, it became apparent that the nematode hosts share a mutualistic symbiosis with the bacterium. The nematode species have coevolved with *Wolbachia* in such a way that the worm now relies on the bacteria for proper embryogenesis, larval development, and survival [8-11]. As previously mentioned, experiments in which worms were treated with tetracycline to rid the gonad of *Wolbachia* showed that nematodes at the four-cell stage no longer displayed proper axis

polarity patterning [10]. This shows that *Wolbachia*-depleted filarial nematodes do not produce viable offspring, presenting another chance to disrupt transmission of these diseases with chemotherapeutics. Additionally, *Wolbachia*-depleted filarial nematodes do not survive after 1 to 2 years following antibiotic treatment [33, 34]. Lastly, the filarial nematode *Loa loa* is completely void of *Wolbachia* endosymbionts, resolving the risk of killing this species when treating patients coinfected with both *L. loa* and *O. volvulus*. Targeting *Wolbachia* is the perfect means to prevent transmission of microfilariae, kill the adult nematodes, and avoid adverse side effects of treating individuals with *Loa loa* coinfection in certain regions of Africa [35-37].

DRUG SCREENING

While *Wolbachia* is an obligate symbiont and cannot be cultured outside of its host cells, a *Wolbachia*-infected cell line exists. A collaborator of the Sullivan Lab, Dr. Alain Debec, created an immortal *Wolbachia*-infected cell line from naturally infected *Drosophila* cells known as JW18 [38]. A former graduate student in the lab, Dr. Pamela White, spearheaded the work to develop a high-throughput cell culture screen that would test small molecule compounds on these naturally *Wolbachia*-infected insect cells. With the help of the UCSC Chemical Screening Center, Dr. White's initial drug screen tested 4,926 compounds from two separate drug compound libraries, and identified 40 candidate hits which reduced *Wolbachia* titer in the JW18 cells [39]. Dr. White's screening protocol has since been adapted by several institutions over the years to screen for antiwolbachial drugs in addition to screening for *Drosophila* host genes that affect *Wolbachia* titers [40-42].

Upon joining the PhD program under the direction of Dr. Bill Sullivan, I began my thesis project by testing the hit compounds found from Dr. White's screen in a secondary screen utilizing *Wolbachia*-infected *Drosophila melanogaster*. Compounds that significantly reduced *Wolbachia* titer in this fruit fly assay were considered secondary hits, and were subsequently tested in a filarial nematode model, *Brugia pahangi* (and in some instances,

Brugia malayi). Interestingly, I found that some drugs did not share the same effect on *Wolbachia* abundance in both species, most likely due in part to the different species of *Wolbachia* that infect *D. melangoster* (wMel) versus that which infects *B. pahangi* (wBp). This work can be found in the supplemental section of this dissertation titled "Unpublished Screening Data."

Through a collaboration with the California Institute of Biomedical Research (Calibr), a division of The Scripps Research Institute in La Jolla, California, I continued screening hit compounds in my tertiary filarial nematode assay. Calibr is a nonprofit drug discovery institution specializing in synthetic and medicinal chemistry with the resources and facilities available for large-scale drug screening protocols. Researchers at Calibr modified Dr. White's initial high-throughput cell screen to increase the number of compounds tested. This effort resulted in the screening of 300,368 small molecule compounds and the discovery of 288 hit candidate compounds [40]. My role in this project was to verify hits and their subsequent chemical analogs in a filarial nematode assay. This work resulted in identifying two promising compounds with potent antiwolbachial activity which proceeded to be tested, with success, in two nematode-infected mammalian models [43]. Chapter 2 outlines these screening endeavors.

In the effort to identify antiwolbachial compounds that can be used to treat and cure filarial diseases, drug resistance is an ever-present risk in mass drug administration programs. Due to this resistance, it has become increasingly important to understand the effects of antibiotics on Wolbachia endosymbionts in filarial worms. My dissertation explores different effects of antibiotics on Wolbachia, and addresses the questions: Can a high-throughput drug screen in insect cell culture identify compounds that convey the same effects in filarial nematodes? How does Wolbachia in filarial nematodes respond to common antibiotics at differing concentrations? Can a potent antiwolbachial compound maintain Wolbachia reduction in the filarial nematode germline over a long-course timeframe, and is

this potential Wolbachia reduction enough to rid a mammalian host of the parasitic worms indefinitely?

From researching this last question, I discovered a novel morphology of the Wolbachia endosymbiont in filarial nematodes. I found antibiotic-resistant clustering bacteria harbored within endothelial cells, known as sheath cells, of the filarial nematode germline tissue.

In Chapter 3, I will outline several key findings about Wolbachia response to varying concentrations of common antibiotics. I will show that Wolbachia in filarial nematodes exhibit the Eagle Effect, a known phenomenon seen in other bacterial pathogens. The Eagle Effect describes the paradox in which higher concentrations of antibiotics tend to convey a reduced ability to kill these pathogens, and lower concentrations tend to be more successful at reducing pathogen titer. This work is particularly important to the field of antiwolbachial drugs because knowing the appropriate concentration to aid in Wolbachia elimination is crucial for treating patients.

In Chapter 4, I will discuss the effects on Wolbachia and filarial nematode abundance seen in a Rifampicin-treated mammalian model. Briefly, eight months following a week-long treatment with the antibiotic Rifampicin, recrudescence of Wolbachia was seen in the germline of the filarial nematodes. This work is especially important for the field because most mammalian model experiments only study the effects of drugs after about 17 weeks. The short duration of these studies misses the critical timepoint in which the bacteria rebound, drawing into question the efficacy of all shortened timeframe mammalian model drug testing. This work is critical for the use of antiwolbachial drugs in the treatment of filariasis because rebound of the bacteria must be considered when developing drugs for mass drug administration programs.

In Chapter 5, I will outline different characteristics of these never-before published bacteriocytes found in filarial nematodes and identify compounds which reduce the number of bacteriocytes in these parasitic worms.

REFERENCES

1. Knowlton N and Rohwer F. *Multispecies Microbial Mutualisms on Coral Reefs: The Host as a Habitat.* The American Naturalist, 2003. **162**(S4): S51-S62.

2. Lindström K and Mousavi SA. *Effectiveness of nitrogen fixation in rhizobia.* Microbial Biotechnology, 2020. **13**(5): 1314-1335.

3. Davenport ER, Sanders JG, Song SJ, Amato KR, Clark AG, Knight R. *The human microbiome in evolution*. BMC Biology, 2017. **15**(1): 127.

4. Hilgenboecker K, et al. *How many species are infected with Wolbachia? —A statistical analysis of current data.* FEMS Microbiology Letters, 2008. **281**(2): 215-220.

5. Serbus LR, et al. *The genetics and cell biology of Wolbachia-host interactions.* Annual Review of Genetics, 2008. **42**: 683-707.

6. Maróti G and Kondorosi É. *Nitrogen-fixing* Rhizobium-*legume symbiosis: are polyploidy and host peptide-governed symbiont differentiation general principles of endosymbiosis?* Front Microbiol. 2014. **5**(326).

7. Foster J, Ganatra M, Kamal I, Ware J, Makarova K, et al. *The Wolbachia Genome of Brugia malayi: Endosymbiont Evolution within a Human Pathogenic Nematode.* PLOS Biology, 2005. **3**(4): e121.

8. Taylor MJ, Hoerauf A, Bockarie M. *Lymphatic filariasis and onchocerciasis.* The Lancet, 2010. **376**(9747): 1175–1185.

9. Townson S, Hutton D, Siemienska J, Hollick L, Scanlon T, Tagboto SK, Taylor MJ. *Antibiotics and Wolbachia in filarial nematodes: antifilarial activity of rifampicin, oxytetracycline and chloramphenicol against Onchocerca gutturosa, Onchocerca lienalis and Brugia pahangi.* Ann Trop Med Parasitol, 2000. **94**(8): 801-816.

10. Landmann F, Foster JM, Michalski ML, Slatko BE, Sullivan W. *Co-evolution between an Endosymbiont and Its Nematode Host: Wolbachia Asymmetric Posterior Localization and AP Polarity Establishment.* PLOS Neg Trop Dis, 2014. **8**(8): e3096.

11. Landmann F, Voronin D, Sullivan W, Taylor MJ. *Anti-filarial Activity of Antibiotic Therapy Is Due to Extensive Apoptosis after Wolbachia Depletion from Filarial Nematodes*. PLOS Pathogens, 2011. **7**(11): e1002351.

12. Sullivan W. Wolbachia, bottled water, and the dark side of symbiosis. Mol Biol Cell, 2017. **28**(18): 2343-2346.

13. Serbus LR, Sullivan W. *A Cellular Basis for Wolbachia Recruitment to the Host Germline*. PLOS Pathogens, 2007. **3**(12): e190.

14. Charlat S, Merçot H. *Wolbachia, mitochondria and sterility.* Trends in Ecology & Evolution, 2001. **16**(8): 431-432.

15. Landmann F. 2019. *The Wolbachia Endosymbionts*. Microbiology Spectrum, 2021. **7**(2):10.1128.

16. Côrtes N, Lira A, Prates-Syed W, Dinis Silva J, Vuitika L, Cabral-Miranda W, Durães-Carvalho R, Balan A, Cabral-Marques O, Cabral-Miranda G. *Integrated control strategies for dengue, Zika, and Chikungunya virus infections*. Front Immunol, 2023. **14**:1281667.

17. Frentiu FD, Robinson J, Young PR, McGraw EA, O'Neill SL. *Wolbachia-mediated resistance to dengue virus infection and death at the cellular level*. PLoS One, 2010. **5**:e13398.

18. Lim JT, Bansal S, Chong CS, Dickens B, Ng Y, Deng L, Lee C, Tan LY, Chain G, Ma P, Sim S, Tan CH, Cook AR, Ng LC. *Efficacy of Wolbachia-mediated sterility to reduce the incidence of dengue: a synthetic control study in Singapore*. Lancet Microbe, 2024. **S2666-5247**(23)00397-X.

19. Velez ID, et al. *Reduced dengue incidence following city-wide wMel Wolbachia mosquito releases throughout three Colombian cities: Interrupted time series analysis and a prospective case-control study.* PLoS Negl Trop Dis, 2023. **17**(11): e0011713.

20. Ogunlade ST, Adekunle AI, Meehan MT, McBryde ES. *Quantifying the impact of Wolbachia releases on dengue infection in Townsville, Australia.* Sci Rep, 2023. **13**(1):14932.

21. Bouchery T, Lefoulon E, Karadjian G, Nieguitsila A, Martin C. *The symbiotic role of Wolbachia in Onchocercidae and its impact on filariasis.* Clinical Microbiology and Infection, 2013. **19**(2): 131-140.

22. American Heartworm Society. “The State of Heartworm Incidence in the U.S.” (2020) Duke C and Carithers D. Available from: https://todaysveterinarypractice.com/parasitology/the-state-of-heartworm-incidence-in-the-united-states (Accessed Feb 2024).

23. World Health Organization. “Lymphatic filariasis.” (2023) Available from: https://www.who.int/news-room/fact-sheets/detail/lymphatic-filariasis (Accessed March 2024).

24. Institute for Health Metrics and Evaluation (IHME). “GBD Results.” (2020) Seattle, WA: IHME, University of Washington. Available from: https://vizhub.healthdata.org/gbd-results (Accessed March 2024).

25. World Health Organization. “Onchocerciasis.” (2022) Available from: https://www.who.int/news-room/fact-sheets/detail/onchocerciasis (Accessed March 2024).

26. Centers for Disease Control and Prevention. “Parasites – Lymphatic filariasis.” (2023) Available from: https://www.cdc.gov/parasites/lymphaticfilariasis/ (Accessed March 2024).

27. Centers for Disease Control and Prevention. “Parasites – Onchocerciasis (also known as River Blindness).” (2023) Available from: https://www.cdc.gov/parasites/onchocerciasis/ (Accessed March 2024).

28. Molyneux DH, Bradley M, Hoerauf A, Kyelem D, Taylor MJ. *Mass drug treatment for lymphatic filariasis and onchocerciasis*. Trends Parasitol, 2003. **19**: 516–522.

29. Gardon J, Gardon-Wendel N, Demanga-Ngangue , Kamgno J, Chippaux JP, Boussinesq M. *Serious reactions after mass treatment of onchocerciasis with ivermectin in an area endemic for Loa loa infection.* Lancet, 1997. **350**: 18–22.

30. Boussinesq M, Gardon J, Gardon-Wendel N, Chippaux J-P. *Clinical picture, epidemiology and outcome of Loa-associated serious adverse events related to mass ivermectin treatment of onchocerciasis in Cameroon.* Filaria J, 2003. 2 Suppl 1: S4.

31. Kozek WJ. *Transovarially-transmitted intracellular microorganisms in adult and larval stages of Brugia malayi.* The Journal of Parasitology, 1977. **63**(6): 992-1000.

32. McLaren DJ, Worms MJ, Laurence BR, Simpson MG. *Micro-organisms in filarial larvae (Nematoda).* Transactions of the Royal Society of Tropical Medicine and Hygiene, 1975. **69**(5-6): 509-514.

33. Taylor MJ, Makunde WH, McGarry HF, Turner JD, Mand S, Hoerauf A. *Macrofilaricidal activity after doxycycline treatment of Wuchereria bancrofti: a double-blind, randomised placebo-controlled trial*. Lancet, 2005. **365**: 2116–2121.

34. Debrah AY, Specht S, Klarmann-schulz U, Batsa L, Mand S, Marfo-Debrekyei Y, et al. *Doxycycline Leads to Sterility and Enhanced Killing of Female Onchocerca volvulus Worms in an Area With Persistent Microfilaridermia After Repeated Ivermectin Treatment: A Randomized, Placebo-Controlled, Double-Blind Trial*. Clin Infect Dis, 2015. **61**: 517–526.

35. Slatko BE, Luck AN, Dobson SL, Foster JM. *Wolbachia endosymbionts and human disease control*. Mol Biochem Parasitol, 2014. **195**: 88–95.

36. Hoerauf A, Volkmann L, Hamelmann C, Adjei O, Autenrieth IB, Fleischer B, et al. *Endosymbiotic bacteria in worms as targets for a novel chemotherapy in filariasis*. Lancet, 2000. **355**: 1242–1243.

37. Taylor MJ, Hoerauf A, Townson S, Slatko BE, Ward SA. *Anti-Wolbachia drug discovery and development: safe macrofilaricides for onchocerciasis and lymphatic filariasis*. Parasitology, 2014. **141**: 119–127.

38. Debec A, Megraw TL, and Guichet A. *Methods to Establish Drosophila Cell Lines*. Methods Mol Biol, 2016. **1478**: 333-351.

39. Serbus LR, Landmann F, Bray WM, White PM, Ruybal J, Lokey RS, Debec A, and Sullivan W. *A cell-based screen reveals that the albendazole metabolite, albendazole sulfone, targets Wolbachia*. PLoS Pathogens, 2012. **8**(9): e1002922.

40. Bakowski M, et al. *Discovery of short-course antiwolbachial quinazolines for elimination of filarial worm infections.* Science Translational Medicine, 2019. **11**(491): eaav3523.

41. White PM, Serbus LR, Debec A, Codina A, Bray W, Guichet A, Lokey RS, Sullivan W. *Reliance of Wolbachia on high rates of host proteolysis revealed by a genome-wide RNAi screen of Drosophila cells*. Genetics, 2017. **205**: 1473–1488.

42. Grobler Y, Yun CY, Kahler DJ, Bergman CM, Lee H, Oliver B, Lehmann R. *Whole genome screen reveals a novel relationship between Wolbachia levels and Drosophila host translation*. PLoS Pathog, 2018. **14**(11): e1007445.

43. Hübner MP, Gunderson E, Vogel I, Bulman CA, Lim KC, Koschel M, Ehrens A, et al. *Short-course quinazoline drug treatments are effective in the Litomosoides sigmodontis and Brugia pahangi jird models*. Int J Parasitol Drugs Drug Resist, 2020. **12**:18-27.

Chapter 2: Discovery of short-course antiwolbachial quinazolines for elimination of filarial worm infections

This chapter contains a reprint of the previously published work of which I am a coauthor (Bakowski et al., 2019). Before I joined the Sullivan Lab, a former graduate student, Dr. Pamela White, initiated a high-throughput cell screening assay to identify drug compounds that could significantly reduce *Wolbachia* titer in *Drosophila melanogaster* cells. Dr. White utilized a cell line created from naturally *Wolbachia*-infected fruit fly cells, known as the JW18 cell line, to test 4,926 compounds and their effects on *Wolbachia* titer. From this screen, Dr. White created a candidate list of 40 hits which significantly reduced *Wolbachia* titer in these cells. During her graduate work, Dr. White initiated a collaboration with the California Institute for Biomedical research, Calibr, in La Jolla, California, to continue the high-throughput screening assay. While the UCSC Chemical Screening Center provided amazing help with their equipment, facilities, and staff support, the facilities at Calibr are more expansive and can screen an extremely high number of drugs in comparison. Researchers at Calibr used the same *Wolbachia*-infected cell line and a slightly modified version of Dr. White's cell screening protocol.

My role in this work involved developing an *in vitro* nematode assay in which to test anti-*Wolbachia* drugs in a *Brugia pahangi* filarial worm model. Of the three filarial nematode species which infect humans, *Brugia malayi*, *Brugia timori*, and *Wuchereria bancrofti*, only *B. malayi* is cultured in a Mongolian jird rodent system and distributed for research purposes. Even though *B. malayi* is capable of being cultured in rodents, they are not the preferred host, and the number of worms that can be ordered is limited. For this reason, I chose to use the *B. pahangi* species for my screening assay because it is closely related to *B. malayi* and is more conducive to being cultured in the rodent model. It should be noted that *B. pahangi* do not infect humans. This was a good compromise for increasing the productivity of my

assay and studying a filarial nematode system closely related to those that pose relevance to human disease.

I worked closely with collaborators at Calibr to verify hit compounds from their high-throughput cell screen in this *in vitro* nematode model. Out of 300,368 small molecules screened, Calibr researchers identified 288 with potent anti-*Wolbachia* properties, and tested 134 in their own nematode validation assay. Of these compounds tested, only 32 showed similar anti-*Wolbachia* properties in the filarial worm. At this point in the project, Calibr was nearing the end of their funding timeline and were ready to discontinue the research. One of the lead scientists on this project, Malina Bakowski, was scheduled to begin another international project, and was no longer available to perform the nematode assays. Not wanting these lead compounds to go to waste, I stepped in and offered to pick up where Malina left off.

Calibr designed and synthesized analog compounds of their hit compounds to assess important chemical moieties for anti-*Wolbachia* activity, while I tested these serial rounds of drug analogs in my nematode assay. Each round of testing produced a clearer idea of which chemical attunements made a more potent anti-wolbachial compound. Through several rounds of synthesizing and testing analog chemical compounds, we arrived at two top hits: CBR417 and CBR490. My work on this project was critical in moving forward with the hit compounds that ultimately resulted in two separate publications. The results of this work are reported below.

ABSTRACT

Parasitic filarial nematodes cause debilitating infections in people in resource-limited countries. A clinically validated approach to eliminating worms uses a 4- to 6-week course of doxycycline that targets *Wolbachia*, a bacterial endosymbiont required for worm viability and reproduction. However, the prolonged length of therapy and contraindication in children and pregnant women have slowed adoption of this treatment. Here, we describe discovery and optimization of quinazolines CBR417 and CBR490 that, with a single dose, achieve >99% elimination of *Wolbachia* in the *in vivo Litomosoides sigmodontis* filarial infection model. The efficacious quinazoline series was identified by pairing a primary cell-based high-content imaging screen with an orthogonal *ex vivo* validation assay to rapidly quantify *Wolbachia* elimination in *Brugia pahangi* filarial ovaries. We screened 300,368 small molecules in the primary assay and identified 288 potent and selective hits. Of 134 primary hits tested, only 23.9% were active in the worm-based validation assay, 8 of which contained a quinazoline heterocycle core. Medicinal chemistry optimization generated quinazolines with excellent pharmacokinetic profiles in mice. Potent antiwolbachial activity was confirmed in *L. sigmodontis*, *Brugia malayi*, and *Onchocerca ochengi in vivo* preclinical models of filarial disease and *in vitro* selectivity against *Loa loa* (a safety concern in endemic areas). The favorable efficacy and *in vitro* safety profiles of CBR490 and CBR417 further support these as clinical candidates for treatment of filarial infections.

INTRODUCTION

Parasitic filarial nematodes, including ones that cause lymphatic filariasis and onchocerciasis (also known as river blindness), were estimated in 2013 to infect 43.8 million and 17 million people world- wide, respectively [1] with more than a billion at risk of infection [2]. Neither lymphatic filariasis nor onchocerciasis is commonly lethal; however, they are a recognized source of considerable morbidity and suffering [3]. In addition to acute symptoms, these long-term infections often result in disfigurement and social discrimination and

contribute to increased poverty of the afflicted individuals and their families. Both lymphatic filariasis and onchocerciasis are caused by long-lived filarial nematodes (roundworms) transmitted by blood-feeding insect vectors. Onchocerciasis is caused exclusively by *Onchocerca volvulus*, and lymphatic filariasis is caused mainly by *Wuchereria bancrofti* and by the closely related *Brugia* species (*Brugia malayi* and *Brugia timori*). Although the adults (macrofilariae) persist within human hosts for up to 15 years, they release thousands of microfilariae each day that either are the main cause or contribute to symptoms of disease and are also the developmental stage responsible for transmission back to the insect vector.

There is no short-course cure for these infections, and current control treatments have been centered on mass drug administration (MDA) campaigns to interrupt transmission and to alleviate symptoms for the duration of the reproductive life span of adult female parasites, variably estimated at 5 to 8 years [4]. The recommended treatment for onchocerciasis is the drug ivermectin (Mectizan), administered at least once yearly to all at risk of infection. Ivermectin works by killing microfilariae and temporarily sterilizing, but not killing, adult worms. Current recommended treatment for lymphatic filariasis varies by geography: albendazole together with ivermectin in Africa where onchocerciasis is coendemic with lymphatic filariasis and albendazole with diethylcarbamazine in the rest of the world. These treatments likewise lead to the death of microfilariae, not the adult parasites, and these drug regimens must be maintained for at least 5 years. Although MDA of ivermectin for onchocerciasis has been ongoing for more than 25 years [5], there are concerns over development of drug resistance [6], which has already been reported in veterinary medicine [7, 8]; the extensive MDA coverage that must be achieved to meet elimination targets [9, 10]; and with overall compliance of at-risk populations [11, 12]. In addition, treatments with diethylcarbamazine or ivermectin are contraindicated in patients with a high load of microfilariae of the African eye worm *Loa loa* (>30,000 to 50,000 microfilariae/ml of blood) due to severe adverse events [13]. Lower densities of microfilariae can also cause other,

non-neurological adverse events, and overall concern over the potential for *L. loa*–associated side effects can reduce adherence to MDA campaigns [12].

An attractive and clinically validated strategy for developing a treatment to selectively kill adult worms is targeting the bacterial endosymbiont of onchocerciasis- and lymphatic filariasis–causing worms, *Wolbachia*, which is absent from *L. loa* nematodes. *Wolbachia* are Gram-negative obligate intracellular bacteria that are widely distributed among a variety of arthropods, where they are considered to be reproductive parasites, known for induction of parthenogenesis, feminization, and male killing [14]. In filarial nematodes, *Wolbachia* are essential endosymbionts, needed by adult worms for both reproduction and viability. Early experiments have shown that tetracycline treatment could prevent experimental infections of rodents with *Brugia* [15] and *Litomosoides sigmodontis* but not with the *Wolbachia*-free species *Acanthocheilonema viteae* [16]. The finding that *Wolbachia* is widely distributed among filarial nematodes [17] stimulated great interest in antibiotic antifilarial therapy [18]. Subsequently, it has been shown in humans that treatment with doxycycline over a period of 4 to 6 weeks to eliminate *Wolbachia* from adult worms is sterilizing and eventually macrofilaricidal, with the life span of *Wolbachia*-depleted worms reduced by 70 to 80% (from ~10 years to 2 to 3 years) [19-22]. An added benefit of this approach is potential reduction of inflammation because adverse inflammatory reactions to anthelmintic treatment have been associated with *Wolbachia* released in patient plasma [23, 24]. However, doxycycline is contraindicated for treatment of pregnant women and children under 8 years of age. The prolonged length of treatment also represents potential challenges with compliance and contributes to cost of therapy, highlighting the need for faster, safer, and more effective therapies. Here, we describe the identification of quinazolines CBR417 and CBR490 that are able to achieve very rapid clearance of *Wolbachia* from filarial nematodes in *in vivo* preclinical models of disease and offer the potential for development of a short-course cure to treat filarial worm infections.

RESULTS

Primary high-throughput phenotypic screen identifies compounds with specific antiwolbachial activity

Because no nematode cell lines have been established to date, to rapidly identify compounds with antiwolbachial activity, we adapted and miniaturized an *in vitro* high-content imaging assay, which relied on *Drosophila melanogaster* cells naturally infected with *w*Mel strain of *Wolbachia* [25]. In the adapted assay, we used the LDW1 cell line [26] and two fluorescence in situ hybridization (FISH) probes specific to *Wolbachia* 16*S* ribosomal RNA (rRNA) to unambiguously stain *Wolbachia* and measure bacterial load inside host cells (Fig. 2.1, A to C). *Wolbachia* are sensitive to tetracycline and rifamycin antibiotics [27, 28], and these controls demonstrated specific antiwolbachial activity in the assay, with doxycycline's half-maximal inhibitory concentration IC_{50} = 279 nM and rifampicin IC_{50} = 5 nM (Fig. 2.1D). Optimized assay conditions yielded a robust assay with *Z′* factors of >0.5. Further miniaturization to 1536-well format did not reduce assay quality (Fig. 2.1C and Table 2.1). Using this optimized assay, we screened ~300,368 small molecules from established libraries, including ReFRAME [29], for antiwolbachial activity, with an overall hit rate of 0.70%. Reconfirmed hits were tested against *Wolbachia* in dose response and for cytotoxicity in the mammalian human embryonic kidney (HEK) 293T and HepG2 cell lines. Overall, we identified and reconfirmed 299 potent (IC_{50} < 1 μM) and selective [half-maximal cytotoxic concentration (CC_{50}):IC_{50} > 10] antiwolbachial compounds (Fig. 2.1, D to H).

We identified a number of known drugs and bioactive molecules among our potent and selective hits including antibiotics, signal transduction modulators, antineoplastics, antifungals, and antivirals (Fig. 2.2). Antibiotics made up the largest category (46%) of the identified known drugs and included tetracyclines, rifamycins, peptide deformylase inhibitors,

Fig. 2.1 A primary cell-based high-throughput phenotypic screen identifies compounds with potent and selective antiwolbachial activity. (A) Schematic of primary antiwolbachial screen workflow. conA, concanavalin A; PFA, paraformaldehyde; FBS, fetal bovine serum. (B) Representative images from dimethyl sulfoxide (DMSO)– and doxycycline-treated wells. One field of view (covering nearly the entire surface of each well) and a zoomed in segment with or without analysis overlays are shown (outline of LDW1 cell nuclei in blue, perimeter of analysis area extending beyond the nucleus in purple, and the identified *Wolbachia* spots are demarcated with a transparent red mask). In the merged image, *Wolbachia* 16*S* rRNA FISH signal is colored magenta, and DNA signal [4′,6-diamidino-2-phenylindole (DAPI)] is colored green. Raw and normalized (Norm.) values (see Materials and Methods) calculated from the images shown in (A) are listed. Scale bars, 100 μm. avg, average. (C) Heat map images of analysis results from plates ran in triplicate. Normalized activity values (%) for *Wolbachia* signal and cell numbers are indicated according to the scale bar. DMSO-treated wells in column 45 and individual positive control-treated wells (blocks of wells with 12.5 μM doxycycline, 0.125 μM rifampicin, or 12.5 uM puromycin) in column 46. (D) Eleven-point 1:3 dose-response curves of known antibiotics with activity against *Wolbachia*, including puromycin cell toxicity positive control. (E) LDW1 cell number dose-response data. (F) Mammalian HEK293T cytotoxicity dose-response data. Puromycin CC_{50} is shown. (G) Powder reconfirmation results for Bioactive and Diversity libraries and (H) the ReFRAME library, where the *w*Mel IC_{50} values of each compound are plotted against their mammalian cytotoxicity (HEK293T CC_{50} values). Compounds are color-coded on the basis of library origin. Hit potency and selectivity criteria (IC_{50} < 1 μM and CC_{50}:IC_{50} > 10) are shown as solid lines, and grayed out areas represent values that do not meet these thresholds. Dotted lines represent maximal concentrations tested in dose-response studies (e.g., 12.5 μM in the antiwolbachial primary assay).

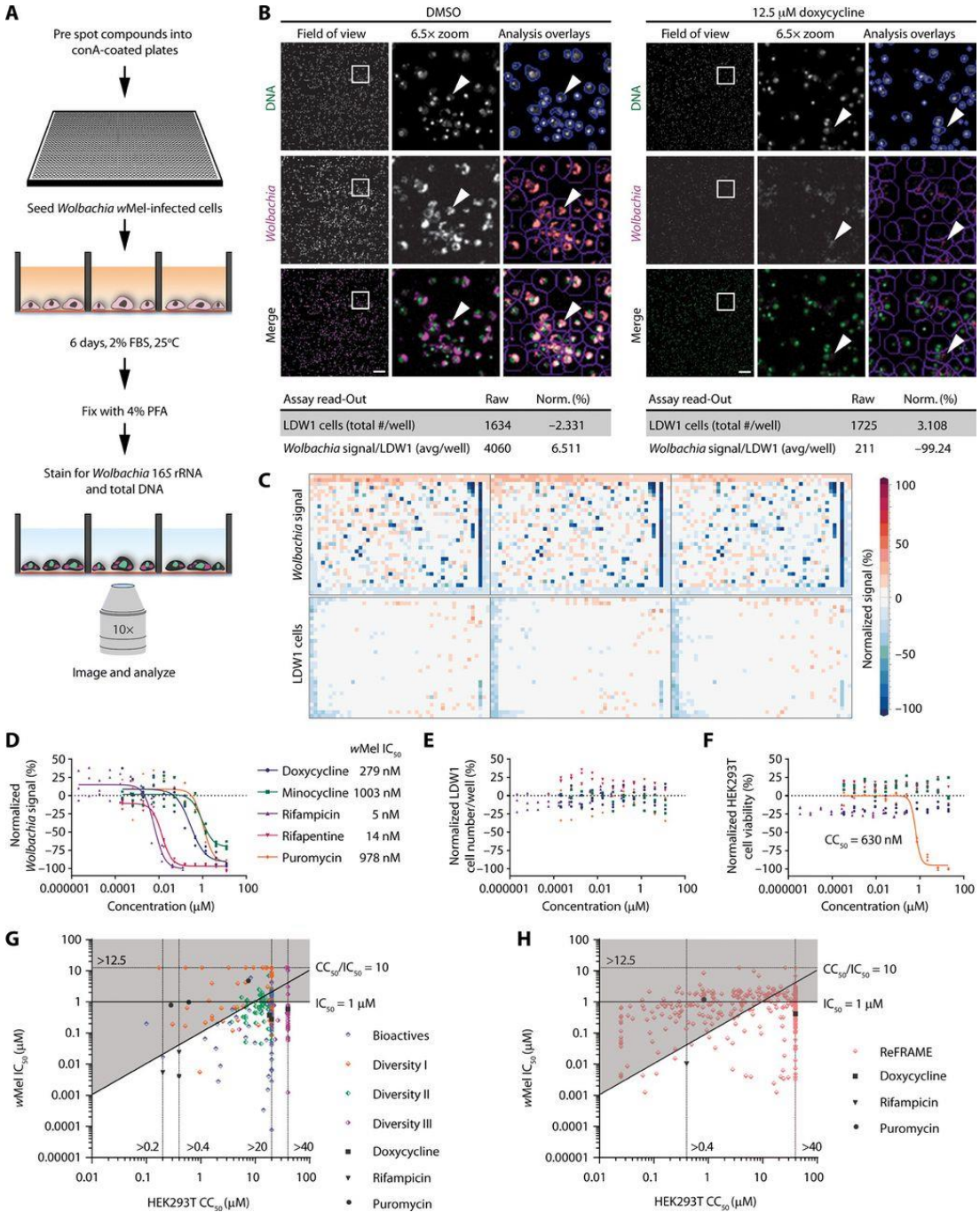
A
Pre spot compounds into conA-coated plates
Seed Wolbachia wMel-infected cells
6 days, 2% FBS, 25°C
Fix with 4% PFA
Stain for Wolbachia 16S rRNA and total DNA
10×
Image and analyze
B
DMSO
12.5 μM doxycycline
Field of view
6.5× zoom
Analysis overlays
DNA
Wolbachia
Merge
Assay read-Out Raw Norm. (%)
LDW1 cells (total #/well) 1634 −2.331
Wolbachia signal/LDW1 (avg/well) 4060 6.511
Assay read-Out Raw Norm. (%)
LDW1 cells (total #/well) 1725 3.108
Wolbachia signal/LDW1 (avg/well) 211 −99.24
C
Wolbachia signal
LDW1 cells
Normalized signal (%)
100
50
0
−50
−100
D
wMel IC50
Doxycycline 279 nM
Minocycline 1003 nM
Rifampicin 5 nM
Rifapentine 14 nM
Puromycin 978 nM
Normalized Wolbachia signal (%)
Concentration (μM)
E
Normalized LDW1 cell number/well (%)
Concentration (μM)
F
Normalized HEK293T cell viability (%)
CC50 = 630 nM
Concentration (μM)
G
>12.5
CC50/IC50 = 10
IC50 = 1 μM
wMel IC50 (μM)
HEK293T CC50 (μM)
>0.2
>0.4
>20
>40
Bioactives
Diversity I
Diversity II
Diversity III
Doxycycline
Rifampicin
Puromycin
H
>12.5
CC50/IC50 = 10
IC50 = 1 μM
wMel IC50 (μM)
HEK293T CC50 (μM)
>0.4
>40
ReFRAME
Doxycycline
Rifampicin
Puromycin

	Screen hit	Failed subseries lead	Successful subseries lead	Advanced leads		Optimized leads	
	CBR008	**CBR063**	**CBR422**	**CBR625**	**CBR715**	**CBR417**	**CBR490**
Subseries	Amide	Amide	Oxadiazole	Oxadiazole	Methylpyridine	Oxadiazole	Methylpyridine
	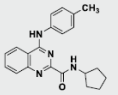	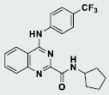		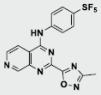		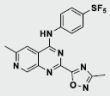	
MW	346.179	400.151	371.099	430.064	380.15	444.079	438.094
In vitro HCI cell-based assay: Anti-*Wolbachia w*Mel in *D. melanogaster* LDW1 cells							
Anti-*Wolbachia w*Mel IC_{50} (nM)	293	89	7	6	21	24	33
Anti-*Wolbachia w*Mel IC_{90} (nM)	735	200	43	52	182	1640	283
Ex vivo worm-based assay: Anti-*Wolbachia w*Bp in *Brugia pahangi* ovaries							
Anti-*Wolbachia w*Bp EC_{50} (nM)	242	97	26	66	51	356	<111
Anti-*Wolbachia w*Bp EC_{90} (nM)	799	221	189	346	396	777	<111
% *Wolbachia w*Bp elimination at 1 mM	86.3%	98.0%	93.5%	95.5%	94.5%	88.0%	95.5%
In vitro mammalian cytotoxicity assay and compound selectivity							
HEK293T CC_{50} (μM)	10.4	18.6	34.95	15.7	26.8	12.6	2.2
HepG2 CC_{50} (μM)	21.2	30.0	>40	11.3	13.7	9.7	1.6
HEK293T CC_{50}/IC_{50}	35	209	5081	2735	1299	525	66
HepG2 CC_{50}/IC_{50}	72	336	>5816	1968	663	294	49
In vitro *L. loa* microfilaria selectivity							
L. loa microfilaria motility IC_{50} (μM) (ivermectin control IC_{50} = 11.3 μM)	*n/d*	*n/d*	*n/d*	*n/d*	>100	86.9	63.6

Table 2.1 Structures and activities of quinazoline antiwolbachials. MW, molecular weight; n/d, not determined; EC_{50}, half-maximal effective concentration.

pleuromutilins, fluoroquinolones, and aminocoumarins. Many of these displayed exquisite potencies against *Wolbachia in vitro* (e.g., coumermycin IC_{50} = 1.5 nM). Among the antiwolbachial antibiotic hits, we also identified macrolide antibiotics tylosin and its derivative tylvalosin, with *w*Mel IC_{50} values of 720 and 350 nM, respectively. However, poor bioavailability, previously identified toxicity liabilities, challenging and costly synthesis, and, most importantly, lack of retained activity against filarial *Wolbachia* made these unattractive for repurposing or further development.

We also identified a number of novel compounds among the hits. To determine whether these antiwolbachial hits were *Wolbachia*-specific and/or had antibiotic activity, we screened them against a panel of extracellular bacteria. As expected, antibiotics and known

drugs showed activity against many bacterial species, but very few novel small molecules inhibited microbial growth, even at the highest concentration tested of 20 μM (Fig. 2.2). This suggests that the novel chemical scaffolds identified in our screen had *Wolbachia*-specific activity or acted on a host cell process required for *Wolbachia*'s intracellular survival. Likewise, the optimized quinazoline leads CBR417 and CBR490 did not generally inhibit extracellular bacterial growth.

A worm-based *ex vivo* assay rapidly identifies hits with antifilarial *Wolbachia* activity

Our primary cell-based assay identified compounds with activity against *w*Mel, a strain of *Wolbachia* that infects *D. melanogaster*. Validation of antiwolbachial compound activity against filarial *Wolbachia* commonly requires *in vivo* models, which is not amenable to rapid compound optimization cycles and has impeded drug discovery efforts. To overcome this limitation, we developed an orthogonal *ex vivo* validation assay that would allow us to prioritize hits in a native context against filarial *Wolbachia* (Figs. 2.3 and 2.4A). On the basis of previous studies [25], we selected quantification of filarial *Wolbachia* stained via 16*S* rRNA FISH near a convenient landmark for quantification, the ovary distal tip cell (DTC), of *B. pahangi* to validate our primary screen hits. The *Wolbachia* distribution in the ovaries is predictable and consistent compared to the variable distribution in hypodermal chords, with highest concentrations near the DTC (Fig. 2.3, A to F) [30]. This population appears more refractive to compound treatment in the 3-day *ex vivo* assay compared to the population found in the hypodermis (Fig. 2.3, G and H), as has also been observed in *Onchocerca ochengi* worms *in vivo* [31]. Moreover, the reproductive tract is a relevant site for antiwolbachial drug action, and clearance in germline stem cells is likely critical to prevent recrudescence of the bacteria after cessation of treatment.

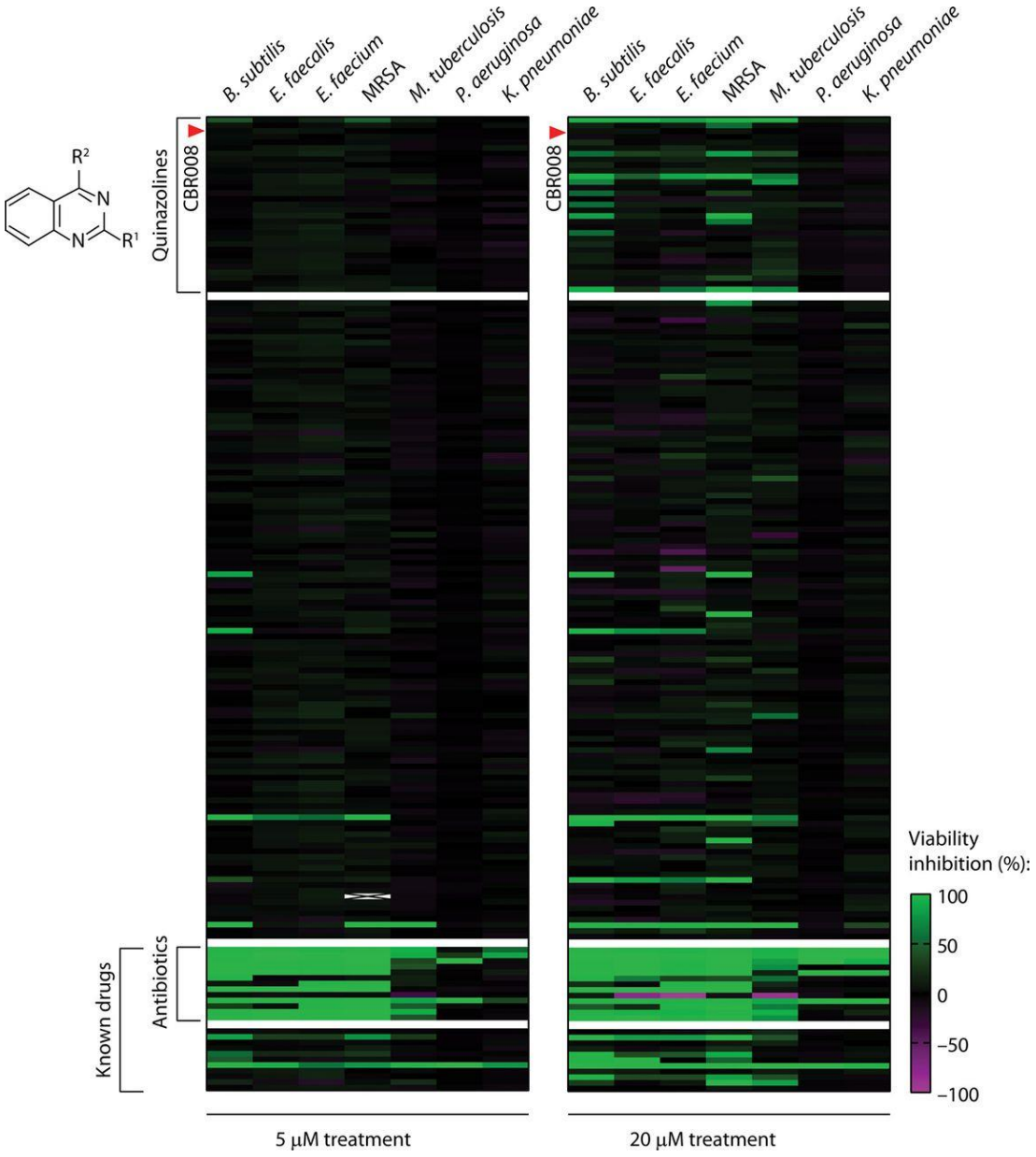

Fig. 2.2 Novel small molecules with antiwolbachial activity have a narrow antibacterial spectrum. Select powder stocks of compounds identified from Bioactive, Diversity I, and Diversity II libraries that displayed potent and selective antiwolbachial activity were tested against a panel of Gram-positive and Gram-negative bacteria. Bacterial viability inhibition after treatment with 5 or 20 μM of each compound was determined by optical density measurements. MRSA, methicillin-resistant *Staphylococcus aureus*.

Fig. 2.3 *Wolbachia* populations in *B. pahangi* adult female worms demonstrate differential susceptibility to antiwolbachial treatment. The effects of short antiwolbachial *ex vivo* treatments on *Wolbachia* populations within adult female *B. pahangi* worms were evaluated. Worms were treated *ex vivo* for 3 days with doxycycline or antiwolbachial series lead CBR422, and *Wolbachia* load was quantified using *Wolbachia*-specific 16*S* rRNA FISH and imaging (in distal ovaries) or quantitative reverse transcription polymerase chain reaction (qRT-PCR; in whole worms or tissues). DAPI (green) and *Wolbachia*-specific 16*S* rRNA FISH (white or magenta) staining in ovaries of (A and D) DMSO-, (B and E) 1 μM doxycycline–, and (C and F) 0.33 μM CBR422–treated worms. (A to C) Images of dissected and stained ovaries acquired using a 10× objective of a confocal microscope. Distal ovaries are indicated with boxes and arrowheads; oviducts and distal uteri are indicated with dashed lines and arrows. Scale bars, 100 μm. (D to F) Images of distal ovaries shown in (A) to (C), acquired using a 63× objective of a confocal microscope. Scale bars, 10 μm. *Wolbachia* elimination (%) determined using high-content image analysis is indicated for each section. (G) *Wolbachia* quantities in distal ovaries compared to those in whole worms after doxycycline (*n* = 3) or CBR422 (*n* = 2) treatment. (H) *Wolbachia* quantities in distal ovaries compared to those in the entire reproductive tract or body wall tissues after doxycycline treatment (*n* = 1). Values for each experiment were normalized to DMSO-treated controls, and means ± SD are shown.

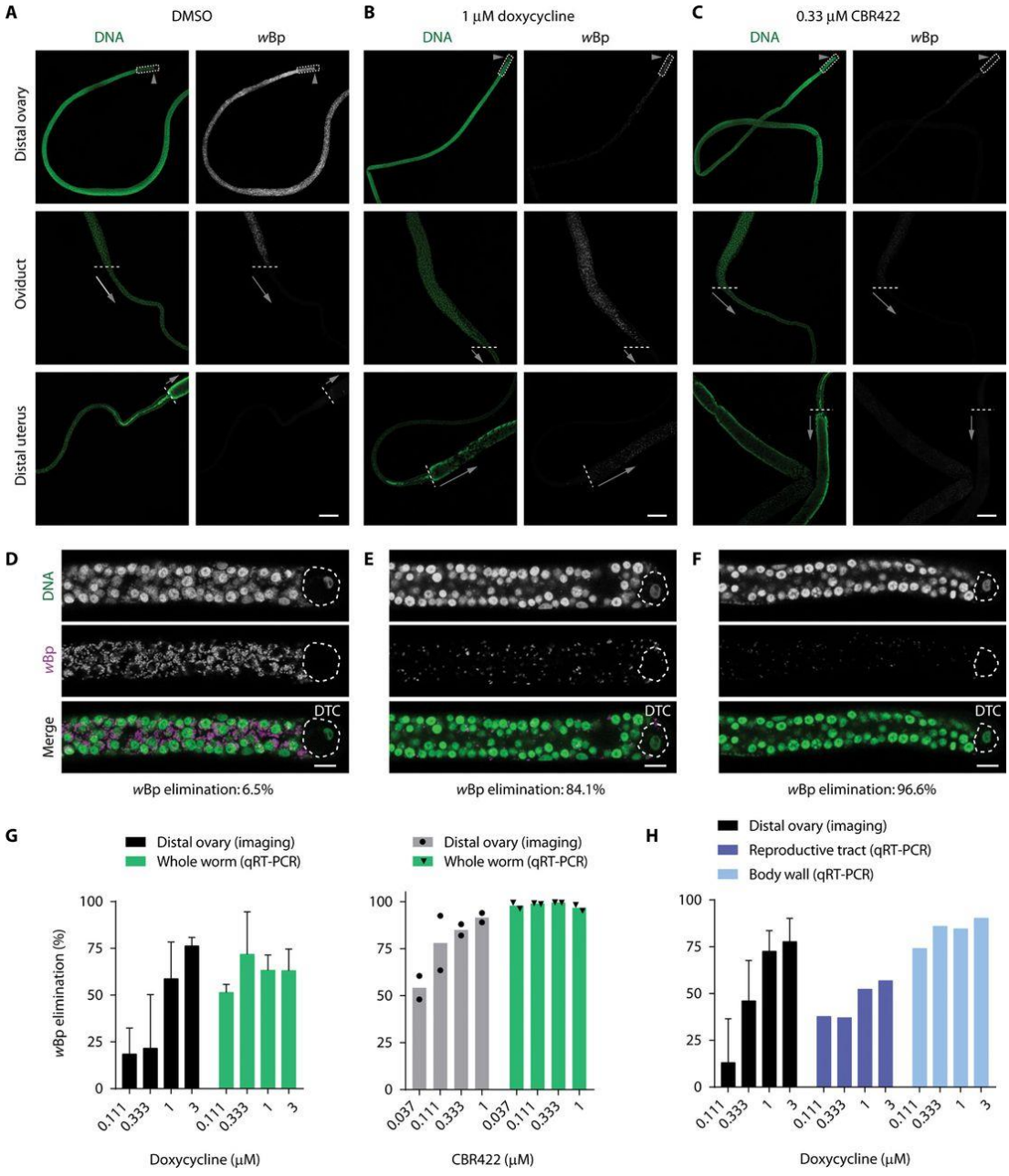
A
DMSO
DNA
wBp
Distal ovary
Oviduct
Distal uterus
B
1 µM doxycycline
C
0.33 µM CBR422
D
E
F
DTC
wBp elimination: 6.5%
wBp elimination: 84.1%
wBp elimination: 96.6%
G
Distal ovary (imaging)
Whole worm (qRT-PCR)
wBp elimination (%)
Doxycycline (µM)
CBR422 (µM)
H
Reproductive tract (qRT-PCR)
Body wall (qRT-PCR)

Fig. 2.4 An *ex vivo* worm-based validation assay rapidly identifies compounds with antifilarial *Wolbachia* activity. (A) Schematic of secondary *ex vivo* validation screen workflow to assess *Wolbachia* elimination in *B. pahangi* adult worm ovaries. Two worms (yielding a maximum of four ovaries) were included in each treatment. (B) Characterization of doxycycline activity against *Wolbachia* within *B. pahangi* ovaries treated *ex vivo*. The shaded green region indicates the selected validation threshold of >75% *Wolbachia* elimination after 1 μM treatment. Data from >3 separate experiments are plotted as means ± SD. (C) Representative images from DMSO- and (D) 1 μM doxycycline–treated ovaries stained with DAPI (green) and *Wolbachia* (magenta). Analysis overlays used to quantify *Wolbachia*-specific signal are represented as a semitransparent red mask. The DTC is indicated with a dashed outline. Scale bars, 10 μm. Boxes surround areas that are magnified 2.6× to the right of each image; arrows indicate *Wolbachia*-specific signal. (E) Validation results for potent and selective primary screen hits, tested in the assay at 1 μM. Results are grouped and colored by the library from which each hit originated. Control compounds tested at 1 μM. DOX, doxycycline; MIN, minocycline; RIF, rifampicin. Data are represented as means ± SD (one to four ovaries per treatment). Gray area in the graph represents activities below the set validation threshold. (F) *w*Bp elimination in *B. pahangi* worm ovaries plotted against *w*Mel IC_{50} values obtained in the primary insect cell-based assay. Doxycyline, minocycline, and rifampicin controls are indicated, and test compounds are colored by the library from which they originated. Data for quinazolines are indicated as donuts. Gray area in the graph represents activities below secondary assay's validation threshold. (G) *w*Bp EC_{50} values obtained for select compounds validated in the secondary worm assay plotted against *w*Mel IC_{50} values obtained in the primary insect cell-based assay. Compounds are labeled according to library origin. Quinazolines are indicated as donuts, and the structure of the most potent, CBR008, is shown. The coefficient of determination (R^2) calculated for all compounds is shown in blue (with the associated regression line; dashed blue) and in green for just the quinazolines.

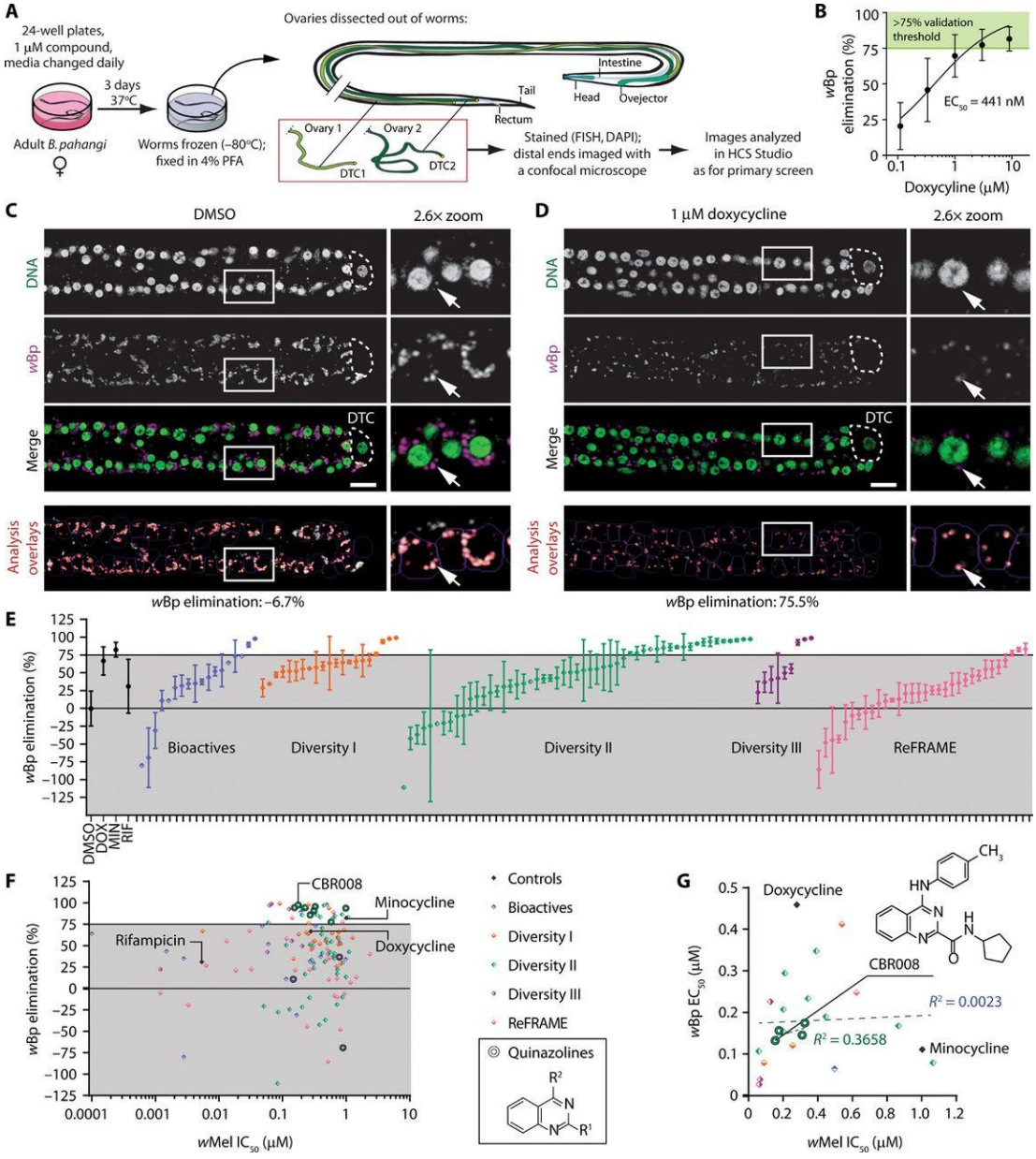
A
24-well plates, 1 µM compound, media changed daily
3 days 37°C
Adult B. pahangi
Worms frozen (–80°C); fixed in 4% PFA
Ovaries dissected out of worms:
Intestine
Tail
Head
Ovejector
Rectum
Ovary 1
Ovary 2
DTC1
DTC2
Stained (FISH, DAPI); distal ends imaged with a confocal microscope
Images analyzed in HCS Studio as for primary screen
B
>75% validation threshold
wBp elimination (%)
EC50 = 441 nM
Doxycyline (µM)
C
DMSO
2.6× zoom
DNA
wBp
Merge
DTC
Analysis overlays
wBp elimination: –6.7%
D
1 µM doxycycline
2.6× zoom
wBp elimination: 75.5%
E
wBp elimination (%)
Bioactives
Diversity I
Diversity II
Diversity III
ReFRAME
DMSO
DOX
MIN
RIF
F
CBR008
Minocycline
Rifampicin
Doxycycline
wBp elimination (%)
wMel IC50 (µM)
Controls
Bioactives
Diversity I
Diversity II
Diversity III
ReFRAME
Quinazolines
G
Doxycycline
CBR008
Minocycline
R² = 0.0023
R² = 0.3658
wBp EC50 (µM)
wMel IC50 (µM)

Doxycycline treatment of up to 9 μM was insufficient to completely clear *w*Bp from *B. pahangi* ovaries in 3 days, but 1 and 3 μM treatments eliminated about 75% of *Wolbachia*, with an estimated EC_{50} of 441 ± 64 nM (Fig. 2.4, B to D). A similar result was observed with *w*Bm strain of *Wolbachia* in *B. malayi* nematodes, where a 1 μM doxycycline treatment eliminated 72.5% of *Wolbachia*. Benchmarking on this doxycycline activity, we established a validation threshold for our candidate antiwolbachial compounds of ≥75% *w*Bp elimination from the distal ovary at a compound concentration of 1 μM (Fig. 2.4B).

The *ex vivo* validation assay could be performed in 11 days, considerably reducing optimization cycle times versus the 3-month-long *in vivo* validation assays but was labor intensive, relying on nematode dissection and confocal imaging. Thus, on the basis of activity and structural similarity clustering, we chose to test 137 of our 299 primary hits (i.e., the most potent of any closely related analogs; Fig. 2.4E). Of these, 32 showed a ≥75% *w*Bp elimination at 1 μM, for a validation rate of 23.4%. The percent elimination of *w*Bp in worm ovaries was not generally correlated to compound potency observed in the primary *D. melanogaster* cell-based assay (R^2 = 0.00048; Fig. 2.4F). Motility of worms was not affected by most of the compounds assayed, with the exception of methylene blue. Structure analysis of novel molecules demonstrated an enrichment of a quinazoline scaffold among validated compounds: Of 11 quinazolines tested in the secondary assay, 8 quinazolines showed activity superior to doxycycline (Fig. 2.4F). Members of this series displayed *in vitro* activity that correlated more with their activity in the *ex vivo* validation assay (R^2 = 0.3658) compared to all validated compounds (R^2 = 0.0023; Fig. 2.4G). Because quinazoline heterocycles are present in many of biologically active compounds including antibacterials [32, 33], we focused on this series to improve their physiochemical properties and metabolic stability and their activity against filarial *Wolbachia*.

Quinazoline series demonstrates potent antifilarial *Wolbachia* activity *ex vivo* and drug-like properties

We carried out a medicinal chemistry campaign to optimize the potency, safety, and physiochemical and pharmacokinetic properties of the quinazoline series, starting with the screen hit CBR008. This involved iterative profiling of analogs in the *in vitro* cell-based and *ex vivo* worm-based assays to determine their antiwolbachial activity. Compounds with ≥90% *w*Bp elimination at 1 μM in the worm-based assay underwent absorption, distribution, metabolism, and excretion (ADME) profiling to assess cytochrome P450 (CYP) and human ether-a-go-go related gene (hERG) inhibition (to understand potential drug-drug interaction and cardiotoxicity liabilities of the compounds, respectively), metabolism in human and mouse liver microsomes, permeability in Caco-2 cells, kinetic solubility, and plasma protein binding. Analogs with favorable properties (CBR422, CBR625, CBR715, CBR417, and CBR490) were advanced for pharmacokinetic studies in mice (Fig. 2.5) to determine whether their profiles were suitable for once-a-day (QD) or twice-a-day (BID) dosing in the *in vivo* preclinical models of infection (e.g., when dosed orally in mice at ≤50 mg/kg maintained plasma exposure over their *w*Bp EC_{90} values for at least 8 hours). As for doxycycline, the quinazoline series compounds had comparable antiwolbachial activity in *B. pahangi* and *B. malayi* worms in the *ex vivo* assay (determined for CBR422 and CBR625).

Briefly, we found that replacing the amide with an oxadiazole isostere or methylpyridine at the C2 position of the quinazoline core and the trifluoromethyl with a pentafluorosulfanyl group improved the *in vitro* and *ex vivo* potencies while increasing metabolic stability and pharmacokinetic properties of the compounds. This effort led to the initial lead CBR422 and the advanced (CBR625 and CBR715) and optimized (CBR417 and CBR490) quinazolines that had excellent potency, selectivity, and ADME properties (Table 2.1). Specifically, compared to screen hit CBR008, these analogs demonstrated improved *in vitro* and *ex vivo* potencies (*w*Mel IC_{50} ≤ 33 nM; *w*Bp EC_{50} ≤ 356 nM) and an acceptable selectivity index, were orally bioavailable in mice, and had excellent pharmacokinetic properties with a prolonged blood plasma exposure time over EC_{90} when dosed at ≤50 mg/kg (>12 to >24 hours; Fig. 2.5). The identified CYP and hERG liabilities of the series (CYP1A2

inhibition IC_{50} of 0.33 μM for initial lead CBR422 and hERG inhibition IC_{50} of 5 μM for CBR625) were markedly reduced in CBR417 (CYP inhibition IC_{50} of ≥30 μM for all isoforms and hERG inhibition IC_{50} of 19.5 μM) and partially addressed in CBR490 (CYP1A2 inhibition IC_{50} of 6.4 μM and hERG inhibition IC_{50} of 7 μM), whereas low kinetic solubility and high protein binding continued to be a feature of the analogs. The advanced and optimized quinazolines were selective against *L. loa* microfilariae (that do not contain *Wolbachia*) in an *in vitro* motility assay, with IC_{50} values of >100 μM for CBR715, 87 μM for CBR417, and 64 μM for CBR490 versus the 11.3 μM IC_{50} of ivermectin (Table 2.1).

Optimized quinazoline series demonstrates *in vivo* efficacy with shortened duration of treatment in preclinical model of filarial infection

A gold-standard *in vivo* preclinical model for assessing activity of antifilarial compounds within a reasonable period of time uses mice infected with a filarial parasite of rodents, *L. sigmodontis* (Fig. 2.6A) [16, 34]. Because *L. sigmodontis* are hosts to the *Wolbachia* endosymbiont, this is also an excellent preclinical model to assess antiwolbachial compound action, which is performed using qPCR to determine the *Wolbachia ftsZ* gene to the *L. sigmodontis* actin gene ratio in female adult worms recovered from mice at the end of the experiment (4 to 6 weeks after treatment start and 65 to 77 days after infection). A series of studies in this model demonstrated that quinazoline potency in the *ex vivo* worm-based assay, together with the ability of the compounds to achieve good exposure after oral dosing, were essential for achieving efficacy. For example, an early analog, CBR063, with good *ex vivo* potency (IC_{50} = 89 nM; EC_{50} = 97 nM) failed to achieve *Wolbachia* clearance *in vivo* (Fig. 2.6B), likely due to a comparably inferior pharmacokinetic profile (C_{max} = 119 ± 38.3 ng/ml; Fig. 2.5A). However, quinazoline analogs CBR422, CBR625, CBR715, CBR417, and CBR490, with excellent *ex vivo* potency and pharmacokinetic profiles, all proved efficacious *in vivo* with <14-day dosing regimens (≤60 mg/kg BID; >99% median *Wolbachia* clearance)

and were significantly ($P < 0.05$ to $P < 0.0001$) superior to the 14-day doxycycline control (40 mg/kg BID) ran in parallel (Fig. 2.6B and Table 2.2).

Ability to achieve efficacy in preclinical models with a shortened duration of treatment (≤7 days) is a desired profile because a reduced dosing schedule for an antiwolbachial medication has the potential to facilitate treatment and improve compliance. Therefore, we explored shortened treatment regimens for the efficacious quinazoline analogs. Efficacy (99.80% *Wolbachia* elimination) was achieved with CBR625 7-day dosing (60 mg/kg BID) and near-target efficacy (98.95% elimination) with dosing (60 mg/kg QD; Table 2.2). Likewise, an oral 7- and 12-day treatment of CBR715 at 50 mg/kg BID eliminated 98.86 and 99.80% of *Wolbachia*, respectively (Fig. 2.6B and Table 2.2). Sparse pharmacokinetics (PK) sampling during *in vivo* studies confirmed relative exposures of the tested quinazolines. Furthermore, an oral 4-day treatment at 60 mg/kg QD with the optimized quinazolines eliminated 99.80% (CBR490) and 99.96% (CBR417) of *Wolbachia* in *L. sigmodontis* adult female worms, significantly superior ($P = 0.0013$ for CBR490 and $P < 0.0001$ for CBR417) to the 14-day doxycycline control ran in parallel (95.21% elimination; Fig. 2.6B and Table 2.2).

Because of the demonstrated potency and favorable exposures of optimized quinazolines CBR417 and CBR490 (time over EC_{90} of 72 hours for a single oral dose [100 mg/kg]), we investigated whether an even more markedly abbreviated efficacious dosing regimen with these compounds was attainable. Both CBR417 and CBR490 were dosed at 100 mg/kg once per week over a 2-week period (two doses total) in the mouse/*L. sigmodontis* model, and a single dose (200 mg/kg) was also evaluated. All treatment regimens eliminated >99% of *Wolbachia* in *L. sigmodontis* adult female worms, significantly superior ($P < 0.01$) to the 14-day doxycycline control ran in parallel (95.21% elimination; Fig. 2.6B and Table 2.2). Examination of *in vivo* efficacy in response to diverse dosing regimens showed that the dose of CBR490 was equally correlated to *in vivo* efficacy ($R^2 = 0.7263$) as was total dose ($R^2 = 0.713$). Too few data points were available for CBR417 to make a conclusive analysis.

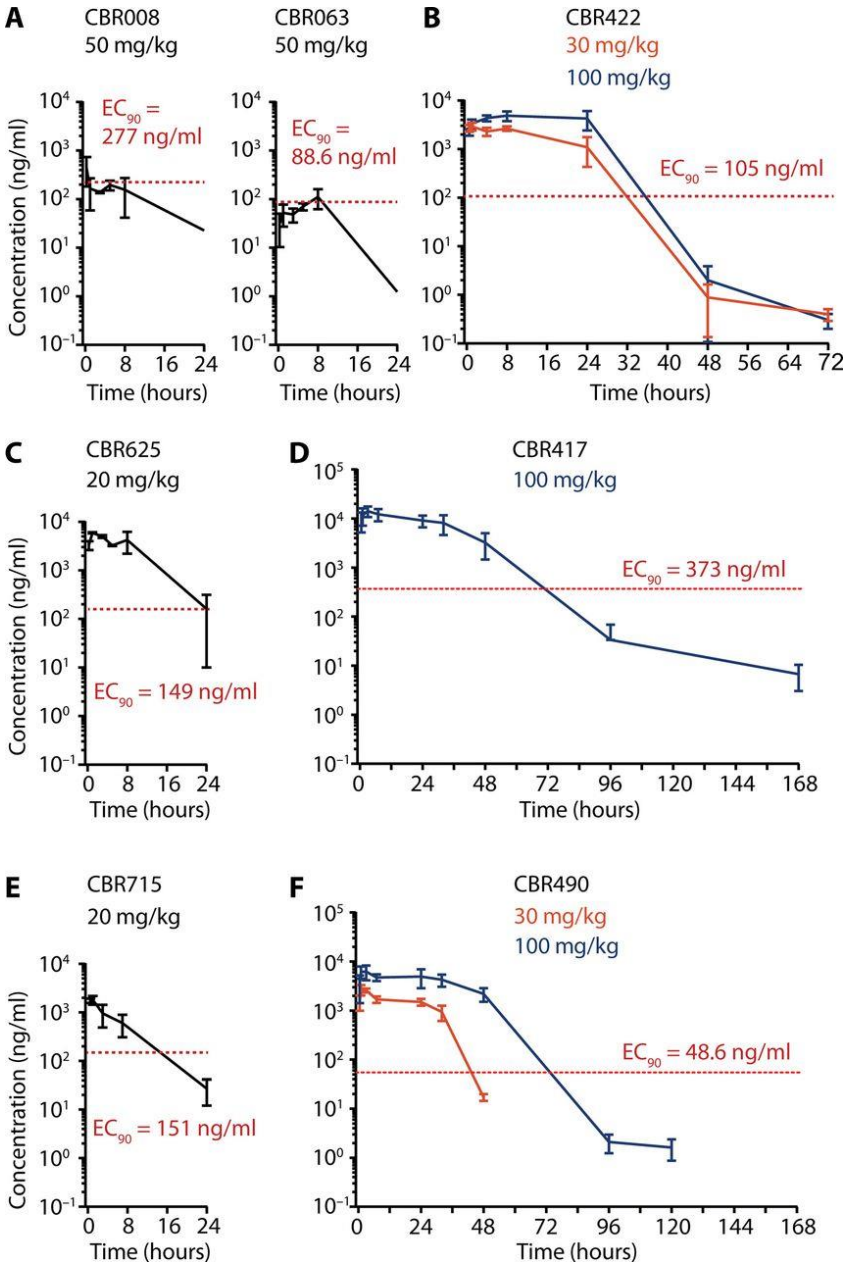

Fig. 2.5 Optimized quinazoline antiwolbachials demonstrate superior pharmacokinetic profiles. Mice were dosed orally with compounds at indicated amounts. Concentration of each compound in plasma was monitored for at least 24 hours. For each compound, *wBp* EC_{90} values established in the worm-based *ex vivo* assay are indicated by a red dashed line. Exposure profiles of (A) the primary screen hit amide CBR008 and its more potent analog CBR063, (B) the oxadiazole series lead CBR422, (C) the advanced lead oxadiazole CBR625, (D) the optimized series lead oxadiazole CBR417, (E) the advanced lead methylpyridine CBR715, and (F) the optimized series lead methylpyridine CBR490. CBR008 and CBR063 were formulated in polyethylene glycol 300/5% dextrose in water (3:1, v/v); all other compounds were formulated in 40% (2-hydroxypropyl)-β-cyclodextrin. Means ± SD (*n* = 3 mice) are shown.

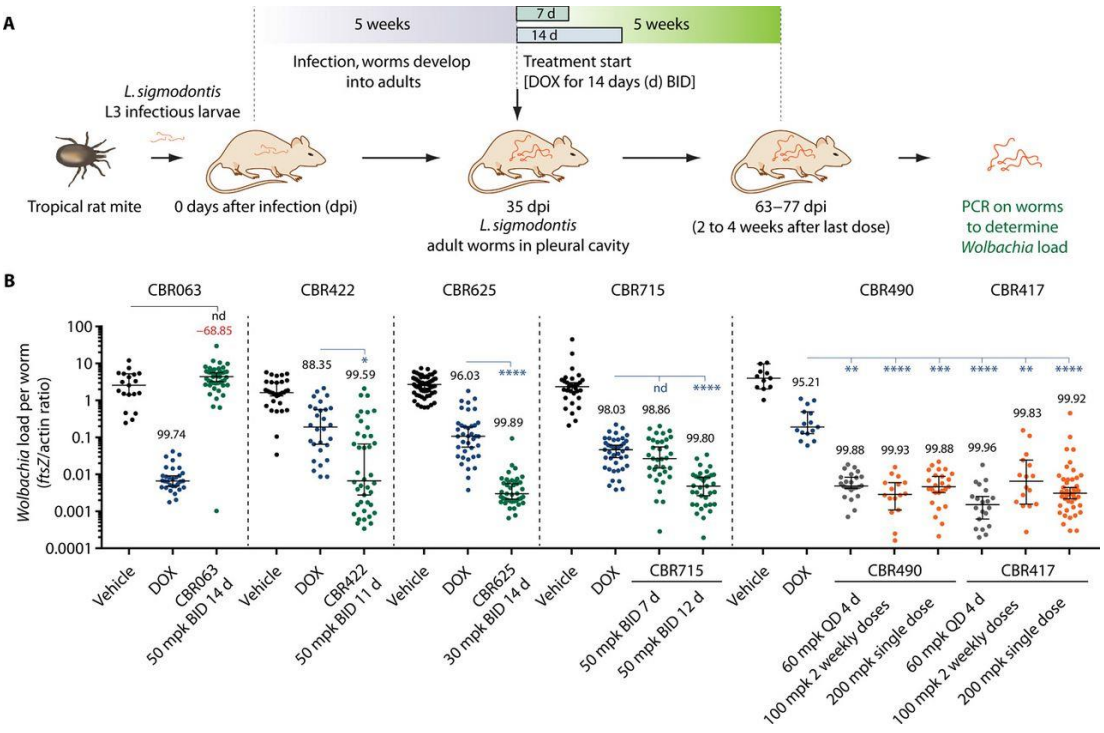

Fig. 2.6 Quinazolines demonstrate antiwolbachial efficacy in mouse model of *L. sigmodontis* filarial infection. (A and B) Advanced antiwolbachial compounds were assayed in an *in vivo* model of *L. sigmodontis* filarial infection where mice (n = 4 to 6 per group) infected with adult *L. sigmodontis* filarial worms (infected by mites carrying *L. sigmodontis* infectious larvae) are dosed for up to 14 days with a compound of interest. (B) *Wolbachia* load per worm was determined by the ratio of *Wolbachia ftsZ* gene to that of filarial actin. Vehicle control and a 14-day doxycycline control (40 mg/kg BID) were included in each independent experiment. Medians with 95% confidence interval are shown, and median elimination (%) is reported. mpk, mg/kg; nd, no significant difference. *P < 0.05, **P < 0.01, ***P < 0.001, ****P < 0.0001.

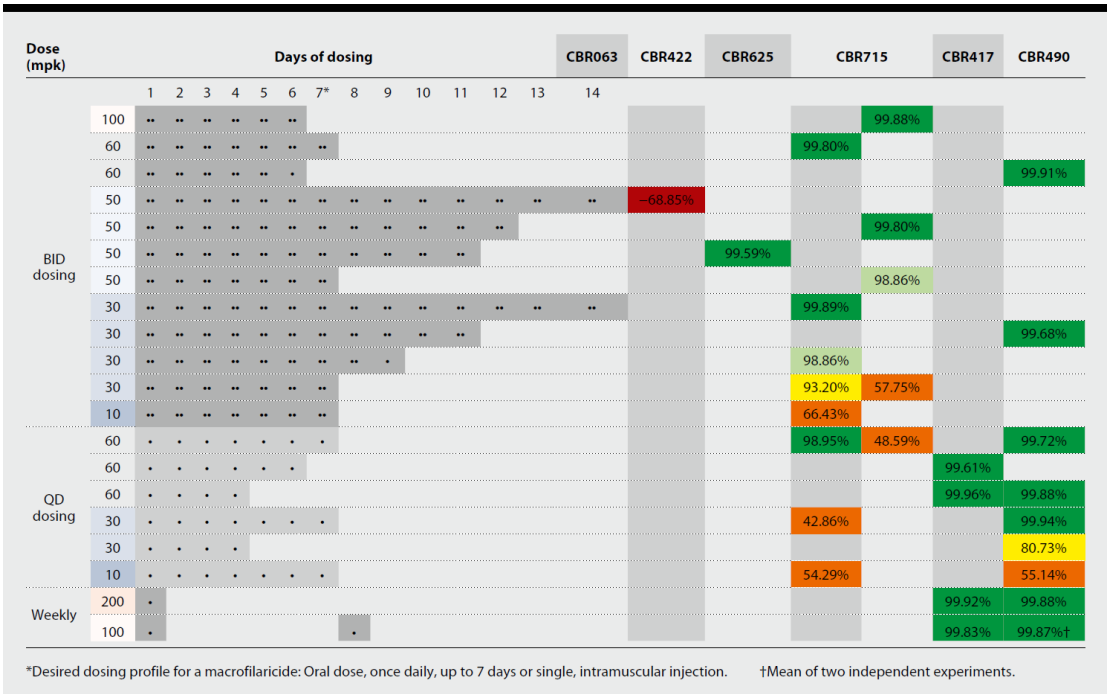

Table 2.2 *Wolbachia* elimination from female adult worms achieved after quinazoline treatment in the mouse/*L. sigmodontis in vivo* model of filarial infection. For ease of interpretation, efficacy values are presented in table cells colored on a sliding scale with excellent efficacy (>99 to 98% elimination of *Wolbachia*) in green, medium levels of efficacy (95 to 80% elimination) in yellow, and inferior levels in orange (70 to 40% elimination) and red (<30% elimination). *Desired dosing profile for a macrofilaricide: Oral dose, once daily, up to 7 days or single, intramuscular injection. †Mean of two independent experiments.

	CBR417 Oxadiazole	CBR490 Methylpyridine
Molecular weight (Da)	444.079	438.094
Solubility (pH 6.8) (μM)	1	1
Melting point (°C)	149–153	250–253
Lipohilicity (cLogP)	4.44	6.18
Plasma protein binding	>99.9% (human)	98.08% (human)
	>99.9% (mouse)	>99.9% (mouse)
Permeability Caco-2		
Papp A-B (10^{-6} cm/s)	2.08	0.14
Papp B-A (10^{-6} cm/s)	1.79	0.26
Metabolic stability (M/R/D/H)		
Extraction ratio (%)	52/20/30/41	86/35/39/63
$T_{1/2}$ (min)	56/145/145/88	10/85/100/35
CL_{int} (μL/min per mg)	25/10/10/16	137/16/14/39
hERG (cardiotoxicity)—manual patch clamp		
% Inhibition at 5 μM	20.5	27.1
IC_{50} (μM)	19.5	7.1
Cardiac panel safety profiling*	No significant inhibition	No significant inhibition
Mini-Ames (genotoxicity)	Negative	Negative
Micronucleus induction (mutagenicity)	Negative	Negative
CYP isoform (IC_{50}) (μM)		
Reversible 1A2	29.52	6.38
Reversible 2C19	>50	11.25
Reversible 2C9	45.34	6.81
Reversible 2D6	>50	13.00
Time-dependent inhibition 3A4	>50	>50
CYP induction, PXR functional assay	>30	>30
Safety pharmacology profiling† (selected receptors, ion channels, transporters, kinases, etc.)	4 with >45% binding/ inhibition	14 with >45% binding/inhibition
P-glycoprotein inhibition, MDCK-MDR1 IC_{50} (μM)	6.5	1.49

*Table S8. †Table S9.

Table 2.3 *In vitro* ADME and safety profiling data for optimized leads. CBR417 and CBR490. T1/2, half-life; M/R/D/H, mouse/rat/dog/human; CLint, intrinsic clearance; MDCK-MDR1, Madin-Darby canine kidney cells transfected with the human MDR1 gene; Papp, apparent permeability coefficient.

CBR417 and CBR490 demonstrate favorable safety profiles in preclinical studies

CBR417 and CBR490 safety profiles were more extensively assessed (Table 2.3). Both compounds were well tolerated in mouse *in vivo* efficacy studies, even when administered at high doses (200 mg/kg; single dose) or for prolonged periods of time (CBR490 daily total dose [60 mg/kg] for 11 days). Neither compound showed intrinsic mutagenic potential based on negative results in mini-Ames, in either the absence or the presence of rat liver S9 mix for metabolic activation. Micronucleus assays also did not reveal inherent genotoxicity potential. The CBR417 oxadiazole did not strongly inhibit hERG or CYP enzymes (the latter assessed for potential drug-drug interactions), and neither compound caused human pregnane X receptor (PXR) activation (a hallmark of CYP3A4 induction). A prospective cardiovascular liability due to hERG inhibition was identified for CBR490 in preliminary profiling assays (IC_{50} = 7.07 μM); however, a cardiac safety panel revealed no significant hits for either compound. To explore other potential off-target effects that could lead to *in vivo* toxicity, the Eurofins Cerep-Panlabs safety screen against 44 selected targets was carried out and identified 12 targets significantly inhibited (>50%) by CBR490 and only three inhibited by CBR417. In summary, these findings demonstrate the favorable safety profiles of CBR417 and CBR490 quinazolines.

Advanced quinazoline lead eliminates *Wolbachia* in *B. malayi* and *Onchocerca* adult worms *in vivo*

Because of the demonstrated efficacy of optimized quinazoline analogs against *Wolbachia* in *L. sigmodontis*, we assayed one of these advanced leads (CBR715) for efficacy in preclinical murine models of *B. malayi* and *Onchocerca* adult worm infections. Retention of compound activity in the *Onchocerca* model was of particular concern because both the *Wolbachia* endosymbionts and the *Onchocerca* hosts are more distantly related from the above host/endosymbiont models: *Wolbachia* of *Onchocerca* species belong to supergroup C, whereas *Wolbachia* of the more closely related *L. sigmodontis* and *Brugia* spp.

belong to supergroup D [35-37]. The only available *in vivo* model of *Onchocerca* adult worms uses the bovine parasite *O. ochengi* [38], which is a sister species and the closest relative of the human river blindness parasite, *O. volvulus* [39].

The severe combined immunodeficient (SCID) mouse *B. malayi* and *O. ochengi* models were previously described and, similar to the mouse/*L. sigmodontis* efficacy model, rely on qPCR for quantification of filarial *Wolbachia* [38]. In the *B. malayi in vivo* model (Fig. 2.7A), treatments with CBR715 (7- and 14-day dosing schedules at 50 mg/kg BID) eliminated >99% *Wolbachia* in *B. malayi* adult females, with the 14-day CBR715 treatment eliminating significantly more *Wolbachia* ($P = 0.0464$) compared to the 42-day doxycycline control (Fig. 2.7B). Doxycycline (42 days) and both CBR715 treatments eliminated all circulating microfilariae (Fig. 2.7C), and although a general trend of reduced adult worm burden was observed, these differences were not statistically significant ($P > 0.05$; Fig. 2.7D). Likewise, in the *O. ochengi in vivo* model (Fig. 2.7E), 7- and 14-day treatments with CBR715 eliminated >99% *Wolbachia* in *O. ochengi* adult males, on par with the 28-day doxycycline treatment control (Fig. 2.7F), and no difference in percent recovery of implanted males was observed (Fig. 2.7G). These data confirm the broad spectrum of activity of the optimized antiwolbachial quinazoline series and the continued superior performance of this series compared to doxycycline in *in vivo* preclinical rodent models of diverse filarial infections.

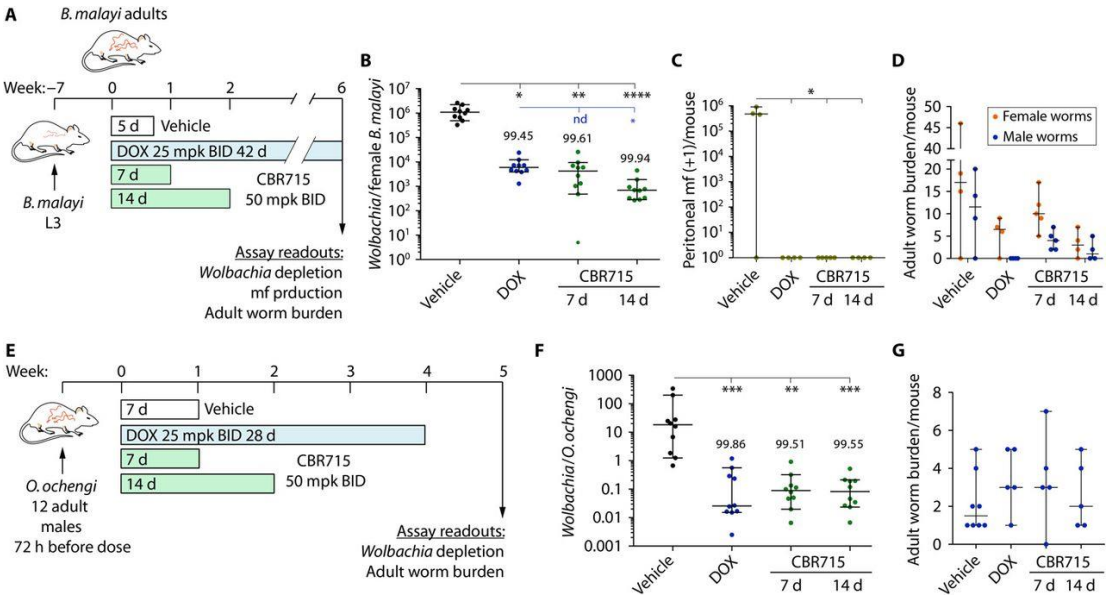

Fig. 2.7 Quinazoline CBR715 demonstrates antiwolbachial efficacy in mouse models of *B. malayi* and *O. ochengi* filarial infection. (A) Efficacy of CBR715 against *Wolbachia* in *B. malayi* was assessed in a mouse model of infection where mice (*n* = 6 per group) are inoculated with infectious L3 larvae of *B. malayi*. (B) *Wolbachia* content in adult worms determined 6 weeks after the beginning of treatment is shown. Effect of CBR715 and doxycycline control treatments on (C) the number of microfilariae (mf) circulating in the blood and (D) total *B. malayi* worm burden at the end of the *in vivo* experiments is shown. (E) Advanced lead CBR715 efficacy against *Wolbachia* in *O. ochengi* was assessed in a mouse model of infection where mice (*n* = 6 per group) are implanted with *O. ochengi* adult male worms. (F) *Wolbachia* content in adult worms determined 5 weeks after the beginning of treatment. (G) Effect of CBR715 and doxycycline control treatments on total *O. ochengi* male worms recovered at the end of the *in vivo* experiments. To assess significance between treatment groups, we used the nonparametric Kruskal-Wallis test with Dunn's multiple comparison test. Black lines indicate significant differences between vehicle control and treatment groups, and blue lines indicate significant differences between doxycycline and treatment groups. **P* < 0.05, ***P* < 0.01, ****P* < 0.001, *****P* < 0.0001.

DISCUSSION

Here, we describe an accelerated drug discovery platform for the identification of antiwolbachial compounds and translation of these to efficacious leads in *in vivo* models of filarial infection. Previous screening efforts using high-throughput insect cell-based assays have identified antiwolbachial compounds active *in vitro*, yet translation of these hits to *in vivo* models and the clinic has been challenging for a number of reasons. First, *Wolbachia* are obligate intracellular bacteria and may only be propagated within appropriate host cells. Because no nematode cell lines have been developed, for high-throughput screening drug discovery, researchers have relied on insect cell lines infected with *Wolbachia* strains that are specific to these hosts [25, 28, 40-42]. Fortuitously, there are substantial similarities in the genetics and cell biology of the *Wolbachia* species that warrant using the infected insect cell lines as a primary screen and a high-throughput proxy for filarial *Wolbachia*-based assays. However, there are also considerable differences between *Wolbachia* strains, demonstrated not only by host range but also by their genomes. For example, Foster *et al.* [43] reported a greater reduction of *B. malayi Wolbachia w*Bm genome (in total size and predicted gene number) compared to *D. melanogaster Wolbachia w*Mel. Thus, compounds identified in whole-cell screens against insect *Wolbachia* may hit targets that are sufficiently divergent or even absent in filarial *Wolbachia*. Similarly, compounds that target a host cell factor to reduce *Wolbachia* load may be absent in filarial nematodes. Last, filarial nematodes may shelter *Wolbachia* from compound action through limited permeability, compound metabolism, and/or excretion.

To address these limitations, following up on initial studies [25], we developed an orthogonal assay in filarial nematodes that allowed us to rapidly assess antifilarial *Wolbachia* activity of our primary screen hits. We used *B. pahangi*, a filarial parasite of cats that can also infect humans [44], because these worms are closely related to *B. malayi* [45] but can be maintained in an animal host (jirds) in larger quantities and, therefore, are more readily available. We focused our evaluation of *Wolbachia* load within

worm ovaries for a number of reasons because this population appeared less sensitive to compound treatment than *Wolbachia* in the hypodermal chords of the animals, providing a more rigorous and pertinent readout of antiwolbachial compound action. A similar differential susceptibility to compound action in the hypodermis versus the ovaries has been previously observed *in vivo* in *O. ochengi* adult worms after antibiotic treatments in cattle [31]. The difficulty in eliminating different clades of *Wolbachia* from ovaries of different species of worms (*Wolbachia* supergroup D in *Brugia* spp. reported here and supergroup C in *Onchocerca* spp.) further supports the relevance of this tissue for assessment of antiwolbachial compound efficacy. We used *Wolbachia* 16*S* rRNA FISH to detect the bacteria in both the cell-based high-throughput assay and the *ex vivo* worm-based assay. In addition to its inherent specificity, rRNA provides a more sensitive viability metric because it is less stable than DNA, allowing us to observe *Wolbachia* elimination in worm ovaries after only a relatively short 3-day treatment *ex vivo*. Although true markers of viability can be challenging to use in high-throughput screens, this approach gave us confidence in our ability to select fast-acting, antifilarial *Wolbachia* compounds.

In our primary insect cell-based screen, we identified known drugs with potent and selective antiwolbachial activity. Among these were antineoplastics and signal transduction modulators, which potentially exert their activity by affecting host cell processes exploited or required by this obligate intracellular bacterium. For example, *Wolbachia* has been found to alter lipid metabolism of mosquitoes [46], and insulin signaling and the target of rapamycin (TOR) complex 1 pathway have been implicated in controlling *Wolbachia* titers in *D. melanogaster* [47, 48]. Accordingly, in our screen, we identified mammalian target of rapamycin (mTOR) inhibitors and drugs affecting cellular metabolism (e.g., drugs for diabetes and liver X receptor agonists). We also identified many antibiotics with antiwolbachial activity, including ones belonging to antibiotic classes that have been previously identified in similar insect cell-based screens and assays [tetracyclines, rifamycins, pleuromutilins, fluoroquinolones, and macrolides (ABBV-4083, an orally available derivative of the macrolide

antibiotic tylosin, is currently being developed as an antiwolbachial therapy) [27, 28, 41, 49, 50] and others that, to our knowledge, have not been previously reported (aminocoumarins and peptide deformylase inhibitors). We found that most of these known drugs and antibiotics did not efficiently eliminate *Wolbachia* from *B. pahangi* ovaries in our *ex vivo* validation assay, regardless of their impressive potency *in vitro*. Therefore, although we relied on the high-throughput assay to identify potential antiwolbachials, developing and using an orthogonal assay that evaluated compound efficacy against *Wolbachia* in parasitic worms allowed us to prioritize molecules with rapid antifilarial *Wolbachia* activity for further medicinal chemistry optimization.

The desired profile for an antiwolbachial macrofilaricide compound is the ability to cause >99% depletion of *Wolbachia* in adult worms within 7 days of dosing in all three preclinical models of filarial disease (*L. sigmodontis*, *B. malayi*, and *O. ochengi*). The oxadiazole and methylpyridine leads (CBR625, CBR417, CBR715, and CBR490) proved efficacious *in vivo*, causing a >99% *Wolbachia* elimination in adult *L. sigmodontis* worms within the mandated dosing schedule of ≤7 days. In addition, the advanced methylpyridine lead CBR715 recapitulated this *in vivo* efficacy against *Wolbachia* in human parasite *B. malayi* and a close surrogate of *O. volvulus* (*O. ochengi*), demonstrating real promise in translation of the quinazoline series to a cure for human filarial infections. Our optimization strategy ultimately led to synthesis of leads CBR490 and CBR417 that, with just a single dose, were efficacious *in vivo* at eliminating >99% of *Wolbachia* from adult *L. sigmodontis* female worms. Abbreviated dosing schedules have a real advantage in treating infections in resource-limited countries and elsewhere because compliance and point of care distribution are greatly facilitated. Last, both CBR417 and CBR490 demonstrated safety in initial *in vivo* and *in vitro* preclinical profiling and did not show strong activity *in vitro* against *L. loa* microfilariae (IC_{50} = 87 and 64 μM, respectively) compared to the ivermectin control (IC_{50} = 11.3 μM), suggesting that they would be appropriate for administration to patients in *L. loa*–endemic regions after further safety assessments against *L. loa* microfilariae *in vivo*.

Despite the promise of these results, we note limitations and outstanding questions that need to be addressed before clinical translation of this work. Because of the length of time (years) needed for adult worm death after *Wolbachia* elimination, reduction in worm numbers in the murine assays is not anticipated and was not observed. However, the more immediate phenotype of worm sterilization was observed in the *B. malayi* murine model. Currently, we also have no evidence that the observed *Wolbachia* elimination is sustained beyond 4 to 5 weeks after treatment, and studies using *in vivo* jird models that can accommodate patent filarial infections for at least 6 months [51] are necessary to determine the lowest efficacious dose of quinazolines that prevent *Wolbachia* recrudescence. Last, treatment of the large, long-lived female worms belonging to the *Onchocerca* spp. represents the ultimate challenge, with females containing 20× more *Wolbachia* than males [52]. Therefore, further assessment of quinazoline efficacy in models that support *Onchocerca* female worms *in vivo* (such as the bovine model of infection) will likewise be required to determine efficacious dosing regimens.

Recently, chemical optimization of the thienopyrimidine series identified in high-throughput screening led to the generation of AWZ1066, a compound with a quinazoline scaffold and increased efficacy against both insect and filarial *Wolbachia* [53]. However, quinazoline heterocycles are present in many biologically active compounds, and whether CBR417, CBR490, and AWZ1066 share the same mechanism of action is uncertain. Genetic manipulation of *Wolbachia* has not been developed, and its obligate intracellular lifestyle complicates target identification efforts, such as evolution of resistance and confirmation of putative targets via genetic means. AWZ1066 and many novel scaffolds identified in our primary screen, including the prototypical quinazoline CBR008, demonstrated very specific antibacterial spectrum of activity, which may indicate a *Wolbachia*- or *Wolbachia* host–specific target. This also suggests that the quinazolines may be narrow spectrum antibiotics, a favorable profile for treating filarial nematode infections while reducing the effects of treatment on the microbiomes of treated individuals.

In summary, our antiwolbachial drug development platform enabled the path toward a short-course oral therapy for elimination of *Wolbachia*-reliant filarial nematodes, including ones that cause lymphatic filariasis and onchocerciasis. Our work supports advancement of the oxadiazole and methylpyridine quinazoline subseries for additional preclinical safety assessment and indicates that quinazolines are a selective treatment for currently intractable filarial worm infections.

MATERIALS AND METHODS

Study design

The objective of this study was to identify antifilarial *Wolbachia* compounds with efficacy superior to that of doxycycline when administered with an abbreviated dosing schedule (≤7 days). *Wolbachia*-infected *Drosophila* cell-based high-content imaging assay was used to screen for potent antiwolbachial compounds, and putative hits were counterscreened in mammalian cells. Activity of potent and selective compounds was validated in an ex vivo whole-worm assay observing filarial *Wolbachia* reduction in *B. pahangi* adult female ovaries, benchmarking on doxycycline activity. *In vivo* experiments were designed to compare *Wolbachia* reduction in *L. sigmodontis*, *O. ochengi*, or *B. malayi* adult worms between different treatment groups, a gold standard doxycycline and a vehicle control, in a randomized design with multiple arms and shared controls. The *Wolbachia* single gene *ftsZ*/worm actin ratios were compared to the vehicle and doxycycline treatment. Where applicable, sample size, selection, blinding schemes, and replicates are provided in the figure legends, and in the Materials and Methods.

Primary *in vitro* cell-based assay

Wolbachia-infected LDW1 cells [26] were maintained in Shields and Sang M3 (SSM3) insect medium (Sigma-Aldrich) supplemented with 10% heat-inactivated FBS (qualified, One Shot format, Gibco) at 25°C, in flasks with unvented caps. Assay plates (Greiner, part nos. 789071

and 789091) were prepared by coating with 0.5 mg/ml (384-well plates) or 1 mg/ml (1536-well plates) solution of concanavalin A lectin (MP Biomedicals). Compounds were acoustically transferred into coated plates using the Echo 555 Liquid Handler (Labcyte Inc.). Cells were trypsinized (TrypLE Express, Gibco), scraped, and seeded at 12,000 cells per well (384-well plates) or 4000 cells per well (1536-well plates) in SSM3 medium supplemented with 2% FBS. Plates were spun at 800 rpm for 3 min and incubated at 25°C. Six days after seeding, cells were fixed with 4% PFA for at least 10 min and washed with phosphate buffered saline (pH 7) and 0.1% Tween 20 (PBS-T). FISH was used to stain *Wolbachia*, and 3 μM DAPI was used to stain DNA.The MultiFlo FX Multi-Mode Dispenser (BioTek) was used for concanavalin A coating, cell fixation, and staining of 384-well plates, and the “bottle valve” dispenser with an angled head (Kalypsys Inc.) was used for processing of 1536-well plates. Plates were imaged using the CX5 CellInsight Cellomics high-content imaging instrument with a 10× objective (Thermo Fisher Scientific). Each well was analyzed using compartmental analysis in HCS Studio (Thermo Fisher Scientific) for cell number and *Wolbachia* content.

Orthogonal ex vivo *Brugia* validation assay

Adult *B. pahangi* and *B. malayi* females cultivated in and extracted from peritoneal cavities of jirds (*Meriones unguiculatus*) were obtained mainly from TRS Laboratories. *B. pahangi* were also provided by B. T. Beerntsen (University of Missouri) and the National Institutes of Health (NIH)/National Institute of Allergy and Infectious Diseases (NIAID) Filariasis Research Reagent Resource Center for distribution by BEI Resources, NIAID, NIH [adult female *B. pahangi* (live), NR-48903]. After shipment, worms were immediately separated into 24-well plates, one animal per well, and allowed to recover for 2 days in high-glucose RPMI 1640 medium (the American Type Culture Collection modification; Gibco) supplemented with 10% minimum essential medium (Gibco) and 10% heat-inactivated HyClone FBS (GE Healthcare Life Sciences). Media were changed daily, and compounds were tested at indicated concentrations (0.1% DMSO). Gross motility of worms was observed by eye during treatment

and compared to DMSO controls. After 3 days of treatment, animals were frozen at −80°C, thawed, and fixed for 20 min with 3.2% PFA in PBS-T. Ovaries were dissected out, stained for *Wolbachia* using a modified FISH protocol, mounted on slides using VECTASHIELD with DAPI mounting medium (H-1200, Vector Laboratories Inc.) and imaged using a confocal microscope (see Supplementary Materials and Methods). To reduce variability, worms originating from a single jird were used in each experiment. The experiments were carried out partially blinded because, with the exception of DMSO and doxycycline controls, the identity of tested compounds was masked during treatment, imaging, and analysis.

Statistical analysis

Percentage *Wolbachia* reduction in macrofilariae was normalized to median vehicle control values derived from the same experimental infection and screen. Where available, repeat experimental data were pooled after normalization. For analysis of *Wolbachia* depletion in *in vivo* experiments, where the majority of grouped data failed the D'Agostino and Pearson normality test ($P > 0.05$), a nonparametric Kruskal-Wallis test with Dunn's correction for multiple comparisons was used to determine significance, and medians with 95% confidence intervals are shown. Comparisons between vehicle and all treatment groups and doxycycline and all treatment groups were preselected. All statistics were computed using GraphPad Prism v6.0h.

REFERENCES

1. Global Burden of Disease Study 2013 Collaborators, Global, regional, and national incidence, prevalence, and years lived with disability for 301 acute and chronic diseases and injuries in 188 countries, 1990-2013: A systematic analysis for the Global Burden of Disease Study 2013. *Lancet* **386**, 743–800 (2015).

2. World Health Organization, *Investing to Overcome the Global Impact of Neglected Tropical Diseases: Third WHO Report on Neglected Diseases 2015* (World Health Organization, 2015).

3. World Health Organization, “Global health estimates 2014 summary tables: YLD by cause, age and sex, 2000–2012” (2014).

4. D. Gems, Longevity and ageing in parasitic and free-living nematodes. *Biogerontology* **1**, 289–307 (2000).

5. J. Lawrence, Y. K. Sodahlon, K. T. Ogoussan, A. D. Hopkins, Growth, challenges, and solutions over 25 years of mectizan and the impact on onchocerciasis control. *PLOS Negl. Trop. Dis.* **9**, e0003507 (2015).

6. M. Y. Osei-Atweneboana, K. Awadzi, S. K. Attah, D. A. Boakye, J. O. Gyapong, R. K. Prichard, Phenotypic evidence of emerging ivermectin resistance in *Onchocerca volvulus*. *PLOS Negl. Trop. Dis.* **5**, e998 (2011).

7. C. N. Pulaski, J. B. Malone, C. Bourguinat, R. Prichard, T. Geary, D. Ward, T. R. Klei, T. Guidry, G. Smith, B. Delcambre, J. Bova, J. Pepping, J. Carmichael, R. Schenker, R. Pariaut, Establishment of macrocyclic lactone resistant *Dirofilaria immitis* isolates in experimentally infected laboratory dogs. *Parasit. Vectors* **7**, 494 (2014).

8. R. M. Kaplan, A. N. Vidyashankar, An inconvenient truth: Global worming and anthelmintic resistance. *Vet. Parasitol.* **186**, 70–78 (2012).

9. R. J. Kastner, C. M. Stone, P. Steinmann, M. Tanner, F. Tediosi, What is needed to eradicate lymphatic filariasis? A model-based assessment on the impact of scaling up mass drug administration programs. *PLOS Negl. Trop. Dis.* **9**, e0004147 (2015).

10. K. K. Frempong, M. Walker, R. A. Cheke, E. J. Tetevi, E. T. Gyan, E. O. Owusu, M. D. Wilson, D. A. Boakye, M. J. Taylor, N. K. Biritwum, M. Osei-Atweneboana, M. G. Basanez, Does increasing treatment frequency address suboptimal responses to ivermectin for the control and elimination of river blindness? *Clin. Infect. Dis.* **62**, 1338–1347 (2016).

11. B. V. Babu, G. R. Babu, Coverage of, and compliance with, mass drug administration under the programme to eliminate lymphatic filariasis in India: A systematic review. *Trans. R. Soc. Trop. Med. Hyg.* **108**, 538–549 (2014).

12. L. Senyonjo, J. Oye, D. Bakajika, B. Biholong, A. Tekle, D. Boakye, E. Schmidt, E. Elhassan, Factors associated with ivermectin non-compliance and its potential role in sustaining *Onchocerca volvulus* transmission in the west region of Cameroon. *PLOS Negl. Trop. Dis.* **10**, e0004905 (2016).

13. D. H. Molyneux, A. Hopkins, M. H. Bradley, L. A. Kelly-Hope, Multidimensional complexities of filariasis control in an era of large-scale mass drug administration programmes: A can of worms. *Parasit. Vectors* **7**, 363 (2014).

14. R. Stouthamer, J. A. Breeuwer, G. D. Hurst, *Wolbachia pipientis*: Microbial manipulator of arthropod reproduction. *Annu. Rev. Microbiol.* **53**, 71–102 (1999).

15. S. C. Bosshardt, J. W. McCall, S. U. Coleman, K. L. Jones, T. A. Petit, T. R. Klei, Prophylactic activity of tetracycline against *Brugia pahangi* infection in jirds (*Meriones unguiculatus*). *J. Parasitol.* **79**, 775–777 (1993).

16. A. Hoerauf, K. Nissen-Pähle, C. Schmetz, K. Henkle-Dührsen, M. L. Blaxter, D. W. Büttner, M. Y. Gallin, K. M. Al-Qaoud, R. Lucius, B. Fleischer, Tetracycline therapy targets intracellular bacteria in the filarial nematode *Litomosoides sigmodontis* and results in filarial infertility. *J. Clin. Invest.* **103**, 11–18 (1999).

17. C. Bandi, T. J. Anderson, C. Genchi, M. L. Blaxter, Phylogeny of Wolbachia in filarial nematodes. *Proc. Biol. Sci.* **265**, 2407–2413 (1998).

18. M. J. Taylor, *Wolbachia* bacteria of filarial nematodes in the pathogenesis of disease and as a target for control. *Trans. R. Soc. Trop. Med. Hyg.* **94**, 596–598 (2000).

19. A. Hoerauf, Filariasis: New drugs and new opportunities for lymphatic filariasis and onchocerciasis. *Curr. Opin. Infect. Dis.* **21**, 673–681 (2008).

20. A. Hoerauf, S. Specht, M. Büttner, K. Pfarr, S. Mand, R. Fimmers, Y. Marfo-Debrekyei, P. Konadu, A. Y. Debrah, C. Bandi, N. Brattig, A. Albers, J. Larbi, L. Batsa, M. J. Taylor, O. Adjei, D. W. Buttner, *Wolbachia* endobacteria depletion by doxycycline as antifilarial therapy has macrofilaricidal activity in onchocerciasis: A randomized placebo-controlled study. *Med. Microbiol. Immunol.* **197**, 335 (2008).

21. M. J. Taylor, W. H. Makunde, H. F. McGarry, J. D. Turner, S. Mand, A. Hoerauf, Macrofilaricidal activity after doxycycline treatment of *Wuchereria bancrofti*: A double-blind, randomised placebo-controlled trial. *Lancet* **365**, 2116–2121 (2005).

22. M. Walker, S. Specht, T. S. Churcher, A. Hoerauf, M. J. Taylor, M. G. Basanez, Therapeutic efficacy and macrofilaricidal activity of doxycycline for the treatment of river blindness. *Clin. Infect. Dis.* **60**, 1199–1207 (2015).

23. J. D. Turner, S. Mand, A. Y. Debrah, J. Muehlfeld, K. Pfarr, H. F. McGarry, O. Adjei, M. J. Taylor, A. Hoerauf, A randomized, double-blind clinical trial of a 3-week course of doxycycline plus albendazole and ivermectin for the treatment of *Wuchereria bancrofti* infection. *Clin. Infect. Dis.* **42**, 1081–1089 (2006).

24. H. F. Cross, M. Haarbrink, G. Egerton, M. Yazdanbakhsh, M. J. Taylor, Severe reactions to filarial chemotherapy and release of Wolbachia endosymbionts into blood. *Lancet* **358**, 1873–1875 (2001).

25. L. R. Serbus, F. Landmann, W. M. Bray, P. M. White, J. Ruybal, R. S. Lokey, A. Debec, W. Sullivan, A cell-based screen reveals that the albendazole metabolite, albendazole sulfone, targets *Wolbachia*. *PLOS Pathog.* **8**, e1002922 (2012).

26. P. M. White, L. R. Serbus, A. Debec, A. Codina, W. Bray, A. Guichet, R. S. Lokey, W. Sullivan, Reliance of *Wolbachia* on high rates of host proteolysis revealed by a genome-wide RNAi screen of *Drosophila* cells. *Genetics* **205**, 1473–1488 (2017).

27. F. Fenollar, M. Maurin, D. Raoult, *Wolbachia pipientis* growth kinetics and susceptibilities to 13 antibiotics determined by immunofluorescence staining and real-time PCR. *Antimicrob. Agents Chemother.* **47**, 1665–1671 (2003).

28. P. G. Hermans, C. A. Hart, A. J. Trees, *In vitro* activity of antimicrobial agents against the endosymbiont *Wolbachia pipientis*. *J. Antimicrob. Chemother.* **47**, 659–663 (2001).

29. J. Janes, M. E. Young, E. Chen, N. H. Rogers, S. Burgstaller-Muehlbacher, L. D. Hughes, M. S. Love, M. V. Hull, K. L. Kuhen, A. K. Woods, S. B. Joseph, H. M. Petrassi, C. W. McNamara, M. S. Tremblay, A. I. Su, P. G. Schultz, A. K. Chatterjee, The ReFRAME library as a comprehensive drug repurposing library and its application to the treatment of cryptosporidiosis. *Proc. Natl. Acad. Sci. U.S.A.* **115**, 10750–10755 (2018).

30. V. Foray, M. M. Pérez-Jiménez, N. Fattouh, F. Landmann, *Wolbachia* control stem cell behavior and stimulate germline proliferation in filarial nematodes. *Dev. Cell* **45**, 198–211.e3 (2018).

31. G. S. Bah, E. L. Ward, A. Srivastava, A. J. Trees, V. N. Tanya, B. L. Makepeace, Efficacy of three-week oxytetracycline or rifampin monotherapy compared with a combination regimen against the filarial nematode *Onchocerca ochengi*. *Antimicrob. Agents Chemother.* **58**, 801–810 (2014).

32. V. Alagarsamy, K. Chitra, G. Saravanan, V. R. Solomon, M. T. Sulthana, B. Narendhar, An overview of quinazolines: Pharmacological significance and recent developments. *Eur. J. Med. Chem.* **151**, 628–685 (2018).

33. I. Khan, S. Zaib, S. Batool, N. Abbas, Z. Ashraf, J. Iqbal, A. Saeed, Quinazolines and quinazolinones as ubiquitous structural fragments in medicinal chemistry: An update on the development of synthetic methods and pharmacological diversification. *Bioorg. Med. Chem.* **24**, 2361–2381 (2016).

34. S. Specht, K. M. Pfarr, S. Arriens, M. P. Hübner, U. Klarmann-Schulz, M. Koschel, S. Sternberg, C. Martin, L. Ford, M. J. Taylor, A. Hoerauf, Combinations of registered drugs reduce treatment times required to deplete *Wolbachia* in the *Litomosoides sigmodontis* mouse model. *PLOS Negl. Trop. Dis.* **12**, e0006116 (2018).

35. M. Gerth, M. T. Gansauge, A. Weigert, C. Bleidorn, Phylogenomic analyses uncover origin and spread of the *Wolbachia* pandemic. *Nat. Commun.* **5**, 5117 (2014).

36. F. Comandatore, R. Cordaux, C. Bandi, M. Blaxter, A. Darby, B. L. Makepeace, M. Montagna, D. Sassera, Supergroup C *Wolbachia*, mutualist symbionts of filarial nematodes, have a distinct genome structure. *Open Biol.* **5**, 150099 (2015).

37. M. Blaxter, G. Koutsovoulos, The evolution of parasitism in Nematoda. *Parasitology* **142** (suppl. 1), S26–S39 (2015).

38. A. Halliday, A. F. Guimaraes, H. E. Tyrer, H. M. Metuge, C. N. Patrick, K. O. Arnaud, T. D. Kwenti, G. Forsbrook, A. Steven, D. Cook, P. Enyong, S. Wanji, M. J. Taylor, J. D. Turner, A murine macrofilaricide pre-clinical screening model for onchocerciasis and lymphatic filariasis. *Parasit. Vectors* **7**, 472 (2014).

39. R. Morales-Hojas, R. A. Cheke, R. J. Post, Molecular systematics of five *Onchocerca* species (Nematoda: Filarioidea) including the human parasite, *O. volvulus*, suggest sympatric speciation. *J. Helminthol.* **80**, 281–290 (2006).

40. K. L. Johnston, D. A. N. Cook, N. G. Berry, W. David Hong, R. H. Clare, M. Goddard, L. Ford, G. L. Nixon, P. M. O'Neill, S. A. Ward, M. J. Taylor, Identification and prioritization of novel anti-*Wolbachia* chemotypes from screening a 10,000-compound diversity library. *Sci. Adv.* **3**, eaao1551 (2017).

41. K. L. Johnston, L. Ford, I. Umareddy, S. Townson, S. Specht, K. Pfarr, A. Hoerauf, R. Altmeyer, M. J. Taylor, Repurposing of approved drugs from the human pharmacopoeia to target *Wolbachia* endosymbionts of onchocerciasis and lymphatic filariasis. *Int. J. Parasitol. Drugs Drug Resist.* **4**, 278–286 (2014).

42. R. H. Clare, D. A. Cook, K. L. Johnston, L. Ford, S. A. Ward, M. J. Taylor, Development and validation of a high-throughput anti-*Wolbachia* whole-cell screen: A route to macrofilaricidal drugs against onchocerciasis and lymphatic filariasis. *J. Biomol. Screen.* **20**, 64–69 (2015).

43. J. Foster, M. Ganatra, I. Kamal, J. Ware, K. Makarova, N. Ivanova, A. Bhattacharyya, V. Kapatral, S. Kumar, J. Posfai, T. Vincze, J. Ingram, L. Moran, A. Lapidus, M. Omelchenko, N. Kyrpides, E. Ghedin, S. Wang, E. Goltsman, V. Joukov, O. Ostrovskaya, K. Tsukerman, M. Mazur, D. Comb, E. Koonin, B. Slatko, The *Wolbachia* genome of *Brugia malayi*: Endosymbiont evolution within a human pathogenic nematode. *PLOS Biol.* **3**, e121 (2005).

44. A. Muslim, M. Y. Fong, R. Mahmud, S. Sivanandam, Vector and reservoir host of a case of human *Brugia pahangi* infection in Selangor, peninsular Malaysia. *Trop. Biomed.* **30**, 727–730 (2013).

45. Y. L. Lau, W. C. Lee, J. Xia, G. Zhang, R. Razali, A. Anwar, M. Y. Fong, Draft genome of *Brugia pahangi*: High similarity between *B. pahangi* and *B. malayi*. *Parasit. Vectors* **8**, 451 (2015).

46. J. C. Molloy, U. Sommer, M. R. Viant, S. P. Sinkins, *Wolbachia* modulates lipid metabolism in *Aedes albopictus* mosquito cells. *Appl. Environ. Microbiol.* **82**, 3109–3120 (2016).

47. L. R. Serbus, P. M. White, J. P. Silva, A. Rabe, L. Teixeira, R. Albertson, W. Sullivan, The impact of host diet on *Wolbachia* titer in *Drosophila*. *PLOS Pathog.* **11**, e1004777 (2015).

48. T. Ikeya, S. Broughton, N. Alic, R. Grandison, L. Partridge, The endosymbiont *Wolbachia* increases insulin/IGF-like signalling in *Drosophila*. *Proc. Biol. Sci.* **276**, 3799–3807 (2009).

49. R. T. Jacobs, C. Lunde, Y. R. Freund, V. Hernandez, X. Li, Y. Xia, P. W. Berry, J. Halladay, R. Stefanakis, E. E. Easom, J. J. Plattner, L. Ford, K. L. Johnston, D. A. N. Cook, R. Clare, A. Cassidy, L. Myhill, H. Tyrer, G. Gamble, A. F. Guimaraes, A. Steven, F. Lenz, A. Ehrens, S. J. Frohberger, M. Koschel, A. Hoerauf, M. P. Hübner, C. McNamara, M. A. Bakowski, J. D. Turner, M. J. Taylor, S. A. Ward, Boron-pleuromutilins as anti-*Wolbachia* agents with potential for treatment of onchocerciasis and lymphatic filariasis. *J. Med. Chem.* **62**, 2521–2540 (2018).

50. M. J. Taylor, T. W. von Geldern, L. Ford, M. P. Hubner, K. Marsh, K. L. Johnston, H. T. Sjoberg, S. Specht, N. Pionnier, H. E. Tyrer, R. H. Clare, D. A. N. Cook, E. Murphy, A. Steven, J. Archer, D. Bloemker, F. Lenz, M. Koschel, A. Ehrens, H. M. Metuge, V. C. Chunda, P. W. Ndongmo Chounna, A. J. Njouendou, F. F. Fombad, R. Carr, H. E. Morton, G. Aljayyoussi, A. Hoerauf, S. Wanji, D. J. Kempf, J. D. Turner, S. A. Ward, Preclinical development of an oral anti-*Wolbachia* macrolide drug for the treatment of lymphatic filariasis and onchocerciasis. *Sci. Transl. Med.* **11**, eaau2086 (2019).

51. C. P. Morris, H. Evans, S. E. Larsen, E. Mitre, A comprehensive, model-based review of vaccine and repeat infection trials for filariasis. *Clin. Microbiol. Rev.* **26**, 381–421 (2013).

52. J. Gilbert, C. K. Nfon, B. L. Makepeace, L. M. Njongmeta, I. M. Hastings, K. M. Pfarr, A. Renz, V. N. Tanya, A. J. Trees, Antibiotic chemotherapy of onchocerciasis: In a bovine model, killing of adult parasites requires a sustained depletion of endosymbiotic bacteria (*Wolbachia* species). *J. Infect. Dis* 3 (2005).

53. W. D. Hong, F. Benayoud, G. L. Nixon, L. Ford, K. L. Johnston, R. H. Clare, A. Cassidy, D. A. N. Cook, A. Siu, M. Shiotani, P. J. H. Webborn, S. Kavanagh, G. Aljayyoussi, E. Murphy, A. Steven, J. Archer, D. Struever, S. J. Frohberger, A. Ehrens, M. P. Hubner, A. Hoerauf, P. Roberts, A. T. M. Hubbard, E. W. Tate, R. A. Serwa, S. C. Leung, L. Qie, N. G. Berry, F. Gusovsky, J. Hemingway, J. D. Turner, M. J. Taylor, S. A. Ward, P. M. O'Neill, AWZ1066S, a highly specific anti-*Wolbachia* drug candidate for a short-course treatment of filariasis. *Proc. Natl. Acad. Sci. U.S.A.* **116**, 1414–1419 (2019).

54. A. Heddi, A. M. Grenier, C. Khatchadourian, H. Charles, P. Nardon, Four intracellular genomes direct weevil biology: Nuclear, mitochondrial, principal endosymbiont, and *Wolbachia*. *Proc. Natl. Acad. Sci. U.S.A.* **96**, 6814–6819 (1999).

55. B. M. Fuchs, G. Wallner, W. Beisker, I. Schwippl, W. Ludwig, R. Amann, Flow cytometric analysis of the in situ accessibility of *Escherichia coli* 16S rRNA for fluorescently labeled oligonucleotide probes. *Appl. Environ. Microbiol.* **64**, 4973–4982 (1998).

56. M. A. Perotti, H. K. Clarke, B. D. Turner, H. R. Braig, Rickettsia as obligate and mycetomic bacteria. *FASEB J.* **20**, 2372–2374 (2006).

57. T. Koressaar, M. Remm, Enhancements and modifications of primer design program Primer3. *Bioinformatics* **23**, 1289–1291 (2007).

58. A. Untergasser, I. Cutcutache, T. Koressaar, J. Ye, B. C. Faircloth, M. Remm, S. G. Rozen, Primer3—New capabilities and interfaces. *Nucleic Acids Res.* **40**, e115 (2012).

59. B. W. Li, Z. Wang, A. C. Rush, M. Mitreva, G. J. Weil, Transcription profiling reveals stage- and function-dependent expression patterns in the filarial nematode *Brugia malayi*. *BMC Genomics* **13**, 184 (2012).

60. M. W. Pfaffl, A new mathematical model for relative quantification in real-time RT-PCR. *Nucleic Acids Res.* **29**, e45 (2001).

61. L. Volkmann, O. Bain, M. Saeftel, S. Specht, K. Fischer, F. Brombacher, K. I. Matthaei, Hoerauf, Murine filariasis: Interleukin 4 and interleukin 5 lead to containment of different worm developmental stages. *Med. Microbiol. Immunol.* **192**, 23–31 (2003).

62. J. D. Turner, R. Sharma, G. Al Jayoussi, H. E. Tyrer, J. Gamble, L. Hayward, R. S. Priestley, E. A. Murphy, J. Davies, D. Waterhouse, D. A. N. Cook, R. H. Clare, A. Cassidy, A. Steven, K. L. Johnston, J. McCall, L. Ford, J. Hemingway, S. A. Ward, M. J. Taylor, Albendazole and antibiotics synergize to deliver short-course anti-*Wolbachia* curative treatments in preclinical models of filariasis. *Proc. Natl. Acad. Sci. U.S.A.* **114**, E9712–E9721 (2017).

63. D. Zofou, F. F. Fombad, N. V. T. Gandjui, A. J. Njouendou, A. J. Kengne-Ouafo, P. W. Chounna Ndongmo, F. R. Datchoua-Poutcheu, P. A. Enyong, D. T. Bita, M. J. Taylor, J. D. Turner, S. Wanji, Evaluation of *in vitro* culture systems for the maintenance of microfilariae and infective larvae of *Loa loa*. *Parasit. Vectors* **11**, 275 (2018).

64. S. Wanji, E. E. Eyong, N. Tendongfor, C. Ngwa, E. Esuka, A. Kengne-Ouafo, F. Datchoua-Poutcheu, P. Enyong, A. Hopkins, C. D. Mackenzie, Parasitological, hematological and biochemical characteristics of a model of hyper-microfilariaemic loiasis (*Loa loa*) in the Baboon (*Papio anubis*). *PLOS Negl. Trop. Dis.* **9**, e0004202 (2015).

65. O. A. Fahmi, J. L. Raucy, E. Ponce, S. Hassanali, J. M. Lasker, Utility of DPX2 cells for predicting CYP3A induction-mediated drug-drug interactions and associated structure-activity relationships. *Drug Metab. Dispos.* **40**, 2204–2211 (2012).

66. J. Bowes, A. J. Brown, J. Hamon, W. Jarolimek, A. Sridhar, G. Waldron, S. Whitebread, Reducing safety-related drug attrition: The use of *in vitro* pharmacological profiling. *Nat. Rev. Drug Discov.* **11**, 909–922 (2012).

67. A. Schiefer, A. Schmitz, T. F. Schäberle, S. Specht, C. Lämmer, K. L. Johnston, D. G. Vassylyev, G. M. König, A. Hoerauf, K. Pfarr, Corallopyronin A specifically targets and depletes essential obligate *Wolbachia* endobacteria from filarial nematodes *in vivo*. *J. Infect. Dis.* **206**, 249-257 (2012).

Chapter 3: The Eagle effect in the *Wolbachia*-worm symbiosis

This chapter contains a reprint of the previously published work of which I was a coauthor (Bulman et al., 2021). In this chapter, collaborators from the Sakanari Lab at UCSF and I wanted to further explore an observation we both separately found when treating *Wolbachia*-infected filarial nematodes with higher concentrations of antibiotic. Doxycycline is a common antibiotic known to decrease *Wolbachia* levels in these parasitic nematodes. Throughout our research we noticed that, counterintuitively, higher concentrations of doxycycline resulted in a smaller decrease in *Wolbachia* titer. Reciprocally, lower concentrations of the antibiotic were more effective at eliminating the bacteria. This phenomenon of higher concentrations resulting in lower efficacy of antibiotics is called the Eagle effect, first discovered by Harry Eagle in 1948 when measuring the effects of penicillin on *Streptococcus pyogenes*. The Eagle effect has been seen among other species of bacteria and some species of fungus. However, this effect had not yet been observed in *Wolbachia* until this work.

In addition to the work I performed testing the antibiotic doxycycline at different concentrations to validate the similar observations seen by the Sakanari Lab, my contribution to this project includes the tissue preparation and analysis of nematode germline *Wolbachia* titer via confocal microscopy. This work was crucial to the project to not only validate our collaborators' qPCR quantifications, but to visualize the nature of Wolbachia concentrations specifically in germline tissue of *B. pahangi*. *Wolbachia* exist in two places within the female filarial nematode: the hypodermal chords and the gonads. qPCR analysis was performed on whole worms, masking any tissue-specific effects of the antibiotics. Performing microdissections to isolate the germline tissue and visualizing this tissue type with immunofluorescent staining and microscopy allows one to specifically identify effects on *Wolbachia* levels in oocytes. This is particularly important because *Wolbachia* is known to control anterior-posterior axis formation in the growing embryo. Effects on *Wolbachia* titer in

the germline tissue have implications for the survival of the embryos, and thus transmission of the parasites via microfilarial shedding. While qPCR is a rapid way to quantify *Wolbachia* titer, it does not identify which tissue types experience fluctuations in bacterial amounts. Microscopy allows for a clear picture of tissue-specific effects. My contribution to this work can be seen in Figure 3.5.

ABSTRACT

Onchocerciasis (river blindness) and lymphatic filariasis (elephantiasis) are two human neglected tropical diseases that cause major disabilities. Mass administration of drugs targeting the microfilarial stage has reduced transmission and eliminated these diseases in several countries but a macrofilaricidal drug that kills or sterilizes the adult worms is critically needed to eradicate the diseases. The causative agents of onchocerciasis and lymphatic filariasis are filarial worms that harbor the endosymbiotic bacterium *Wolbachia.* Because filarial worms depend on *Wolbachia* for reproduction and survival, drugs targeting *Wolbachia* hold great promise as a means to eliminate these diseases. To better understand the relationship between *Wolbachia* and its worm host, adult *Brugia pahangi* were exposed to varying concentrations of doxycycline, minocycline, tetracycline and rifampicin *in vitro* and assessed for *Wolbachia* numbers and worm motility. Worm motility was monitored using the Worminator system, and *Wolbachia* titers were assessed by qPCR of the single copy gene *wsp* from *Wolbachia* and *gst* from *Brugia* to calculate IC_{50}s and in time course experiments. Confocal microscopy was also used to quantify *Wolbachia* located at the distal tip region of worm ovaries to assess the effects of antibiotic treatment in this region of the worm where *Wolbachia* are transmitted vertically to the microfilarial stage. Worms treated with higher concentrations of antibiotics had higher *Wolbachia* titers, i.e. as antibiotic concentrations increased there was a corresponding increase in *Wolbachia* titers. As the concentration of antibiotic increased, worms stopped moving and never recovered despite maintaining *Wolbachia* titers comparable to controls. Thus, worms were rendered moribund by the higher

concentrations of antibiotics but *Wolbachia* persisted suggesting that these antibiotics may act directly on the worms at high concentration. Surprisingly, in contrast to these results, antibiotics given at low concentrations reduced *Wolbachia* titers. *Wolbachia* in *B. pahangi* display a counterintuitive dose response known as the “Eagle effect.” This effect in *Wolbachia* suggests a common underlying mechanism that allows diverse bacterial and fungal species to persist despite exposure to high concentrations of antimicrobial compounds. To our knowledge this is the first report of this phenomenon occurring in an intracellular endosymbiont, *Wolbachia*, in its filarial host.

INTRODUCTION

Onchocerciasis and lymphatic filariasis are two human neglected tropical diseases caused by parasitic filarial nematodes. Onchocerciasis, also known as river blindness, is caused by *Onchocerca volvulus*, while lymphatic filariasis is caused by the species *Wuchereria bancrofti*, *Brugia malayi* and *Brugia timori*. Each of these species harbors the endosymbiotic bacterium, *Wolbachia,* in the hypodermal chord and female ovaries, where the endosymbiont is passed through the female germline [1]. These filarial worms depend on *Wolbachia* for their long-term survival and reproduction, and *Wolbachia* also play a role in the clinical pathology of filarial infection [2–9]. The microfilaricidal drug ivermectin, which has been successfully used in mass drug administration (MDA) programs to eliminate onchocerciasis in Central and South America [10, 11], cannot be used in Central and West Africa because of the severe adverse effects in patients co-infected with high numbers of *Loa loa* microfilariae [12, 13]. *Loa loa*, unlike *Onchocerca*, *Wuchereria* and *Brugia*, does not harbor *Wolbachia* [14, 15], thus identifying antibiotics that eliminate *Wolbachia* is an excellent approach to find new drugs to eliminate onchocerciasis and lymphatic filariasis [16–19].

Clinical studies have shown that doxycycline given to patients for 4–6 weeks at 100–200 mg/day was efficacious in reducing disease pathology and microfilaremia in individuals with lymphatic filariasis [20–22] and was also effective in reducing *Wolbachia*, disrupting

worm fertility and causing adult worm death in patients infected with *O. volvulus* [23–26]. Although effective as an anti-*Wolbachia* drug, doxycycline is contraindicated during pregnancy and for young children, and the long course of treatment is not feasible for MDA because of the challenges of patient adherence [15, 27–31]. Antibiotics such as rifampicin and minocycline, as well as novel anti-*Wolbachia* drugs, have also shown promise in pre-clinical models of lymphatic filariasis and onchocerciasis [19, 32–37]. However, there is evidence in pre-clinical models that if insufficient anti-*Wolbachia* treatment is administered, *Wolbachia* can repopulate their host leading to recovery of filarial fecundity [35, 38, 39].

Much remains unknown about the mechanisms by which *Wolbachia* repopulates an antibiotic-treated filarial worm and how the filarial worm regains its reproductive output. While it is clear that *Wolbachia* and its filarial host are co-dependent, the mechanisms by which *Wolbachia* abundance influences worm viability is unknown. This information is critical for both understanding the biology of the *Wolbachia*-worm symbiosis and developing efficacious protocols for treating these devastating diseases. Because of the high costs and difficulties associated with animal studies, *in vitro* studies have provided an excellent means to study the *Wolbachia/Brugia* relationship. Here we tested several antibiotics, doxycycline, tetracycline, minocycline, rifampicin and two novel anti-wolbachial compounds, with adult *B. pahangi* females and males *in vitro* to determine *Wolbachia* titers and their effects on worm viability. Surprisingly, there was a positive correlation between antibiotic concentrations and *Wolbachia* titers, a phenomenon known as the “Eagle effect,” where higher concentrations of antibiotics correlate with increased titers of bacteria [40–43]. We also determined that antibiotics affected worm viability without first reducing *Wolbachia* titers, suggesting that these antibiotics may act directly on the worms *in vitro* at high concentration.

RESULTS

Worm motility is highly correlated to viability in MTT assay

To confirm that worm motility is indicative of worm viability, worms were analyzed using an MTT assay similar to ones used previously [49–51]. Results showed that cell viability as measured by the conversion of MTT to formazan was highly correlated with worm motility (r = 0.889) and that earlier cessation of worm motility was predictive of greater reduction in formazan production on Day 6 (Table 3.1) similar to the results found with *B. malayi* [49] and *O. gutturosa* [50].

	% Inhibition of motility					% Inhibition of formazan production
Compound	**Day 1 (%)**	**Day 2 (%)**	**Day 3 (%)**	**Day 4 (%)**	**Day 6 (%)**	**Day 6 (%)**
Doxycycline (100 μM)	54	94	97	99	99	91
Doxycycline (10 μM)	0	0	9	59	92	46
Doxycycline (1 μM)	0	0	0	2	0	8

Table 3.1 Viability of female worms treated with doxycycline was highly correlated with worm motility. Worms treated with 100 and 10 μM doxycycline showed declining motility over time and were barely motile at 100 μM by Day 2. Viability was assessed on Day 6, as measured by formazan production in an MTT assay. The degree and duration of motility inhibition was predictive of reduced viability in the MTT assay.

Eagle effect in an endosymbiotic bacterium from a filarial worm

To better understand the relationship between *Wolbachia* and its worm host, adult *Brugia pahangi* were exposed to varying concentrations of doxycycline, minocycline, tetracycline, and rifampicin and assessed for *Wolbachia* numbers and worm motility. Results showed that *Wolbachia* titers were significantly reduced at antibiotic concentrations that are at or slightly below the IC_{50}s for worm motility in female worms (Fig. 3.1). In contrast to these results, worms treated with higher concentrations of antibiotics had higher *Wolbachia* titers, i.e. as antibiotic concentrations increased there was a corresponding increase in *Wolbachia*

titers (the Eagle effect). However, as the concentration of antibiotic increased, worms stopped moving and never recovered despite maintaining *Wolbachia* titers comparable to controls. Thus, worms were rendered moribund by the higher concentrations of antibiotics but *Wolbachia* persisted. The same trends in *Wolbachia* titers were observed when *wsp* copy numbers were analyzed both with and without normalization to worm *gst* copy numbers, indicating that changes in the *wsp/gst* ratio reflect changes in *Wolbachia* titer and were not driven by changes in *gst* copy number. *Wolbachia* titers in males treated with doxycycline, minocycline and rifampicin followed a similar pattern as observed in females with a positive correlation between *Wolbachia* titers and compound concentration (correlation coefficient of $r \geq 0.5$). Male worms treated with tetracycline, however, did not show a positive correlation between *Wolbachia* titers and compound concentration (Fig. 3.1).

The motility-based IC_{50}s for doxycycline, minocycline, tetracycline, and rifampicin with female worms after 6 days *in vitro* were: 5.6, 3.6, 15.7 and 5.9 µM, respectively; for male worms, the IC_{50}s for each of the antibiotics were 13.0, 10.9, 77.3 and 29.5 µM, respectively.

Doxycycline and tetracycline inhibited worm motility without reducing *Wolbachia* titers in time course experiments

To further investigate the effects of antibiotics on female and male *B. pahangi,* both *Wolbachia* titers and worm motility at multiple antibiotic concentrations were assessed over time. These time course experiments showed that high concentrations of doxycycline and tetracycline did not reduce *Wolbachia* titers, though lower concentrations did; 100 µM doxycycline did not cause a significant decrease in *Wolbachia* titers in female worms at any time point compared to control worms, yet worm motility was inhibited by 90% on Day 1 and worms were moribund by Day 3 (99% inhibition of motility) (Fig. 3.2A). At 10 µM, motility was inhibited by 96% on Day 3 and 99% on Day 6, also without significant reduction in *Wolbachia*. However, 1 µM doxycycline reduced *Wolbachia* titers by 63% on Day 3 and 82% on Day 6,

Fig. 3.1 *Brugia pahangi* worms exposed to higher concentrations of antibiotics maintained higher *Wolbachia* titers. Female and male worms were treated with 6-point serial dilutions of doxycycline, minocycline, tetracycline and rifampicin *in vitro* for 6 days and assessed for worm motility and *Wolbachia* titers (see also Fig. S1 and Table S1 for statistical significance). For female worms, higher concentrations of antibiotics inhibited worm motility, but surprisingly *Wolbachia* titers did not decrease. Male worms were similarly affected except for those treated with tetracycline, which did not show a positive correlation between *Wolbachia* titers and antibiotic concentration. *Wolbachia* titers were measured by qPCR as a ratio of *wsp/gst* (shown as medians with 95% confidence intervals); antibiotic concentrations are in µM. The percent differences in *wsp/gst* ratios as compared to DMSO controls are shown below each antibiotic concentration. Negative percentages signify a decrease in *Wolbachia* titers, and positive percentages indicate titers that were higher than controls. Percent inhibition of worm motility is also shown below each antibiotic concentration: 0% inhibition indicates that worms were as motile as controls, and 100% inhibition indicates that the worms were not motile. There was an inverse relationship between worm motility and *wsp/gst* ratio ($r \leq -0.5$), except for males treated with tetracycline, which did not show this inverse relationship.

Doxycycline

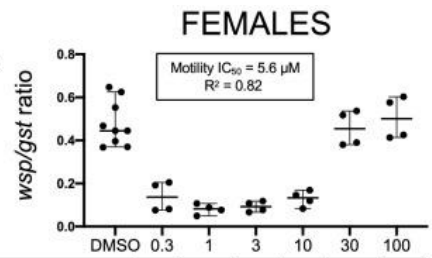

	DMSO	0.3	1	3	10	30	100
% Difference in *wsp/gst* Ratio		-69%	-81%	-79%	-70%	2%	13%
% Inhibition of Motility		28%	0%	2%	92%	100%	99%

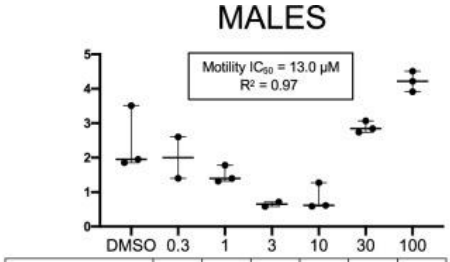

	DMSO	0.3	1	3	10	30	100
% Difference in *wsp/gst* Ratio		3%	-28%	-67%	-69%	46%	116%
% Inhibition of Motility		15%	0%	0%	19%	99%	99%

Minocycline

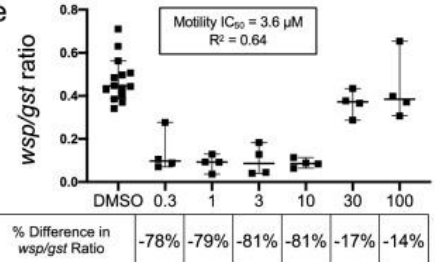

	DMSO	0.3	1	3	10	30	100
% Difference in *wsp/gst* Ratio		-78%	-79%	-81%	-81%	-17%	-14%
% Inhibition of Motility		13%	41%	26%	69%	100%	100%

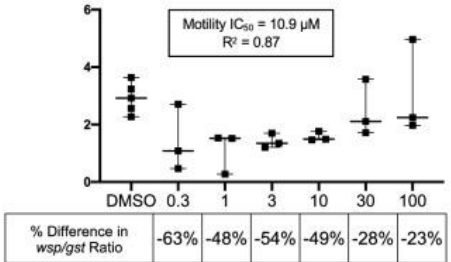

	DMSO	0.3	1	3	10	30	100
% Difference in *wsp/gst* Ratio		-63%	-48%	-54%	-49%	-28%	-23%
% Inhibition of Motility		23%	0%	0%	48%	85%	100%

Tetracycline

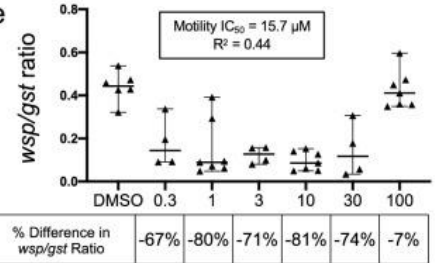

	DMSO	0.3	1	3	10	30	100
% Difference in *wsp/gst* Ratio		-67%	-80%	-71%	-81%	-74%	-7%
% Inhibition of Motility		0%	2%	0%	12%	56%	100%

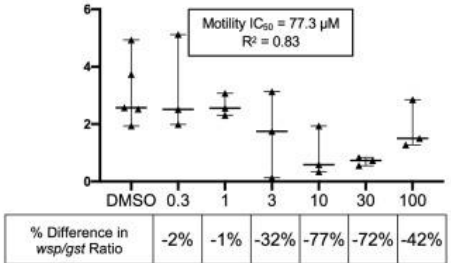

	DMSO	0.3	1	3	10	30	100
% Difference in *wsp/gst* Ratio		-2%	-1%	-32%	-77%	-72%	-42%
% Inhibition of Motility		3%	8%	2%	0%	0%	76%

Rifampicin

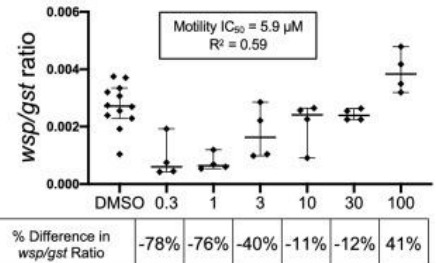

	DMSO	0.3	1	3	10	30	100
% Difference in *wsp/gst* Ratio		-78%	-76%	-40%	-11%	-12%	41%
% Inhibition of Motility		30%	14%	20%	63%	99%	99%

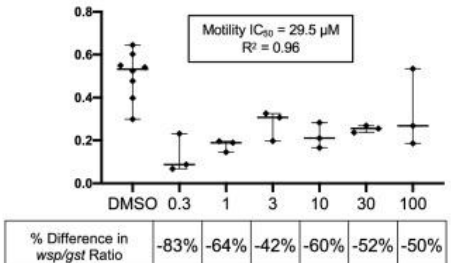

	DMSO	0.3	1	3	10	30	100
% Difference in *wsp/gst* Ratio		-83%	-64%	-42%	-60%	-52%	-50%
% Inhibition of Motility		0%	0%	0%	0%	51%	100%

although worms remained motile for the duration of the assay. Similar results were observed for male *B. pahangi* motility and for the *Wolbachia* titers at high and low concentrations of doxycycline.

Tetracycline fully inhibited worm motility only when worms were exposed to 100 µM tetracycline for 6 days. At this high concentration, worms were immotile but *Wolbachia* titers were similar to those of control worms (Fig. 3.2B). At the lower antibiotic concentrations (1 and 10 µM), *Wolbachia* titers were significantly reduced compared to those from control worms on Days 3 and 6, despite showing active motility. Thus, while both doxycycline and tetracycline showed the expected dose response relationship in terms of motility, the inverse relationship was found for *Wolbachia* titer.

Rifampicin reduced worm motility only at high concentrations but *Wolbachia* titers were reduced at all concentrations in time course experiment

Rifampicin was also used in the time course experiment to assess the relationship between female and male worms and *Wolbachia* titers (Fig. 3.2C). Each concentration of rifampicin tested reduced *Wolbachia* titers but only the highest concentration inhibited motility. Worms treated with 100 µM rifampicin were moribund by Day 6. Rifampicin reduced *Wolbachia* titers at all concentrations starting as early as Day 1 for female worms and Day 3 for male worms. By Day 6 rifampicin reduced *Wolbachia* titers by 50% or more compared to control worms at all concentrations. Figure 3.3 summarizes the effects that doxycycline, tetracycline and rifampicin have on worms (motility) and *Wolbachia* numbers (% reduction) compared to control worms.

Novel anti-*Wolbachia* compounds show trends similar to approved antibiotics

The novel quinazolines CBR417 and CBR490 were tested on *B. pahangi* female worms in a

Fig. 3.2 Time course experiment reveals antibiotics stop worm motility without a corresponding decrease in *Wolbachia* and *vice versa.* A time course experiment was conducted to determine the effects of doxycycline, tetracycline and rifampicin on *B. pahangi* females and *Wolbachia* titers at low (1 µM), intermediate (10 µM) and high (100 µM) concentrations at three time points (Day 1, 3 and 6). Doxycycline (A) and tetracycline (B) decreased worm motility but *wsp/gst* ratios did not fall in response to high antibiotic concentrations; at lower concentrations, worm motility was not impacted but *wsp/gst* ratios were reduced. *Wolbachia* titers were measured by *wsp/gst* ratios; medians with 95% confidence intervals are shown. X-axis labels show antibiotic concentration in µM. Percent differences in *wsp/gst* ratios compared to DMSO controls are shown below each antibiotic concentration. Negative percentages signify a decrease in *Wolbachia* titers, and positive percentages indicate that titers were higher than controls. Percent inhibition of motility is shown below each antibiotic concentration: 0% inhibition indicates that worms were as motile as controls, and 100% inhibition indicates that the worms were fully immotile. Red asterisks indicate statistical significance of the difference between *wsp/gst* ratios in treated worms and DMSO controls. ****$P < 0.0001$, ***$P < 0.001$, **$P < 0.01$, *$P < 0.05$.

FEMALES

a Doxycycline

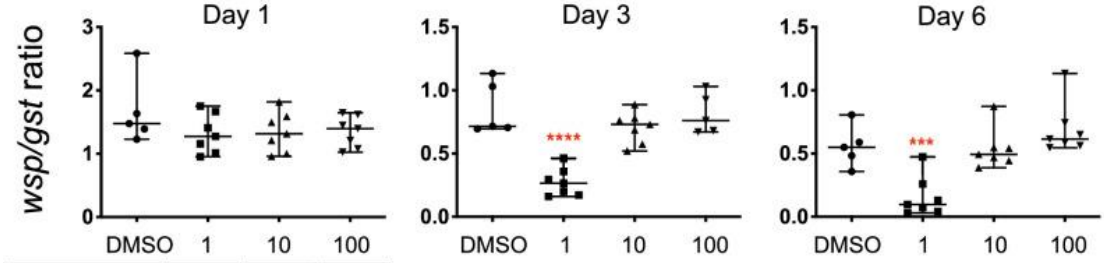

	DMSO	1	10	100
% Difference in *wsp/gst* Ratio		-14%	-11%	-5%
% Inhibition of Motility		0%	0%	90%
% Difference in *wsp/gst* Ratio		-63%	2%	6%
% Inhibition of Motility		0%	96%	99%
% Difference in *wsp/gst* Ratio		-82%	-10%	12%
% Inhibition of Motility		6%	99%	99%

b Tetracycline

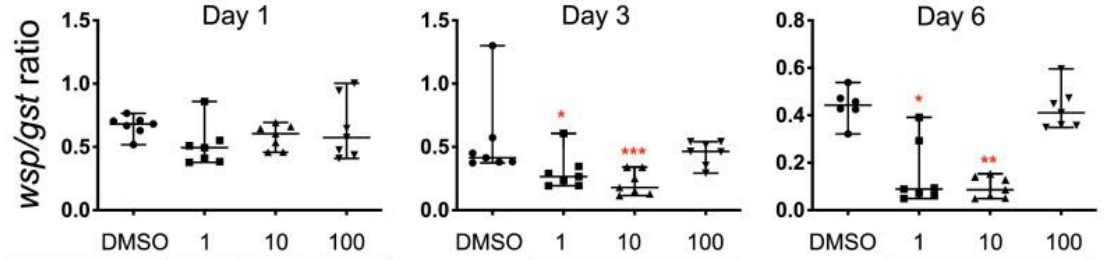

	DMSO	1	10	100
% Difference in *wsp/gst* Ratio		-28%	-11%	-16%
% Inhibition of Motility		0%	0%	8%
% Difference in *wsp/gst* Ratio		-36%	-57%	12%
% Inhibition of Motility		0%	0%	57%
% Difference in *wsp/gst* Ratio		-80%	-81%	-7%
% Inhibition of Motility		2%	12%	100%

c Rifampicin

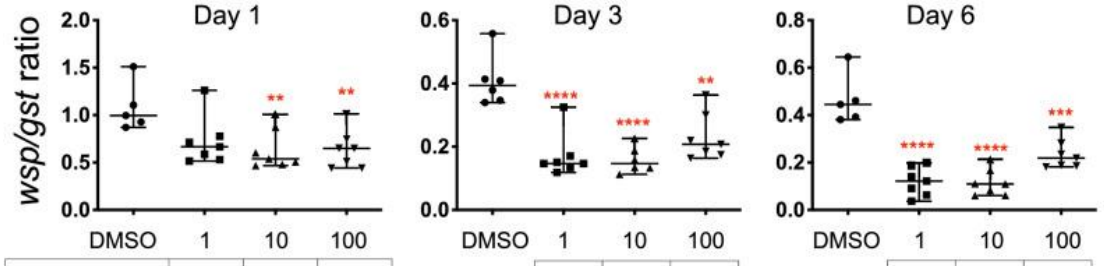

	DMSO	1	10	100
% Difference in *wsp/gst* Ratio		-33%	-46%	-35%
% Inhibition of Motility		0%	0%	0%
% Difference in *wsp/gst* Ratio		-63%	-63%	-47%
% Inhibition of Motility		0%	0%	31%
% Difference in *wsp/gst* Ratio		-73%	-75%	-51%
% Inhibition of Motility		0%	0%	100%

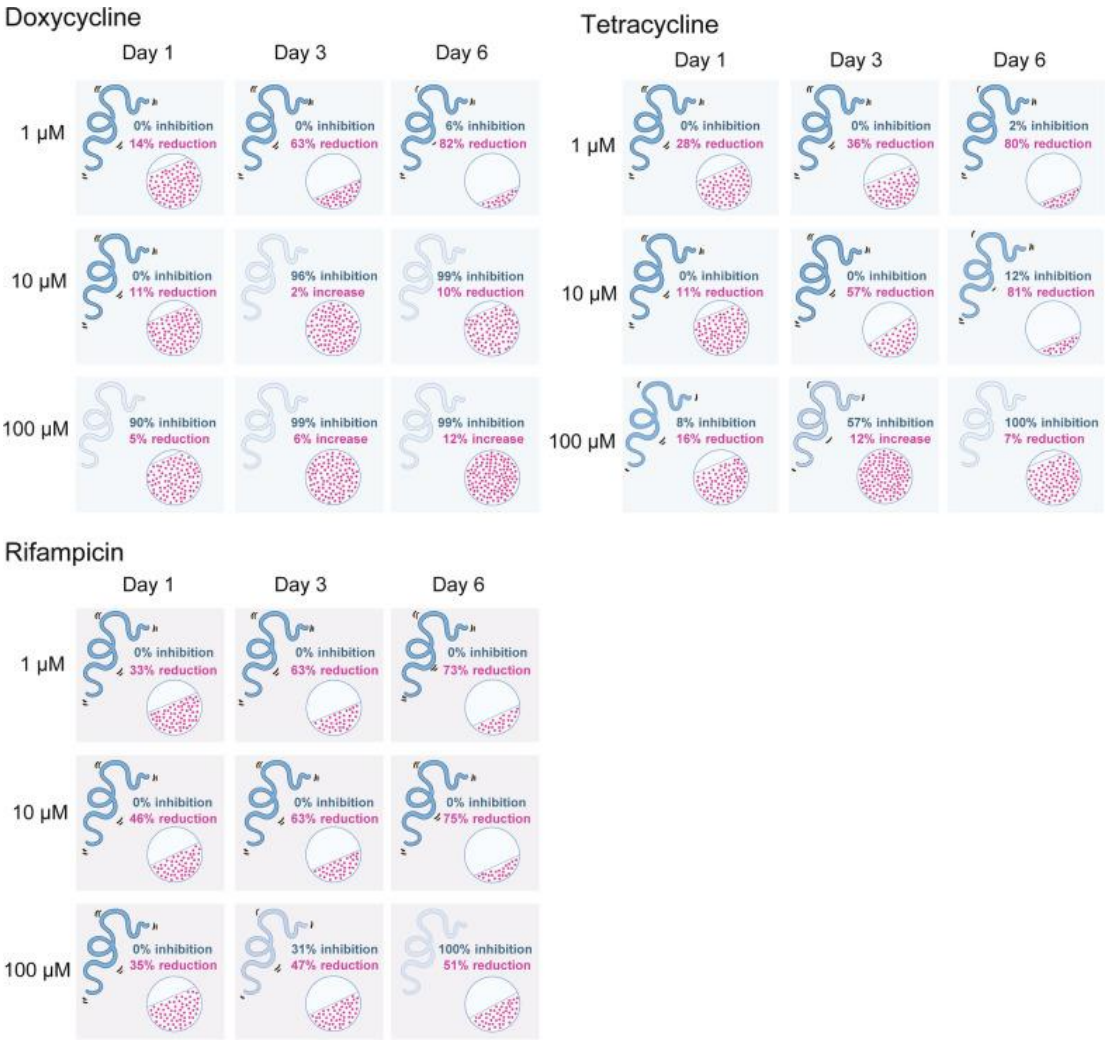

Fig. 3.3 Illustration summarizing the Eagle effect on the endosymbiont *Wolbachia* in its worm host. The illustration depicts the worm and *Wolbachia* response to doxycycline, tetracycline and rifampicin. With doxycycline and tetracycline treatment worms become moribund at high concentration despite the high numbers of *Wolbachia*. Relative inhibition of worm motility is in blue (top), and relative changes in *Wolbachia* titers are in red (bottom). Worm motility is represented by the drawing of the worm: darker blue worms indicate more motility, and lighter blue worms indicate inhibited motility. *Wolbachia* titers are represented by red dots within the circle and are proportional to the *Wolbachia* titers normalized to controls. Illustration created by Mona Luo.

3-day assay (Fig. 3.4). Both CBR417 and CBR490 induced the Eagle effect in *Wolbachia* titers, but as would be expected, inhibition of worm motility increased with compound concentration. Both compounds completely inhibited motility at 100 µM. Treatment with 10 µM CBR417 led to 72% inhibition of motility, while 10 µM CBR490 also inhibited motility by 100%. Similar to doxycycline and tetracycline, *Wolbachia* titers were not reduced even though worms were no longer motile at these concentrations. Conversely at the lowest concentration, 1 µM, *Wolbachia* titers were reduced by approximately 50% compared to the levels found in the controls but worms remained motile.

Confocal microscopy confirms *Wolbachia* reduction in the distal tip cell when exposed to antibiotic treatment

Confocal microscopy of ovaries removed from worms treated with 10 µM doxycycline, minocycline, tetracycline and rifampicin revealed that there were lower numbers of *Wolbachia* in the distal tip region compared to those from worms in the control group. Figure 3.5 shows low and high magnification fluorescence images of fixed and stained untreated worms and worms treated with 10 µM tetracycline and rifampicin. Tetracycline significantly reduced the number of *Wolbachia* by 95% compared to the controls ($P < 0.001$); rifampicin also significantly reduced *Wolbachia* by 83% ($P < 0.05$). Although doxycycline and minocycline had lower *Wolbachia* titers (60 and 73%, respectively) compared to control worms, the reductions were not statistically significant.

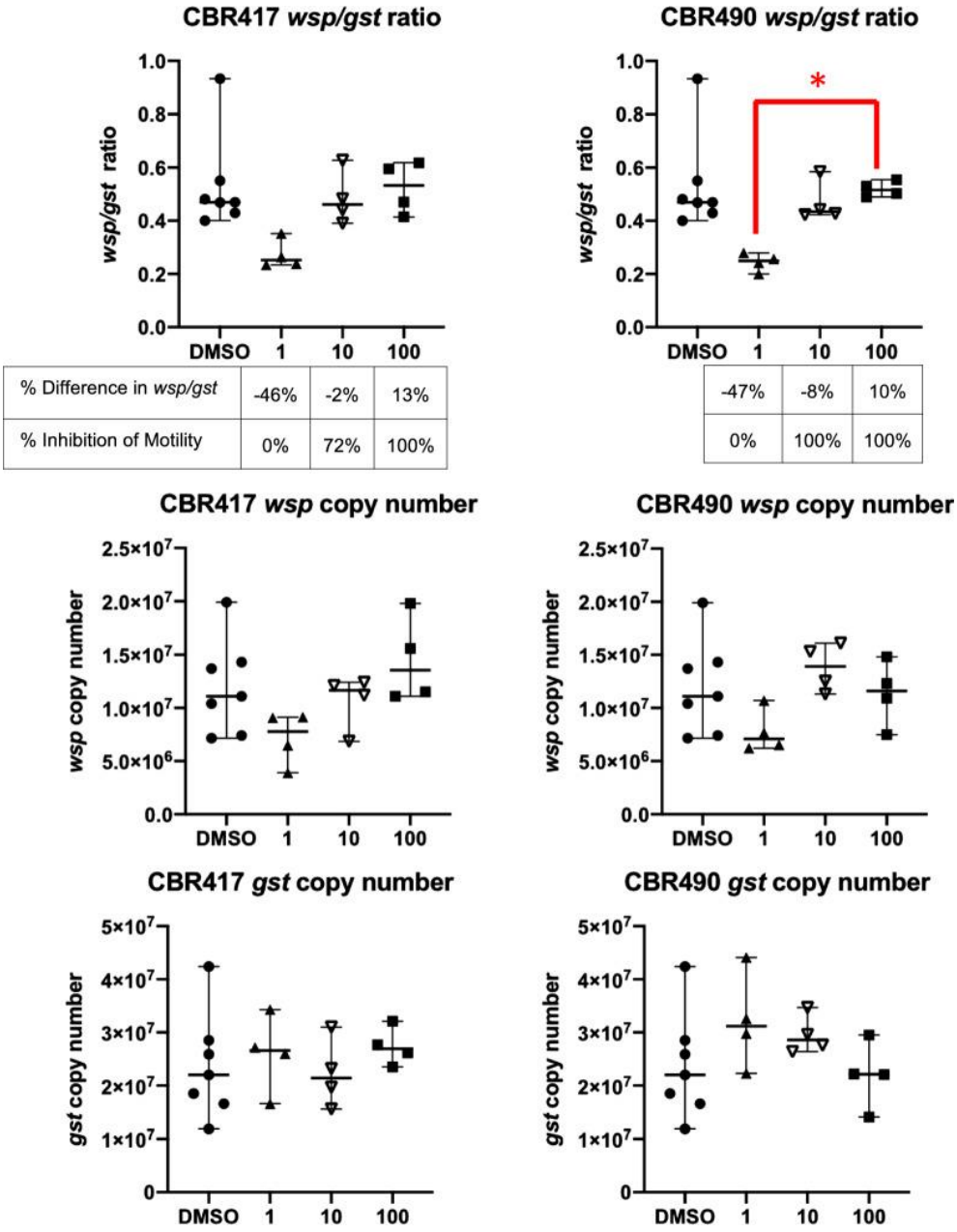

% Difference in *wsp/gst*	-46%	-2%	13%
% Inhibition of Motility	0%	72%	100%

-47%	-8%	10%
0%	100%	100%

Fig 3.4 Quinazolines CBR417 and CBR490 are effective in killing worms at high concentrations and reduce *Wolbachia* numbers at low concentrations. *B. pahangi* adult females were treated with two novel anti-*Wolbachia* compounds, CBR417 and CBR490, for 3 days, *in vitro.* These compounds showed worm killing without *Wolbachia* reduction at 10 and 100 µM and worm survival with reduced *Wolbachia* titers at 1 µM. X-axis shows compound concentrations in µM. The same DMSO control worms were used as a comparator for both CBR417 and CBR490. Both compounds showed a positive correlation between antibiotic concentration and *wsp/gst* ratio ($r \geq 0.6$) and a negative correlation between worm motility and *wsp/gst* ratio ($r \leq -0.9$). The difference between 1 and 100 µM CBR490 was statistically significant (*$P < 0.05$). Inhibition of worm motility compared to DMSO controls at 10 and 100 µM for both compounds was statistically significant ($P < 0.0001$).

Fig. 3.5 *Wolbachia* are depleted in the distal tip region of worm ovaries following antibiotic treatments. Worms were treated with 10 µM doxycycline, minocycline, tetracycline, and rifampicin for 6 days. Negative controls contained 1% DMSO in culture media. (A) Graph shows medians with 95% confidence intervals. ****P* < 0.001; **P* < 0.05. (B) Images of the distal tip region of *B. pahangi* ovaries from worms treated *in vitro* with tetracycline and rifampicin showing the elimination of *Wolbachia* in worm ovaries. Panels on the right are high magnification images of the boxed regions in the distal tip region. *Wolbachia* are the red puncta stained with propidium iodide and DAPI; the nuclei of host cells (worm cells) in the ovaries are stained blue/magenta by DAPI.

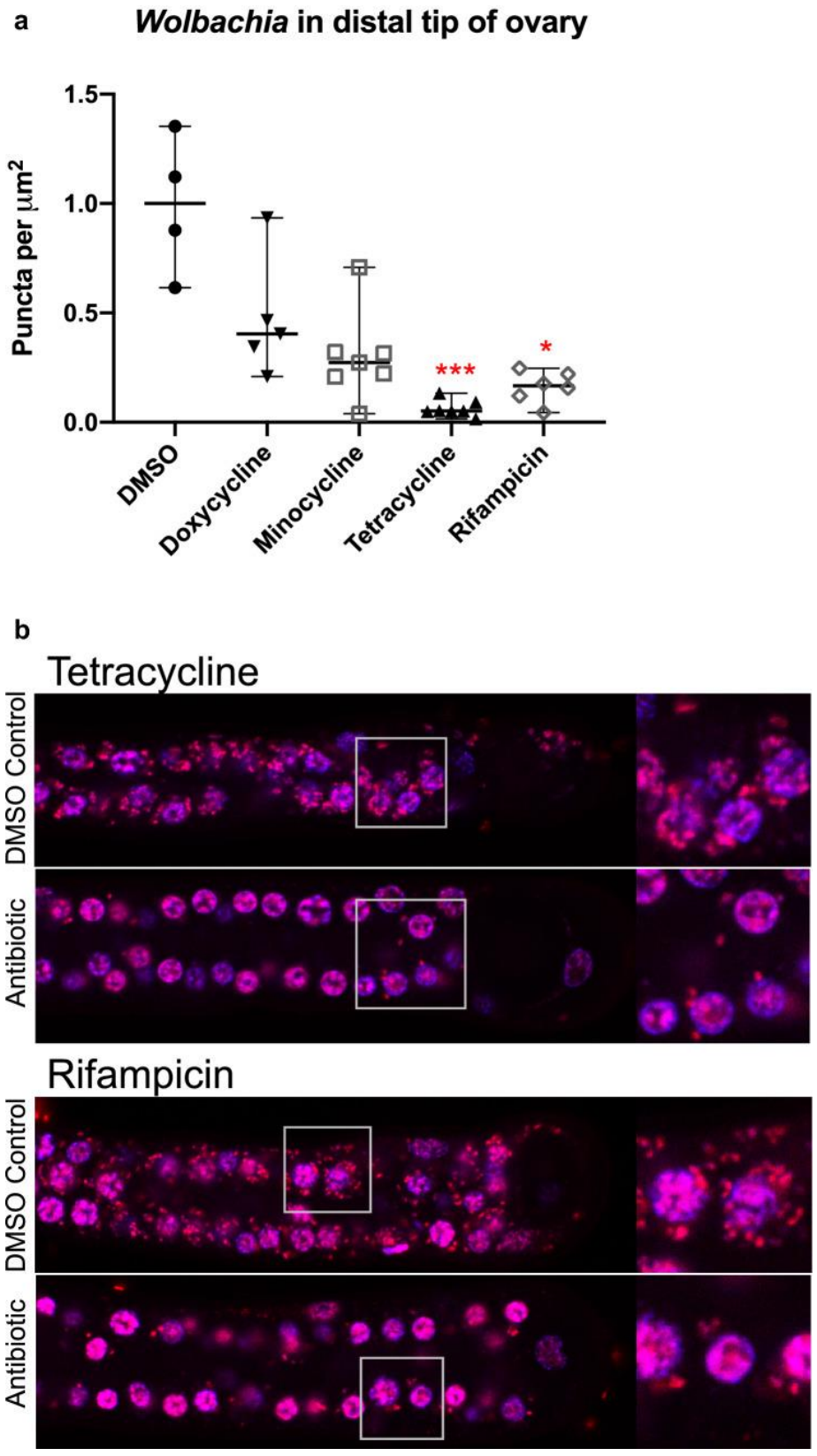
a
Wolbachia in distal tip of ovary
Puncta per μm²
1.5
1.0
0.5
0.0
***
*
DMSO
Doxycycline
Minocycline
Tetracycline
Rifampicin
b
Tetracycline
DMSO Control
Antibiotic
Rifampicin
DMSO Control
Antibiotic

DISCUSSION

While testing known antibiotics and novel anti-*Wolbachia* compounds with *Brugia pahangi* adult worms *in vitro*, we observed a surprising pattern: *Wolbachia* killing occurred at low antibiotic concentrations but *Wolbachia* survived when treated with higher concentrations. The IC_{50} and time course experiments showed that high concentrations of antibiotics failed to clear *Wolbachia* from the adult *Brugia pahangi* worms, while low concentrations decreased *Wolbachia* titers. This phenomenon, known as the Eagle effect, was first described by Eagle [40], who found that *Staphylococcus aureus*, *Enterococcus faecalis* and group B and C *Streptococcus* survived penicillin treatment at concentrations above an optimal point. Since this initial report, the Eagle effect has been reported in numerous species of bacteria and fungi treated with antibiotics across multiple classes [41–43, 56], but to our knowledge this is the first case in which the Eagle effect occurs with the endosymbiont, *Wolbachia*, in its worm host.

Although the underlying mechanisms that drive the Eagle effect are not known, investigators have suggested various possibilities to explain the increased survival of bacteria when treated with antibiotics at concentrations above the minimum inhibitory concentration (MIC), including antibiotic interference with bacterial autolytic enzymes, bacterial tolerance (bacteria transiently remain viable when exposed to high antibiotic concentrations) and the presence of non-replicating persister populations [42, 43]. In the *Wolbachia* endosymbiont-filarial worm relationship, it is possible that one or more of these mechanisms may be at play. Since *Wolbachia* are obligate intracellular bacteria, antibiotics must first pass through cells of the worm host to enter bacterial cells. It is possible that high concentrations of antibiotics such as doxycycline cause direct damage to host cells, which signal *Wolbachia* to initiate replication to maintain their population or to enter a protective, dormant “persister” state to reduce susceptibility to antibiotics. An analogous process occurs in adherent invasive *Escherichia coli* that are triggered to enter a persister state by the stressful conditions of the phagolysosome when phagocytosed by macrophages [57]. Lower antibiotic concentrations

may be insufficient to cause damage to the worm cells, thus allowing the antibiotics to infiltrate the bacteria before signaling mechanisms can be engaged.

In an *in vivo* study by Gunderson et al. [39], *Wolbachia* titers were initially reduced following rifampicin treatment but then returned to normal levels 8 months later. They reported that populations of *Wolbachia* found within clusters were not reduced by antibiotic treatment, but that *Wolbachia* in the areas surrounding the clusters were eliminated, suggesting that these clusters contained *Wolbachia* in a protected state. It is possible that the clusters are affording protection for the *Wolbachia* and act as a privileged site in the worm that allows the bacteria to persist and contribute to the Eagle effect.

Given that worm motility was inhibited at high concentrations independently of *Wolbachia* killing, the antibiotics' effect on worms was likely due to off-target effects. For instance, the tetracycline class of antibiotics (doxycycline, tetracycline, and minocycline) achieve their bacteriostatic effects by binding to the 30S ribosomal subunit, thereby inhibiting bacterial protein synthesis [58, 59], but they are also known to have effects on eukaryotic cells, e.g. inhibit mitochondrial function in both *Wolbachia*-infected and -uninfected *Drosophila simulans* [60], influence apoptosis [61, 62] and inhibit matrix metalloproteinases [63]. *Brugia* are known to have metalloproteinases that play important physiological roles, and the inhibition of these enzymes may play a role in worm killing [64]. These off-target drug effects may also affect worm survival when rifampicin is given at high concentrations *in vitro*. Rifampicin is known to induce reactive oxygen species (ROS) in bacteria [65, 66] in addition to inhibiting bacterial RNA polymerase. The mechanism of action is not yet known for the new quinazolines, CBR417 and CBR490, but these compounds resulted in findings similar to those of rifampicin *in vivo*. Animal studies have shown that these compounds decreased *Wolbachia* titers by 90–99% compared to vehicle controls [33, 36, 39], which suggests that worms recovered from treated animals may correspond to those worms that were exposed to low (1–10 μM) concentrations of antibiotics in the present *in vitro* study. Thus, worms

recovered *in vivo* receive what may be the equivalent of low doses *in vitro*. However, further pharmacokinetic studies are needed to evaluate how *in vitro* results relate to *in vivo* studies.

Observation of the Eagle effect in *Wolbachia* suggests a common underlying mechanism that allows for diverse bacterial and fungal species to persist despite exposure to high concentrations of antimicrobial compounds. Further investigation into the Eagle effect in the *Wolbachia-Brugia* endosymbiotic relationship may shed light on conserved mechanisms by which bacteria evade antibiotic treatment and lead to improved treatments for both filarial and bacterial infections.

MATERIALS AND METHODS

Brugia pahangi worm assays and motility assessment

Adult *B. pahangi* female and male worms were collected from jirds (*Meriones unguiculatus*) and transferred to 24-well plates with 500 µl of culture media (RPMI-1640 with 25 mM HEPES, 2.0 g/L $NaHCO_3$, 5% heat-inactivated FBS and 1X antibiotic/antimycotic solution). To limit variability among individual female worms, only fecund female worms that released at least 50 microfilariae (mf) were used. To determine IC_{50}s, worms were treated with a 6-point serial dilution of 100, 30, 10, 3, 1 and 0.3 µM of doxycycline hyclate (Sigma-Aldrich catalog no. D9891), minocycline hydrochloride (Sigma-Aldrich catalog no. M9511), tetracycline hydrochloride (Sigma-Aldrich catalog no. T7660) or rifampicin (Fisher Scientific catalog no. 50-213-645). To avoid precipitation of the antibiotics in media, we used a maximum concentration of 100 µM, which is below the limit of solubility in water for each of the antibiotics [44–47]. One percent DMSO (Fisher Scientific catalog no. BP231) was used for the control worms. Female worms were plated individually, and male worms were plated four per well. Worms were kept in culture in a 37 °C, 5% CO_2 incubator for the duration of the assay (6 days). Worm motility was recorded on Days 0, 1, 2, 3 and 6 using the Worminator [48], and worms were collected on Day 6 for qPCR analysis.

To confirm that worm motility correlated with worm viability, *B. pahangi* females that had been treated with 100, 10 and 1 µM doxycycline were collected on Day 6 and assayed using a cell viability assay with thiazolyl blue tetrazolium bromide (MTT) (Sigma Aldrich catalog no. M2128) similar to ones used previously [49–51]. Worms were transferred to a 96-well plate containing 200 µl freshly prepared 0.5 mg/ml MTT in PBS per well, incubated at 37°C for 30 min and then transferred to 150 µl DMSO. After 1 h, 100 µl DMSO was transferred to a clear, flat-bottom 96-well plate, and the absorbance of formazan was read at 570 nm.

To compare the effects of two different classes of antibiotics on adult *Brugia*, doxycycline and tetracycline (tetracycline class of antibiotics) and rifampicin (macrocyclic antibiotic) were used in a time course experiment with male and female worms. Worms were treated with different concentrations of antibiotic and assessed over multiple time points. Female worms were treated with 100, 10 and 1 µM antibiotic, and male worms were treated with 100 and 1 µM antibiotic. DMSO (1%) was used as the negative control. Motility was recorded on Days 0, 1, 2, 3, 5 and 6, and worms were collected for qPCR analysis on Days 1, 3 and 6.

Two novel quinazoline compounds, CBR417 and CBR490 (provided by Calibr-Scripps Research Institute, San Diego, CA) [34], were tested with *B. pahangi* females at 100, 10 and 1 µM. Motility was recorded on Days 0–3, and worms were collected on Day 3 for qPCR analysis. All compounds were completely soluble at all concentrations.

Quantification of *wsp* and *gst* copy numbers from *B. pahangi* worms

Treated worms were washed in PBS, frozen in a dry ice/ethanol bath and stored at −80 °C. Genomic DNA from individual female worms was extracted using the Qiagen DNeasy Blood & Tissue Kit, and genomic DNA from four male worms was extracted using the QIAampDNA micro kit. The *Wolbachia* surface protein (*wsp*) and *Brugia pahangi* glutathione S-transferase (*gst*) primers [52] were used with the GeneCopoeia All-in-One SYBR Green qPCR mix and

run in a BioRad CRX Connect thermocycler. pCR4-TOPO plasmid standards containing *wsp* and *gst* genes were used to calculate gene copy numbers from Ct values. The following primer sequences were used: *gst*_fwd 5'-GAGACACCTTGCTCGCAAAC-3'; *gst*_rev 5'-ATCACGGACGCCTTCACAG-3'; *wsp*_fwd 5'-CCCTGCAAAGGCACAAGTTATTG-3'; *wsp*_rev 5'-CGAGCTCCAGCAAAGAGTTTAATTT-3'.

For amplification of *gst*, the reaction mix was heated at 95° C for 15 min, followed by 36 cycles of denaturation at 94 °C for 15 s, annealing at 55 °C for 30 s and elongation at 72 °C for 30 s. After the final cycle, melting curve analysis was conducted by heating the reaction mix at 95° C for 1 min, annealing at 55 °C for 30 s and then heating to 97 °C. For amplification of *wsp*, the reaction mix was heated to 95 °C for 15 min, followed by 40 cycles of denaturation at 94 °C for 10 s, annealing at 57 °C for 20 s and elongation at 72 °C for 15 s. After the final cycle, melting curve analysis was conducted by heating the reaction mix at 95 °C for 1 min, annealing at 55 °C for 30 s and then heating to 95 °C.

Quantification of *Wolbachia* in distal tip region of *B. pahangi* ovaries by immunofluorescence assay

To visually confirm the effects of antibiotics on *Wolbachia*, worms were stained with immunofluorescent dyes and examined by confocal microscopy. As with previous studies [34, 53], quantification was limited to the distal tip region of the ovaries, which has a more consistent distribution of *Wolbachia* in developing oocytes than the hypodermal chords, where *Wolbachia* are often dispersed as regional accumulations of bacteria [1, 53, 54]. Female worms treated with 10 µM doxycycline, minocycline, tetracycline and rifampicin were frozen in drug-free culture media at −80 °C on Day 6 for immunofluorescence staining. Worms were thawed and immediately fixed in 3.2% paraformaldehyde for 25 min and then rinsed with PBST (PBS with 0.1% Triton-X100). Ovaries were dissected from the worm bodies and stained with propidium iodide (1 mg/ml diluted 100X in PBST) for 30 s, then mounted with DAPI VECTASHIELD mounting medium (Vector Labs) and imaged using an

SP5 confocal microscope. *Wolbachia* titers were obtained by counting the number of puncta per μm^2 area.

Statistical analyses

Motility data were normalized to the mean motility of DMSO control worms. Motility data (percent inhibitions) were constrained to 0 and 100% inhibition [55], and IC_{50}s were calculated using GraphPad Prism software (Version 8.1.2). The statistical significance of reductions in motility in the time course experiment was determined using a two-way ANOVA followed by Tukey's multiple comparisons test.

Correlation coefficients (*r*) were determined using the CORREL function in Microsoft Excel for Mac 2011 (version 14.7.7). Correlation coefficients were determined for worm motility *vs* formazan production in the MTT assay, antibiotic concentration *vs wsp/gst* ratios of treated worms and worm motility *vs wsp/gst* ratios of treated worms.

Statistical significance of puncta per μm^2 in the distal tip region of worm ovaries was determined using the Kruskal-Wallis test followed by Dunn's multiple comparisons test with GraphPad Prism version 8.1.2.

To compare *Wolbachia* titers at different antibiotic concentrations in the time course experiment, *wsp/gst* ratios of treated worms were normalized to their respective DMSO controls. Statistical significance was determined using a two-way ANOVA followed by Tukey's multiple comparison test, with comparisons across antibiotic treatments within each time point and across time points within each antibiotic treatment. Percent differences in *Wolbachia* titers compared to DMSO controls were calculated based on the medians of the treatment groups and DMSO controls.

REFERENCES

1. Landmann F, Foster JM, Slatko B, Sullivan W. Asymmetric *Wolbachia* segregation during early *Brugia malayi* embryogenesis determines its distribution in adult host tissues. *PLoS Negl Trop Dis.* 2010; **4**:e758. doi: 10.1371/journal.pntd.0000758.

2. Taylor M, Hoerauf A. *Wolbachia* bacteria of filarial nematodes. *Parasitol Tod.* 1999; **15**:437–442. doi: 10.1016/S0169-4758(99)01533-1.

3. Hoerauf A, Volkmann L, Hamelmann C, Adjei O, Autenrieth IB, Fleischer B, et al. Endosymbiotic bacteria in worms as targets for a novel chemotherapy in filariasis. *Lancet.* 2000; **355**:1242–1243. doi: 10.1016/S0140-6736(00)02095-X.

4. Taylor MJ, Bandi C, Hoerauf A. *Wolbachia* bacterial endosymbionts of filarial nematodes. *Adv Parasitol.* 2005; **60**:245–284. doi: 10.1016/S0065-308X(05)60004-8.

5. Slatko BE, Taylor MJ, Foster JM. The *Wolbachia* endosymbiont as an anti-filarial nematode target. *Symbiosis.* 2010; **51**:55–65. doi: 10.1007/s13199-010-0067-1.

6. Tamarozzi F, Halliday A, Gentil K, Hoerauf A, Pearlman E, Taylor MJ. Onchocerciasis: the role of *Wolbachia* bacterial endosymbionts in parasite biology, disease pathogenesis, and treatment. *Clin Microbiol Rev.* 2011; **24**:459–468. doi: 10.1128/CMR.00057-10.

7. Bouchery T, Lefoulon E, Karadjian G, Nieguitsila A, Martin C. The symbiotic role of *Wolbachia* in Onchocercidae and its impact on filariasis. *Clin Microbiol Infect.* 2013; **19**:131–140. doi: 10.1111/1469-0691.12069.

8. Taylor MJ, Voronin D, Johnston KL, Ford L. *Wolbachia* filarial interactions. *Cell Microbiol.* 2013; **15**:520–526. doi: 10.1111/cmi.12084.

9. Tamarozzi F, Turner JD, Pionnier N, Midgley A, Guimaraes AF, Johnston KL, et al. *Wolbachia* endosymbionts induce neutrophil extracellular trap formation in human onchocerciasis. *Sci Rep.* 2016; **6**:1–13. doi: 10.1038/srep35559.

10. Centers for Disease Control and Prevention Progress toward elimination of Onchocerciasis in the Americas—1993–2012. *Morb Mortal Wkly.* 2013; **62**:405–408.

11. Richards F, Rizzo N, Espinoza CED, Monroy ZM, Valdez CGC, De Cabrera RM, et al. One hundred years after its discovery in Guatemala by Rodolfo Robles, *Onchocerca volvulus* transmission has been eliminated from the central endemic zone. *Am J Trop Med Hyg.* 2015; **93**:1295–1304. doi: 10.4269/ajtmh.15-0364.

12. Boussinesq M, Gardon J, Gardon-Wendel N, Chippaux J-P. Clinical picture, epidemiology and outcome of *Loa*-associated serious adverse events related to mass ivermectin treatment of onchocerciasis in Cameroon. *Filaria J.* 2003; **2**:1–13. doi: 10.1186/1475-2883-2-S1-S4.

13. Bockarie MJ, Taylor MJ, Gyapong JO. Current practices in the management of lymphatic filariasis. *Expert Rev Anti Infect Ther.* 2009; **7**:595–605. doi: 10.1586/eri.09.36.

14. McGarry HF, Pfarr K, Egerton G, Hoerauf A, Akue JP, Enyong P, et al. Evidence against *Wolbachia* symbiosis in *Loa loa*. *Filaria J.* 2003; **2**:9. doi: 10.1186/1475-2883-2-9.

15. Boussinesq M, Fobi G, Kuesel AC. Alternative treatment strategies to accelerate the elimination of onchocerciasis. *Int Heal.* 2018; **10**:i40–i48. doi: 10.1093/inthealth/ihx054.

16. Johnston KL, Ford L, Umareddy I, Townson S, Specht S, Pfarr K, et al. Repurposing of approved drugs from the human pharmacopoeia to target *Wolbachia* endosymbionts of onchocerciasis and lymphatic filariasis. *Int J Parasitol Drugs Drug Resist.* 2014; **4**:278–286. doi: 10.1016/j.ijpddr.2014.09.001.

17. Clare RH, Cook DAN, Johnston KL, Ford L, Ward SA, Taylor MJ. Development and validation of a high-throughput anti-*Wolbachia* whole-cell screen: A route to macrofilaricidal drugs against onchocerciasis and lymphatic filariasis. *J Biomol Screen.* 2015; **20**:64–69. doi: 10.1177/1087057114551518.

18. Bakowski MA, McNamara CW. Advances in anti-wolbachial drug discovery for treatment of parasitic filarial worm infections. *Trop Med Infect Dis.* 2019; **4**:108. doi: 10.3390/tropicalmed4030108.

19. Taylor MJ, Von Geldern TW, Ford L, Hubner MP, Marsh K, Johnston KL, et al. Preclinical development of an oral anti-*Wolbachia* macrolide drug for the treatment of lymphatic filariasis and onchocerciasis. *Sci Transl Med.* 2019; **11**:1–11. doi: 10.1126/scitranslmed.aau2086.

20. Taylor MJ, Makunde WH, McGarry HF, Turner JD, Mand S, Hoerauf A. Macrofilaricidal activity after doxycycline treatment of *Wuchereria bancrofti*: a double-blind, randomised placebo-controlled trial. *Lancet.* 2005; **365**:2116–2121. doi: 10.1016/S0140-6736(05)66591-9.

21. Debrah AY, Mand S, Specht S, Marfo-Debrekyei Y, Batsa L, Pfarr K, et al. Doxycycline reduces plasma VEGF-C/sVEGFR-3 and improves pathology in lymphatic filariasis. *PLoS Pathog.* 2006; **2**:e92. doi: 10.1371/journal.ppat.0020092.

22. Debrah AY, Mand S, Marfo-Debrekyei Y, Batsa L, Pfarr K, Buttner M, et al. Macrofilaricidal effect of 4 weeks of treatment with doxycycline on *Wuchereria bancrofti*. *Trop Med Int Heal.* 2007; **12**:1433–1441. doi: 10.1111/j.1365-3156.2007.01949.x.

23. Hoerauf A, Specht S, Buttner M, Pfarr K, Mand S, Fimmers R, et al. *Wolbachia* endobacteria depletion by doxycycline as antifilarial therapy has macrofilaricidal activity in onchocerciasis: a randomized placebo-controlled study. *Med Microbiol Immunol.* 2008; **197**:335. doi: 10.1007/s00430-007-0072-z.

24. Hoerauf A, Specht S, Marfo-Debrekyei Y, Buttner M, Debrah AY, Mand S, et al. Efficacy of 5-week doxycycline treatment on adult *Onchocerca volvulus*. *Parasitol Res.* 2009; **104**:437–447. doi: 10.1007/s00436-008-1217-8.

25. Walker M, Specht S, Churcher TS, Hoerauf A, Taylor MJ, Basanez MG. Therapeutic efficacy and macrofilaricidal activity of doxycycline for the treatment of river blindness. *Clin Infect Dis.* 2015; **60**:1199–1207. doi: 10.1093/cid/ciu1152.

26. Klarmann-Schulz U, Specht S, Debrah AY, Batsa L, Ayisi-Boateng NK, Osei-Mensah J, et al. Comparison of doxycycline, minocycline, doxycycline plus albendazole and

albendazole alone in their efficacy against onchocerciasis in a randomized, open-label, pilot trial. *PLoS Negl Trop Dis.* 2017; **11**:e0005156. doi: 10.1371/journal.pntd.0005156.

27. Pechère JC, Hughes D, Kardas P, Cornaglia G. Non-compliance with antibiotic therapy for acute community infections: a global survey. *Int J Antimicrob Agents.* 2007; **29**:245–253. doi: 10.1016/j.ijantimicag.2006.09.026.

28. Gualano MR, Gili R, Scaioli G, Bert F, Siliquini R. General population's knowledge and attitudes about antibiotics: a systematic review and meta-analysis. *Pharmacoepidemiol Drug Saf.* 2014; **24**:2–10. doi: 10.1002/pds.3716.

29. Taylor MJ, Hoerauf A, Townson S, Slatko BE, Ward SA. Anti-*Wolbachia* drug discovery and development: safe macrofilaricides for onchocerciasis and lymphatic filariasis. *Parasitology.* 2014; **141**:119–127. doi: 10.1017/S0031182013001108.

30. World Health Organization. Global Action Plan on Antimicrobial Resistance. 2015. http://www.who.int/iris/bitstream/10665/193736/1/9789241509763_eng.pdf?ua=1. Accessed 20 November 2020

31. Pfizer. Vibramycin Product Information. 2017. http://labeling.pfizer.com/ShowLabeling.aspx?id=611. Accessed 20 November 2020

32. Sharma R, Al JG, Tyrer HE, Gamble J, Hayward L, Guimaraes AF, et al. Minocycline as a re-purposed anti-*Wolbachia* macrofilaricide: superiority compared with doxycycline regimens in a murine infection model of human lymphatic filariasis. *Sci Rep.* 2016; **6**:1–11. doi: 10.1038/s41598-016-0001-8.

33. Aljayyoussi G, Tyrer HE, Ford L, Sjoberg H, Pionnier N, Waterhouse D, et al. Short-course, high-dose rifampicin achieves *Wolbachia* depletion predictive of curative outcomes in preclinical models of lymphatic filariasis and onchocerciasis. *Sci Rep.* 2017; **7**:1–12. doi: 10.1038/s41598-016-0028-x.

34. Bakowski MA, Shiroodi RK, Liu R, Olejniczak J, Yang B, Gagaring K, et al. Discovery of short-course anti-wolbachial quinazolines for elimination of filarial worm infections. *Sci Transl Med.* 2019; **11**:eaav3523. doi: 10.1126/scitranslmed.aav3523.

35. Hübner MP, Koschel M, Struever D, Nikolov V, Frohberger SJ, Ehrens A, et al. *In vivo* kinetics of *Wolbachia* depletion by ABBV-4083 in *L. sigmodontis* adult worms and microfilariae. *PLoS Negl Trop Dis.* 2019; **13**:1–19.

36. Hübner MP, Gunderson E, Vogel I, Bulman CA, Lim KC, Koschel M, et al. Short-course quinazoline drug treatments are effective in the *Litomosoides sigmodontis* and *Brugia pahangi* jird models. *Int J Parasitol Drugs Drug Resist.* 2020; **12**:18–27. doi: 10.1016/j.ijpddr.2019.12.001.

37. Hong WD, Benayoud F, Nixon GL, Ford L, Johnston KL, Clare RH, et al. AWZ1066S, a highly specific anti-*Wolbachia* drug candidate for a short-course treatment of filariasis. *Proc Natl Acad Sci.* 2019; **116**:1414–1419. doi: 10.1073/pnas.1816585116.

38. Gilbert J, Nfon CK, Makepeace BL, Njongmeta LM, Hastings IM, Pfarr KM, et al. Antibiotic chemotherapy of onchocerciasis: In a bovine model, killing of adult parasites

requires a sustained depletion of endosymbiotic bacteria (*Wolbachia* species) *J Infect Dis.* 2005; **192**:1483–1493. doi: 10.1086/462426.

39. Gunderson EL, Vogel I, Chappell L, Bulman CA, Lim KC, Luo M, et al. The endosymbiont *Wolbachia* rebounds following antibiotic treatment. *PLOS Pathog.* 2020; **16**:e1008623. doi: 10.1371/journal.ppat.1008623.

40. Eagle H. A paradoxical zone phenomenon in the bactericidal action of penicillin *in vitro*. *Am Assoc Adv Sci.* 1948; **107**:44–45.

41. Eagle H, Musselman AD. The rate of bactericidal action of penicillin *in vitro* as a function of its concentration, and its paradoxically reduced activity at high concentrations against certain organisms. *J Exp Med.* 1948; **88**:99–131. doi: 10.1084/jem.88.1.99.

42. Wu ML, Tan J, Dick T. Eagle effect in nonreplicating persister mycobacteria. *Antimicrob Agents Chemother.* 2015; **59**:7786–7789. doi: 10.1128/AAC.01476-15.

43. Prasetyoputri A, Jarrad AM, Cooper MA, Blaskovich MAT. The Eagle effect and antibiotic-induced persistence: two sides of the same coin? *Trends Microbiol.* 2019; **27**:339–354. doi: 10.1016/j.tim.2018.10.007.

44. Sigma-Aldrich. Doxycycline hyclate D9891 Product Information. https://www.sigmaaldrich.com/content/dam/sigma-aldrich/docs/Sigma/Product_Information_Sheet/d9891pis.pdf. Accessed 06 October 2020

45. Sigma-Aldrich. Minocycline hydrochloride M9511 Product Information. https://www.sigmaaldrich.com/content/dam/sigma-aldrich/docs/Sigma/Product_Information_Sheet/1/m9511pis.pdf. Accessed 06 October 2020

46. Sigma-Aldrich. Tetracycline T7660 Product Specification. https://api.sigmaaldrich.com/deepweb/assets/sigmaaldrich/quality/spec/177/393/T7660-BULK_____SIGMA____.pdf. Accessed 06 October 2020

47. Pubchem. Rifampicin Compound Summary. https://pubchem.ncbi.nlm.nih.gov/compound/135398735#section=Drug-Indication. Accessed 06 October 2020

48. Marcellino C, Gut J, Lim KC, Singh R, McKerrow J, Sakanari J. WormAssay: a novel computer application for whole-plate motion-based screening of macroscopic parasites. *PLoS Negl Trop Dis.* 2012; **6**:e1494. doi: 10.1371/journal.pntd.0001494.

49. Rao RU, Weil GJ. *In vitro* effects of antibiotics on *Brugia malayi* worm survival and reproduction. *J Parasitol.* 2002; **88**:605–611. doi: 10.1645/0022-3395(2002)088[0605:IVEOAO]2.0.CO;2.

50. Townson S, Tagboto S, McGarry HF, Egerton GL, Taylor MJ. *Onchocerca* parasites and *Wolbachia* endosymbionts: Evaluation of a spectrum of antibiotic types for activity against *Onchocerca gutturosa in vitro*. *Filaria J.* 2006; **5**:1–9. doi: 10.1186/1475-2883-5-4.

51. Cho-Ngwa F, Abongwa M, Ngemenya MN, Nyongbela KD. Selective activity of extracts of *Margaritaria discoidea* and *Homalium africanum* on *Onchocerca ochengi*. *BMC Complement Altern Med.* 2010; **10**:62. doi: 10.1186/1472-6882-10-62.

52. McGarry HF, Egerton GL, Taylor MJ. Population dynamics of *Wolbachia* bacterial endosymbionts in *Brugia malayi*. *Mol Biochem Parasitol.* 2004; **135**:57–67. doi: 10.1016/j.molbiopara.2004.01.006.

53. Serbus LR, Landmann F, Bray WM, White PM, Ruybal J, Lokey RS, et al. A cell-based screen reveals that the albendazole metabolite, albendazole sulfone, targets *Wolbachia*. *PLoS Pathog.* 2012; **8**:e1002922. doi: 10.1371/journal.ppat.1002922.

54. Foray V, Pérez-Jiménez MM, Fattouh N, Landmann F. *Wolbachia* control stem cell behavior and stimulate germline proliferation in filarial nematodes. *Dev Cell.* 2018; **45**:198–211. doi: 10.1016/j.devcel.2018.03.017.

55. Bulman CA, Bidlow CM, Lustigman S, Cho-Ngwa F, Williams D, Rascon AA, Jr, et al. Repurposing auranofin as a lead candidate for treatment of lymphatic filariasis and onchocerciasis. *PLoS Negl Trop Dis.* 2015; **9**:e0003534. doi: 10.1371/journal.pntd.0003534.

56. Agudelo M, Rodriguez CA, Zuluaga AF, Vesga O. Nontherapeutic equivalence of a generic product of imipenem-cilastatin is caused more by chemical instability of the active pharmaceutical ingredient (imipenem) than by its substandard amount of cilastatin. *PLoS ONE.* 2019; **14**:e0211096. doi: 10.1371/journal.pone.0211096.

57. Demarre G, Prudent V, Schenk H, Rousseau E, Bringer M-A, Barnich N, et al. The Crohn's disease-associated Escherichia coli strain LF82 relies on SOS and stringent responses to survive, multiply and tolerate antibiotics within macrophages. *PLoS Pathog.* 2019; **15**:e1008123. doi: 10.1371/journal.ppat.1008123.

58. Zakeri B, Wright GD. Chemical biology of tetracycline antibiotics. *Biochem Cell Biol.* 2008; **86**(2):124–136. doi: 10.1139/O08-002.

59. DrugBank. Tetracycline. https://www.drugbank.ca/drugs/DB00759. Accessed 07 January 2020

60. Ballard JW, Melvin RG. Tetracycline treatment influences mitochondrial metabolism and mtDNA density two generations after treatment in *Drosophila*. *Insect Mol Biol.* 2007; **16**:799–802. doi: 10.1111/j.1365-2583.2007.00760.x.

61. Bettany JT, Peet NM, Wolowacz RG, Skerry TM, Grabowski PS. Tetracyclines induce apoptosis in osteoclasts. *Bone.* 2000; **27**:75–80. doi: 10.1016/S8756-3282(00)00297-0.

62. Sapadin AN, Fleischmajer R. Tetracyclines: nonantibiotic properties and their clinical implications. *J Am Acad Dermatol.* 2006; **54**:258–265. doi: 10.1016/j.jaad.2005.10.004.

63. Castro MM, Tanus-Santos JE, Gerlach RF. Matrix metalloproteinases: targets for doxycycline to prevent the vascular alterations of hypertension. *Pharmacol Res.* 2011; **64**:567–572. doi: 10.1016/j.phrs.2011.04.002.

64. Choi YJ, Ghedin E, Berriman M, McQuillan J, Holroyd N, Mayhew GF, et al. A deep sequencing approach to comparatively analyze the transcriptome of lifecycle stages of the filarial worm *Brugia malayi*. *PLoS Negl Trop Dis.* 2011; **5**:e1409. doi: 10.1371/journal.pntd.0001409.

65. Kohanski MA, Dwyer DJ, Hayete B, Lawrence CA, Collins JJ. A common mechanism of cellular death induced by bactericidal antibiotics. *Cell.* 2007; **130**:797–810. doi: 10.1016/j.cell.2007.06.049.

66. Piccaro G, Pietraforte D, Giannoni F, Mustazzolu A, Fattorini L. Rifampin induces hydroxyl radical formation in *Mycobacterium tuberculosis*. *Antimicrob Agents Chemother.* 2014; **58**:7527–7533. doi: 10.1128/AAC.03169-14.

Chapter 4: The endosymbiont *Wolbachia* rebounds following antibiotic treatment

This chapter contains a reprint of the previously published work of which I was a coauthor (Gunderson et al., 2020). In this chapter, we expanded on research from the previous chapter to assess the effects of the antibiotic rifampicin on the filarial nematode *Brugia pahangi* in a mammalian model. Rifampicin was chosen due to its potent anti-*Wolbachia* effects, as seen in Chapter 3, Figure 3.5. To summarize, four different common antibiotics were assessed for their ability to reduce worm motility and *Wolbachia* titer in the female germline of *Brugia pahangi*. While tetracycline showed the greatest reduction of *Wolbachia* titer (95% reduction compared to controls), tetracycline is known to cause adverse side effects in humans. Therefore, we chose to pursue research on the second most potent antibiotic tested (95% reduction compared to controls), as results from this study would prove more applicable for human treatment of filarial disease. Rifampicin was chosen due to its potent anti-*Wolbachia* activity and its relatively safe administration for humans.

This study looked at the long-term effects of both *Wolbachia* levels and nematode survival and reproductive health following a short-course treatment of antibiotics in a nematode-infected mammalian model. Most *in vivo* experiments such as this end after 17 weeks post-treatment. This is mainly due to the high cost and resource demands of animal experiments. We wanted to analyze the effects on survival and reproduction of the parasite well past this 17-week time point. This study treated *Brugia pahangi*-infected Mongolian jirds with a twice daily dose of rifampicin for one week, then analyzed the parasitic nematode and its *Wolbachia* endosymbiont after 1-week, 6-week, 17-week, and 36-week time points.

My contributions to these experiments involved processing and imaging worms from each timepoint to assess for *Wolbachia* titer in the germline of the nematodes utilizing immunofluorescence and confocal microscopy. Because *Wolbachia* control proper embryogenesis within the female germline, it is crucial to understand the tissue-specific effects of anti-*Wolbachia* drugs. My work validated whole-worm qPCR results performed by

the Sakanari Lab, in addition to providing this tissue-specific analysis. I found that *Wolbachia* titers dropped drastically in the 1-week and 6-week timepoints, gradually increased in the 17-week time point, and rebounded to control levels in the 36-week timepoint.

During my data collection, I identified a new clustering morphology of *Wolbachia* seen in the ovaries of the filarial nematode. I analyzed different features of these clustering bacteria, including number, size, and bacterial density of these clusters for both rifampicin- and vehicle-treated worms at the 6-week, 17-week, and 36-week time points. (I did not discover the clustering morphology until analyzing worms from the 6-week time point, so unfortunately, we do not have cluster data from the 1-week time point.) I found no significant differences between rifampicin treatment and vehicle controls for any of the factors analyzed, at any time point, suggesting these clustering bacteria are unaffected by the antibiotic treatment. Because we see *Wolbachia* rebound eight months after antibiotic treatment, and because these clustering bacteria are resistant to the rifampicin treatment, we hypothesize that the source of bacterial rebound comes directly from these *Wolbachia* clusters. These clusters may serve as a protective niche for bacteria to evade antibiotics until the coast is clear and they can repopulate germline tissue. If this is the case, then this has incredibly significant implications in the efforts to identify anti-*Wolbachia* compounds as a means to address human filarial disease. Researchers who are a part of these efforts must consider the specific effects of any potential drug on these clusters to avoid bacterial rebound after antibiotic treatment.

The discovery of this new morphology would not have been possible without my work, underscoring the importance of utilizing microscopy analysis in assessing cellular processes and mechanisms in conjunction with other analyses like qPCR. My work and contributions to this project can be seen in Figure 4.4.

ABSTRACT

Antibiotic treatment has emerged as a promising strategy to sterilize and kill filarial nematodes due to their dependence on their endosymbiotic bacteria, *Wolbachia*. Several studies have shown that novel and FDA-approved antibiotics are efficacious at depleting the filarial nematodes of their endosymbiont, thus reducing female fecundity. However, it remains unclear if antibiotics can permanently deplete *Wolbachia* and cause sterility for the lifespan of the adult worms. Concerns about resistance arising from mass drug administration necessitate a careful exploration of potential *Wolbachia* recrudescence. In the present study, we investigated the long-term effects of the FDA-approved antibiotic, rifampicin, in the *Brugia pahangi* jird model of infection. Initially, rifampicin treatment depleted *Wolbachia* in adult worms and simultaneously impaired female worm fecundity. However, during an 8-month washout period, *Wolbachia* titers rebounded and embryogenesis returned to normal. Genome sequence analyses of *Wolbachia* revealed that despite the population bottleneck and recovery, no genetic changes occurred that could account for the rebound. Clusters of densely packed *Wolbachia* within the worm's ovarian tissues were observed by confocal microscopy and remained in worms treated with rifampicin, suggesting that they may serve as privileged sites that allow *Wolbachia* to persist in worms while treated with antibiotic. To our knowledge, these clusters have not been previously described and may be the source of the *Wolbachia* rebound.

INTRODUCTION

Onchocerciasis, commonly known as river blindness, and lymphatic filariasis (LF), commonly known as elephantiasis, are neglected tropical diseases caused by filarial worms that together affect an estimated 86 million people worldwide [1]. Approximately 1.2 million people are visually impaired due to river blindness, while 12 million people with LF have complications due to elephantiasis [1]. River blindness is caused by the release of thousands of microfilariae (mf) from adult *Onchocerca volvulus* females residing in subcutaneous tissues. Mf migrate through the skin causing severe itching and skin depigmentation and also migrate to the ocular region where they induce an inflammatory response that can lead to blindness [2]. LF is caused by *Wuchereria bancrofti*, *Brugia malayi* and *B*. *timori* worms that reside in the lymphatic tissues where they cause tissue damage. While many infections are asymptomatic, individuals that develop the disfiguring disease often experience pain and severe lymphedema typically in the arms, legs, breasts and genitalia [2]. This can result in stigma associated with elephantiasis and extreme economic loss for individuals suffering from this disease [3]. The years lived with disability (YLDs) for LF and onchocerciasis are estimated to be 1.4 million and 1.3 million, respectively [1].

Current treatments primarily target the mf and not the adult worms, which are capable of surviving in their human host for 10–14 years for *O*. *volvulus* and 6–8 years for *Brugia* spp. [2,4–9]. For this reason, international control programs require annual or biannual mass drug administration of drugs in order to reduce transmission rates. However, given the longevity and high fecundity of these worms and the current lack of drugs that kill the adult worms, it is unlikely that the WHO goal of eliminating LF and onchocerciasis by 2030 will be met when microfilaricidal drugs are used alone [10–15]. The inability to reduce transmission rates with microfilaricides is compounded by the fact that ivermectin (IVM) cannot be distributed in areas co-endemic for another filarial nematode, *Loa loa*, due to the risk of severe adverse events, especially toxic encephalopathy when individuals are co-infected with high loads of *L*. *loa* mf [16,17].

Onchocerca, *Wuchereria* and *Brugia* spp., like many other species of filarial nematodes, harbor an intracellular endosymbiont, *Wolbachia*, which is important for female worm fecundity and survival [18–22]. *Loa loa*, however, lacks this bacterium, and efforts are underway to develop anti-*Wolbachia* drugs to eliminate this bacterium, thereby resulting in death of adult worms. In clinical trials conducted on patients with onchocerciasis and lymphatic filariasis, doxycycline was shown to deplete *Wolbachia* and eventually eliminate the adult worms after about 1–2 years [23,24]. Doxycycline however requires lengthy dosing regimens (100–200 mg daily for 4–6 weeks) and is therefore not practical for mass drug distribution. In addition, doxycycline is contraindicated in children 8 years and younger and because it is in pregnancy category D, should not be given to pregnant women [2].

Several studies have recently shown that short courses of 7- and 14-days of anti-*Wolbachia* compounds hold promise as excellent drugs to treat onchocerciasis and LF [25–29]. Studies by Hübner et al. however, showed that suboptimal treatment regimens of doxycycline in the *Litomosoides sigmodontis* infection model did not lead to a sustained reduction in *Wolbachia* loads in worms 14–18 weeks post-treatment and that longer term studies were needed to assess permanent sterilization of female adult worms [27,29]. Although West African cattle infected with *Onchocerca ochengi* are excellent hosts for long-term studies to evaluate the efficacy of antibiotics for the treatment of human onchocerciasis [30–36], the purpose of our study was to investigate the long-term effects of rifampicin in a rodent model of infection. In the present study, we investigated the use of jirds infected with *Brugia pahangi* to assess the effects of rifampicin on *Wolbachia* and worm survival in an 8-month time course study in which *Wolbachia* titers were determined using adult worms recovered from animals treated with a one-week dosing regimen of rifampicin.

RESULTS

The endosymbiont *Wolbachia* rebound after 8 months following rifampicin treatment without genetic change

The research objective was to determine the long-term effects of antibiotic treatment on filarial worms and their endosymbiont, *Wolbachia*. We hypothesized that rifampicin would deplete worms of *Wolbachia* which would eventually lead to adult worm death in jirds infected with *Brugia pahangi*. *Wolbachia* titers in adult male and female worms were determined by qPCR at 1 week, 6 weeks, 17 weeks and 8 months post-first dose following the protocol by McGarry et al [37]. The relative abundance of single copy genes encoding the *Wolbachia* surface protein (*wsp*) were normalized to that of *Brugia* glutathione-S-transferase gene (*gst*) [28,29,38–40]. At the 1-week timepoint, *Wolbachia* titers were significantly reduced by 95.2% in female worms (Fig 4.1A). By 6 weeks however, the reduction in *Wolbachia* titers was reduced by 81.3% compared to those of control worms and by 17 weeks, titers were reduced by 77%. At 8 months, *Wolbachia* titers returned to levels similar to those of control worms, i.e. there was a 0% reduction in *Wolbachia* titers (Fig 4.1A). *Wolbachia* titers from male worms followed a similar trend of rebound (Fig 4.1B).

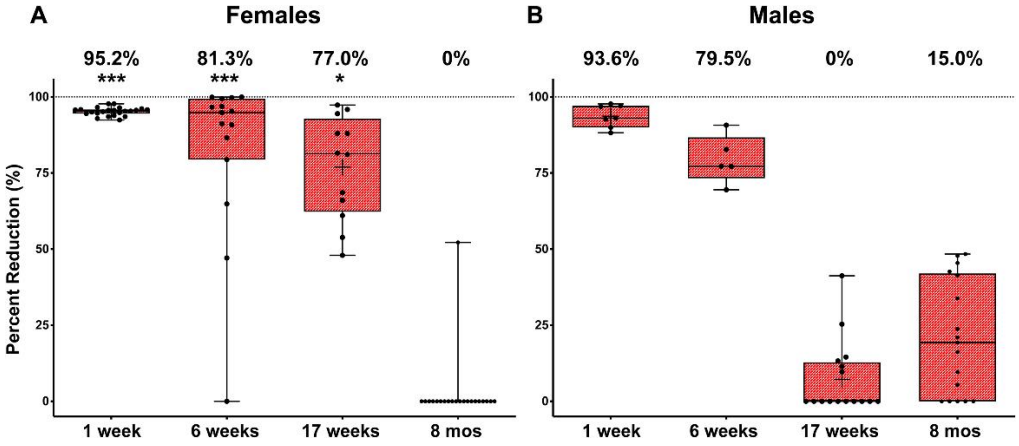

Fig 4.1 *Wolbachia* titers return to control levels 8 months after rifampicin treatment. Female and male *Brugia pahangi* from jirds treated with rifampicin were analyzed by qPCR to determine *Wolbachia* titers at each timepoint. Mean percent reductions of *Wolbachia wsp*/*gst* ratios from female (A) and male (B) adult worms are shown at 1-week, 6-weeks, 17-weeks and 8-months post-first dose. Data shown are medians and the boxes are the 25th and 75th percentiles with ***P<0.001 and *P<0.05. n = 2–9 jirds per treatment group per timepoint.

Although there was a significant effect of rifampicin on *Wolbachia* titers at early timepoints, rifampicin did not reduce the number of adult worms recovered at the time of necropsy at any of the timepoints, i.e. no macrofilaricidal effects were observed.

To determine if the rebound in *Wolbachia* occurred as a result of genome changes (e.g. antibiotic resistance/tolerance), we sequenced *Wolbachia* genomes using hybridization probe-capture method from the treatment and vehicle groups at the 1-week and 8-month timepoints [41]. On average ~90,000 PacBio CCS reads were generated per sample, which amounts to ~150× coverage of the genome. A complete circularized reference genome (1,072,983 bp) was assembled using the 1-week vehicle group and sequence variants were identified in each group with respect to the reference. Variants occurring within the genomic regions likely representing nuclear *Wolbachia* transfers (nuwts [42]) were excluded from the analysis.

One single nucleotide variant (SNV) and five insertion/deletion variants (INDEL) were identified and their allele frequencies were estimated based on the number of reads that support each allele in each sample. The SNV (C-to-T substitution) occurred within the ORF of a short-chain dehydrogenase/reductase family (SDR) oxidoreductase and was predicted to be a synonymous variant and therefore a silent mutation. The allele frequency of this variant increased from 5.1% in the 1-week vehicle group to 35.5% in the 8-month rifampicin group (Fisher's exact test P-value: 3.2×10^{-5}), which was the only variant whose allele frequency displayed a statistically significant change. The INDEL variants invariably occurred within homopolymer regions (9–13 consecutive bases of A or T). Homopolymeric tracts are mutational hotspots because they are vulnerable to slippage errors during replication and transcription [43]. However, INDEL calling is error-prone around homopolymer runs (due to sequencing and PCR errors), and we cannot exclude the possibility that these INDELs are false-positive variants [44]. These data suggest that, despite the population bottleneck and recovery, the genetic change in *Wolbachia* after rifampicin treatment likely did not occur.

Female worm fecundity is significantly reduced shortly after treatment but returns to control levels by 17 weeks

Commensurate with the depletion of *Wolbachia* 1 week after the first dose of rifampicin, we observed a significant impact on embryogenesis 6 weeks post-antibiotic treatment. This was followed by a gradual rebound in *Wolbachia* and return to normal embryogenesis by 17 weeks.

The fecundity of female *B. pahangi* at each timepoint was assessed by counting the number of mf released after worms were removed from the animals and incubated *in vitro* for 18 hours. Worms from rifampicin treated jirds at the 1- and 6-week timepoint showed a significant reduction in the number of mf that were shed compared to worms from the vehicle group (43.4% reduction, P<0.05 and 86.3% reduction, P<0.0001, respectively) (Fig 4.2). Female fecundity returned to control levels after 17 weeks and remained at control levels for up to 8 months.

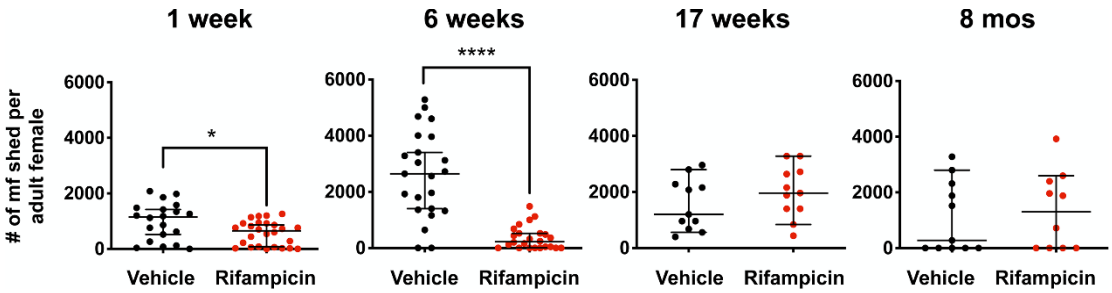

Fig 4.2 Rifampicin decreases mf shedding from female worms up to 6 weeks, followed by a return to normal by 17 weeks.
The number of mf shed overnight by adult female worms that were recovered 1 week, 6 weeks, 17 weeks and 8-months post-first dose is shown for each timepoint. Mf shed overnight at the 1- and 6-week timepoint were significantly reduced (*P<0.05 and ****P<0.0001, respectively). Data are shown as median ± 95% CI. n = 10–26 female worms from n = 2–9 jirds per treatment group per timepoint.

Embryograms of female worms were also analyzed to determine the effects of rifampicin on the developing stages of mf within the reproductive tract of female worms. Results showed that developmental stages from female worms recovered from rifampicin treated jirds at the 6-week timepoint exhibited a significant decrease in healthy embryos and an increase in degenerated embryos compared to those from both the control group at the 6-week timepoint, and the rifampicin group at the 1-week timepoint, where little disruption was observed (Fig 4.3). The decrease in fecundity and disruption of embryogenesis however were not observed at later timepoints suggesting that embryonic development of mf returned to control levels following the rebound of *Wolbachia*.

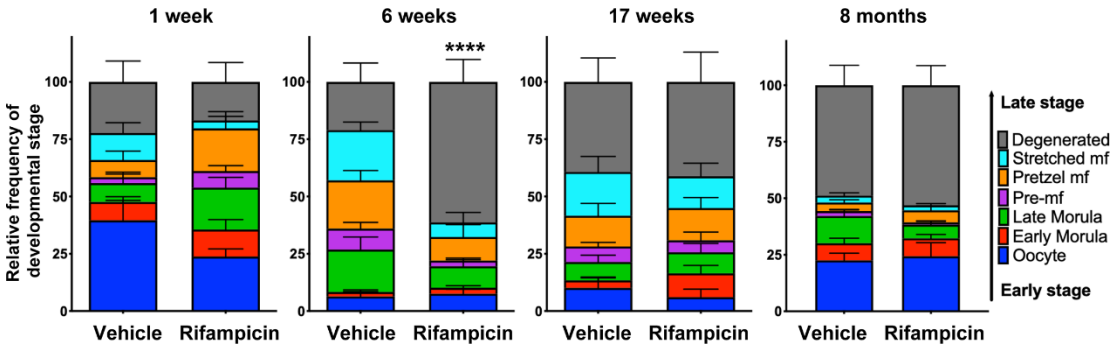

Fig 4.3 Rifampicin treatment leads to impaired embryogenesis by the 6-week timepoint but normal developmental stages return by 17 weeks.
Embryonic stages found within the ovaries and uteri from female worms from the vehicle and treated groups were counted 1 week, 6 weeks, 17 weeks and 8 months post-first dose. There was a significant decrease in the frequency of healthy embryos across all developmental stages of embryogenesis at the 6-week timepoint (****P<0.0001). Percentages of degenerated embryos (gray) were also determined for each timepoint. Data are presented as mean ± SEM. n = 6–9 female worms from n = 2–9 jirds per treatment group per timepoint.

Cellular analysis reveals the rebound is derived from clusters of *Wolbachia*

As an independent method of analyzing *Wolbachia* titer, we performed fluorescence confocal analysis to image *Wolbachia* and host cell nuclei as previously described by Landmann et al., Serbus et al. and Foray et al. [45–49].

Fluorescence imaging of the distal tip region of the ovaries revealed that *Wolbachia* were nearly depleted from germline tissues at the 1-week timepoint, but they began to increase in number at later timepoints (Fig 4.4A). Interestingly, large densely packed "clusters" of *Wolbachia* (Fig 4.4B) were observed in worms recovered from both the vehicle and treated groups at each timepoint. When *Wolbachia* were quantified in each of the clusters from ovaries (Fig 4.4C), results showed there were no significant differences between the treated and control groups with respect to the *Wolbachia* density (puncta per area of cluster, Fig 4.4D). However, *Wolbachia* in the peripheral areas around the clusters were significantly reduced ($P = 0.05$) in the worms from the rifampicin group at 6-weeks but not at the later timepoints (Fig 4.4D).

The presence of clusters with densely packed *Wolbachia* in ovaries from both rifampicin treated and control worms suggests that despite clearance of bacteria from the areas outside the clusters, the *Wolbachia* nevertheless persisted within the clusters and may be the source of the rebound. Analyses were not conducted on male worms as the focus of the work was on female fecundity and embryogenesis. We postulate that similar clusters will be associated with male worms, possibly in the hypodermal areas and, as with females, are likely responsible for the rebound.

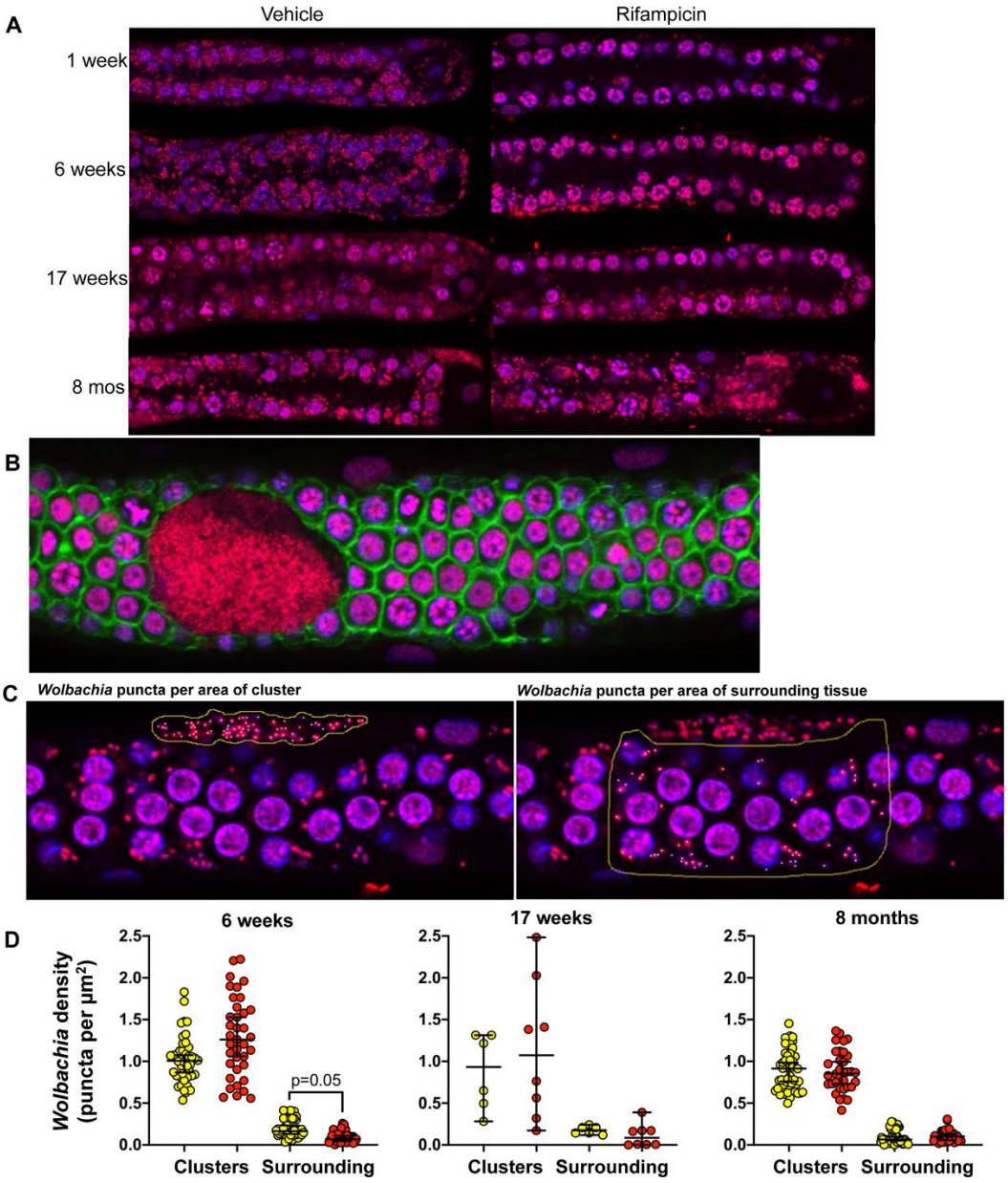

Fig 4.4 Rebound of *Wolbachia* at later timepoints may be driven by clusters. Ovaries were removed from individual female worms, fixed and stained for host nuclei (magenta) and *Wolbachia* (red). (A) *Wolbachia* are depleted at 1- and 6-weeks post-treatment but begin to rebound by 17 weeks. (B) Clusters of *Wolbachia* are seen in ovaries from vehicle and rifampicin worms; actin (green) stained with phalloidin; *Wolbachia* (red) stained with propidium iodide and host nuclei (magenta) stained with DAPI. (C) *Wolbachia* were quantified by counting number of puncta within the clusters (left) and in the periphery of the clusters (right). (D) Clusters were analyzed from worms collected at 6 weeks (n = 36–46), 17 weeks (n = 6–8) and 8 months (n = 34–52). Vehicle control worms in yellow and worms from rifampicin treated groups in red. Peripheral *Wolbachia* were reduced in females recovered from rifampicin treated jirds at the 6-week timepoint only (P = 0.05). Data are presented as median ± 95% CI.

DISCUSSION

Major efforts to identify new drugs to treat the adult stage (macrofilariae) of *Onchocerca volvulus* have led to the discovery of novel anti-*Wolbachia* compounds. These studies demonstrated that their respective anti-*Wolbachia* compounds significantly reduced *Wolbachia* titers in worms from animals treated with short courses of quinazolines and Tylosin analogs after 16–18 weeks post-first dose [26,27,29,40,50]. In addition, a one-week combination treatment of rifampicin and albendazole resulted in a greater than 99% reduction in *Wolbachia* levels in *B*. *malayi* infected SCID mice [28]. Clinical trials further revealed that albendazole either alone or in combination with antibiotics dramatically reduced *Wolbachia* levels [51,52]. With the recent discoveries of new anti-wolbachial drugs, we explored the *Wolbachia*/worm relationship *in vivo* to better understand the outcomes of antibiotic exposure. The aim of this study was to determine the longer-term effects of rifampicin on female worm survival and fecundity and *Wolbachia* titers using the *Brugia pahangi* infected jird model.

Although macrofilaricidal effects were not observed following treatment with rifampicin, *Wolbachia* titers and female fecundity were significantly affected 1 week post-first dose. *Wolbachia* titers were reduced by >95% in female worms from rifampicin treated animals at the 1-week timepoint compared to those of worms from vehicle animals. The extensive reduction of *Wolbachia* titers in adult worms has been previously described in other rodent studies with filarial worms, but the studies were terminated 16–18 weeks post-treatment [26,27,29,40,50], and the long-term effects of antibiotic treatment on filarial worms and their *Wolbachia* were not evaluated in these models.

Our present long-term study showed that even though *Wolbachia* were almost completely eliminated at early timepoints, *Wolbachia* rebounded to levels similar to those of control worms 8 months after rifampicin dosing. Female worms recovered from this timepoint were also fully reproductive, similar to female worms from the control group. Thus, despite qPCR data that showed a >95% reduction in *Wolbachia* titers, *Wolbachia* rebounded and

returned to levels comparable to those of control worms, suggesting that this level of elimination is not sufficient to ensure permanent elimination and permanent female sterility. This finding parallels the rebound of *Wolbachia* titers in *O*. *ochengi* from cattle treated with a short, intensive regimen of oxytetracycline (10 mg/kg QD for 14 days) reported by Gilbert et al. [32], and suggests that this jird model is a suitable alternative for long-term studies (up to 8 months) in situations where cattle models cannot be conducted.

The dosage of rifampicin used in the present study was not likely suboptimal since previous studies with *B*. *malayi* infected SCID mice showed that 25 mg/kg rifampicin twice a day for 7 days resulted in reductions in *Wolbachia* comparable to the clinical dosage of doxycycline that caused >90% *Wolbachia* depletion [25]. While we saw the expected reduction in *Wolbachia* at early timepoints, the reduction was not sustained, and *Wolbachia* rebounded. Comparison of the genetic profiles of *Wolbachia* genomes from the early and late timepoints revealed that despite the population bottleneck and recovery, no genetic changes occurred in *Wolbachia* that could account for the rebound.

The significance of the rebound in this bacteria/worm symbiosis was evident when low titers of *Wolbachia*, which initially led to the reduction of late-stage embryos and microfilariae at 1- and 6- weeks, was later followed by the return of developing embryos and microfilariae released by female worms. This recovery back to control levels was commensurate with *Wolbachia* rebound, in line with evidence showing the dependence of female worms on *Wolbachia* to maintain their reproductive output [21,32,49,53–55].

Direct visualization of worm ovaries using fluorescence confocal microscopy revealed two distinct populations of *Wolbachia*: “clusters” of *Wolbachia* that were found within the female ovaries and “peripheral” *Wolbachia* that were found surrounding the clusters. For the *Wolbachia* within clusters, we found no significant differences in bacterial cluster amount, size, or density between rifampicin and control treatments, suggesting that these clusters do not respond to antibiotics, at least at the dosages used in this study. In contrast, we found that rifampicin significantly reduced the peripheral *Wolbachia* surrounding the clusters at 6

weeks. To our knowledge, these clusters have never before been identified in any *Wolbachia*-nematode system, and we believe that the clusters could serve as a reservoir of bacteria that can repopulate the germline tissue after antibiotic treatment.

Since genome sequencing of the rebounded *Wolbachia* showed there were no gene changes that could account for the persistence, we postulate that the clusters are privileged sites in which *Wolbachia* persist in a low or inactive metabolic state, similar to what occurs with intracellular *Toxoplasma gondii* bradyzoites [56,57] and pathogenic intracellular bacteria including *Mycobacterium tuberculosis*, *Treponema pallidum*, *Chlamydia* spp. and *Salmonella enterica* which can cause persistent and latent infections [58–66]. Interestingly, bacterial toxin-antitoxin (TA) genes of the *RelEB* family thought to cause persister cell formation in insect-associated *Wolbachia*, were absent in *Wolbachia* from filarial nematodes, suggesting that TAs may not be involved in persister formation of *Wolbachia* within the clusters and that other mechanisms are likely at play [67–70].

Although the molecular mechanisms of persister formation is not known in the *Wolbachia*-worm relationship, *Wolbachia* may respond in some manner to their low numbers and repopulate the ovarian tissues by moving from the clusters to the peripheral areas within the ovaries or by migrating into the worm's pseudocoelom [46,71] and back into the ovaries, thereby ensuring their vertical transmission for future generations of microfilariae.

Further studies to define the nature of these clusters and wolbachial persistence will yield new information on the cell biology of this bacteria-worm symbiosis and may reveal similar strategies used by various pathogens that allow them to persist and remain latent within their hosts.

We describe the effects of rifampicin treatment on the *Wolbachia-Brugia pahangi* relationship over an 8-month period in a rodent model. *Wolbachia* numbers were significantly reduced after initial treatment but subsequently rebounded along with a corresponding return of embryogenesis and fecundity in female worms. This *in vivo B*. *pahangi*/jird model serves as a useful tool to evaluate the long-term effects of antibiotics on *Wolbachia* depletion and

female worm fecundity and provides information that may impact the clinical use of antibiotics to treat filarial diseases.

This study also provides insight into the *Wolbachia*-worm relationship with the discovery of two different populations of *Wolbachia* within the ovaries of these filarial worms: clusters of *Wolbachia* and peripheral *Wolbachia*, the former of which may account for the rebound of *Wolbachia* following antibiotic treatment. To our knowledge, clusters of *Wolbachia* have never before been identified in any *Wolbachia*-nematode system and may represent sequestered populations of this endosymbiont within *Brugia pahangi* ovaries.

MATERIALS AND METHODS

Ethics statement

All animal studies were performed under the University of California, San Francisco Institutional Animal Care and Use Committee (IACUC) approvals AN109629-03 and AN173847-02 and adhered to the guidelines set forth in the NIH Guide for the Care and Use of Laboratory Animals and the USDA Animal Care Policies.

Animal infections

For dosing studies on adult worms, male Mongolian jirds 50–60 grams, 5–7 weeks in age (*Meriones unguiculatus*, Charles River Laboratories International, Inc., Wilmington, MA) were injected intraperitoneally (IP) with third-larval stage *Brugia pahangi* (University of Missouri-Columbia) and treated 3 months later when larvae developed into adult worms.

Drug dosages

Rifampicin (Research Products International Corp., Prospect, IL) was dissolved in 55% polyethylene glycol 400 (Sigma), 25% propylene glycol (Sigma), 20% water at a concentration of 5 mg/mL, and animals were given oral doses of 25 mg/kg twice a day for 7 days. We selected the dosage 25 mg/kg BID for 7 days based on findings from Aljayyoussi et

al, 2017 which reported rifampicin dosages of 15 mg/kg QD for 7 days, 35 mg/kg QD for 7 days, or 25 mg/kg BID for 7 days resulted in reductions in *Wolbachia* of 97.7%, 98.2% and 99.5%, respectively [25]. They found 25 mg/kg BID x 7 days to be superior to doxycycline 25 mg/kg BID treatment for four weeks (P>0.0001) and not significantly inferior from doxycycline 25 mg/kg BID treatment for six weeks [25].

PK analyses

To determine the level of exposure of rifampicin in treated animals, blood was collected from the saphenous vein in Am-heparinized tubes and centrifuged at 2,000 x g for 15 min at 4°C. Blood was collected 0.5 hour, 1 hour, 3 hours and 6 hours post-first dose. The second dose was given 8 hours post-first dose and blood was collected 24 hours post-first dose. Plasma was collected and stored at -80°C prior to shipment to Integrated Analytical Solutions (Berkeley, CA) for plasma analysis. Calibration standards, QC samples and study samples were processed for LC/MS/MS analysis by precipitating 10 µL of each sample with 3 volumes of ice cold Internal Standard Solution (acetonitrile containing 50 ng/mL dextromethorphan). The precipitated samples were centrifuged at 6100g for 30 min and an aliquot of each supernatant was transferred to an auto sampler plate and diluted in water with 2 volumes of 0.2% formic acid.

Necropsies

Vehicle and rifampicin treated jirds were necropsied 1 week, 6 weeks, 17 weeks and 8 months post-first dose. Animals were dissected and peritoneal cavities were washed with 100 mL of PBS to collect adult worms and mf that had been released from female worms. Adult worms were separated by sex, counted and processed for subsequent analyses. Mf from the peritoneal cavity were quantified by mixing peritoneal wash 9:1 (v/v) with 0.04% methylene blue:water and counted using an inverted microscope. Data from each timepoint are from three replicate studies, except for the 17-week timepoint, in which the data are from one set.

All animals were euthanized at their intended timepoints and no adverse events were observed. However, one animal had ascites, but was otherwise healthy at the 8-month timepoint.

qPCR analysis of *Wolbachia* in adult *Brugia pahangi*

Adult worms collected during necropsies were snap-frozen in a dry-ice and ethanol bath prior to storage at -80° C. gDNA was extracted from individual female worms or from 4–25 male worms using a DNEasy Blood & Tissue Kit (QIAGEN) according to the manufacturer's instructions. Genomic DNA was quantified using a NanoDrop One^{c} (Thermo Fisher Scientific) and qPCR was performed using a Geneoecopia 2x All-in-One Master Mix (Cat #QP001-01) in a Bio-Rad CFX Connect RT-PCR thermocycler. The single copy gene, *Wolbachia* surface protein (*wsp*), was used to quantify *Wolbachia* titers and the single copy gene, glutathione-S-transferase (*gst*), was used to quantify *Brugia* titers following the protocol of McGarry et al. [37]. Primers used for qPCR were based on *wsp* forward: 5'-CCCTGCAAAGGCACAAGTTATTG-3'; *wsp* reverse: 5'-CGAGCTCCAGCAAAGAGTTTAATTT-3'; *gst* foward: 5'-GAGACACCTTGCTCGCAAAC-3'; *gst* reverse: 5'-ATCACGGACGCCTTCACAG-3'. For *gst* amplification the following cycles were used: 95°C for 15 minutes, followed by 36 cycles of denaturation at 94°C for 15 seconds, annealing at 55° C for 30 seconds and elongation at 72° C for 30 seconds. Melting curve analysis was conducted by heating to 95°C for 1 minute, annealing at 55°C for 30 seconds and heating to 97°C. For *wsp* amplification: samples were heated at 95° C for 15 minutes, followed by 40 cycles of denaturation at 94°C for 10 seconds, annealing at 55°C for 20 seconds and elongation at 72°C for 15 seconds. Melting curve analysis was conducted by heating to 95°C for 1 minute, annealing at 55°C for 30 seconds and heating to 97°C.

Wolbachia genome sequencing

Total genomic DNA was extracted from *Brugia pahangi* worms recovered from 1-week and 8-month timepoints using DNeasy Blood & Tissue Kit (QIAGEN) following the manufacturer's protocol and quantified using Qubit (Invitrogen). Genomic DNA was subjected to hybridization probe-capture (adaptation of the protocol of Geniez et al. and protocol of Lefoulon et al.) to enrich for *Wolbachia* DNA using biotinylated probe-baits and magnetic streptavidin beads [41,72]. Prior to capture, genomic DNA was sheared using NEBNext FSII for 30 min at 37° and ligated to NimbleGen SeqCap adapters (NEBNext Ultra II kit), followed by AMPure bead purification (0.9X), PCR amplification and purification through AMPure beads (0.9X). The barcoded samples were then pooled (~400 ng per sample) and hybridization of DNA with *Wolbachia* specific EZ library probes was performed according to SeqCap EZ HyperCap protocol v1.0 (NimbleGen). The captured DNA library was amplified by PCR, purified using AMPure bead (0.9X), and subjected to PacBio circular consensus sequencing (CCS). A reference *w*Bp genome was assembled with Canu v1.9 [73] from the control sample (1-week vehicle group) after the CCS reads were trimmed to remove residual adapter sequences using seqtk. To minimize assembly errors due to the presence of *B*. *pahangi* sequences derived from nuclear *Wolbachia* transfers (nuwts), a draft assembly was first generated using all available reads, and then reads (longer than 3 kb) that mapped to the assembly without clipping were collected using minimap v2.17 [74] and assembled to produce a second draft assembly, which was then circularized using Circlator [75]. Assembly errors were further corrected through manual curation and Pilon v1.23 [76]. Genome annotation was performed using PGAP [77] and DFAST v1.2.4 [78]. Genetic variants (SNPs and indels) were called across samples by DeepVariant [79] after non-clipped CCS reads were aligned to the *w*Bp reference genome using minimap2. The depth-of-coverage patterns of clipped reads (that span the junctions between nuwts and *B*. *pahangi* DNA) along the *Wolbachia* genome were exploited to infer the location of regions that show sequence similarity to nuwts using samtools [80] and sequana_coverage v0.7.1 [81]. Using VCFtools v0.1.17 [82], false-positive

variants occurring within these putative nuwts regions were filtered and excluded from further analyses. Finally, SnpEff v4.3 [83] was used to annotate and predict the effects of the remaining variants. The statistical significance of allele frequency differences was determined with Fisher's exact test.

Embryograms and microfilariae overnight shed

Individual adult female worms (n = 12–24 females per treatment group) from vehicle and rifampicin treated jirds were maintained overnight in 24-well plates with 500 μL of RPMI-1640, 25mM HEPES, 5% heat inactivated-FBS, and 1x Antibiotic/Antimycotic. Mf that were released from individual females after 18 hours were removed from the wells and counted. For the embryogram analyses, individual adult female worms previously frozen in 0.5mL of 0.1% PBS-Triton X-100 (Sigma) were homogenized using a glass pestle to disrupt the cuticle and expose the reproductive structures. Developing stages from the ovaries and uteri (oocyte, early morula, late morula, pre-mf, pretzel mf and stretched mf, degenerated embryos) were assessed in a blinded fashion for their developmental stages using an inverted microscope and hemocytometer. A minimum of 100 developmental stages were counted from each female and relative proportions were used to determine the means and standard deviations. n = 6–9 females per treatment group per timepoint [45].

Fluorescence imaging of female worm ovaries

Female *B. pahangi* worms removed from jirds from each group were frozen and shipped to UC Santa Cruz for fluorescence analysis. Frozen worms were thawed at room temperature, immediately fixed in 3.2% paraformaldehyde for 25 minutes and rinsed twice in PBST (PBS plus 0.1% Triton-X100). Individual female uteri/ovaries were dissected from fixed tissue and incubated overnight in RNAse A (10mg/mL) in PBST following similar protocols described by Landmann et al., Serbus et al. and Foray et al. [45–49]. Tissues were then stained with propidium iodide (PI) (1mg/mL diluted 100X in PBST) for 30 seconds, rinsed twice in PBST

and then mounted in DAPI Vectashield mounting medium (Vector Labs). The distal tips of the ovarian tissue were imaged on a Leica SP5 confocal microscope and single images were taken at the mid-plane of the ovarian tissue for each distal tip. To measure the average *Wolbachia* titer of each distal tip, *Wolbachia* puncta were counted by hand using the Cell Counter tool in FIJI; the number of puncta was divided by the area of the tissue in each image (puncta/μm^2).

Statistical analyses

Data were first tested for normality using the Shapiro-Wilk test of normality. When data did not pass the normality test, a Mann-Whitney U test was conducted and when data did pass the normality test, a Student's t-test was used. All significance levels were determined as compared to the vehicle worms at the same timepoint. Individual percent reductions of *Wolbachia* were calculated for each worm using the *wsp* copy number normalized to the *Brugia gst* copy number [28,29,38–40]. *Wsp/gst* ratios were calculated for each timepoint by subtracting the *wsp/gst* ratios of treated worms from the mean *wsp/gst* ratio of vehicle worms and then dividing by the mean *wsp/gst* ratio of vehicle worms for each respective timepoint. The means were then calculated to determine the average percent reduction. All statistical analyses were determined using Prism 8 version 8.2.0 (272).

REFERENCES

1. James SL, Abate D, Abate KH, Abay SM, Abbafati C, Abbasi N, et al. *Global, regional, and national incidence, prevalence, and years lived with disability for 354 Diseases and Injuries for 195 countries and territories, 1990–2017: A systematic analysis for the Global Burden of Disease Study 2017*. Lancet. 2018; 1789–1858. pmid:30496104

2. Taylor MJ, Hoerauf A, Bockarie M. *Lymphatic filariasis and onchocerciasis*. Lancet. 2010;376: 1175–1185. pmid:20739055

3. Abdulmalik J, Nwefoh E, Obindo J, Dakwak S, Ayobola M, Umaru J, et al. *Emotional difficulties and experiences of stigma among persons with lymphatic filariasis in Plateau state, Nigeria.* Health Hum Rights. 2018;20: 27–40. pmid:30008550

4. Molyneux DH, Bradley M, Hoerauf A, Kyelem D, Taylor MJ. *Mass drug treatment for lymphatic filariasis and onchocerciasis.* Trends Parasitol. 2003;19: 516–522. pmid:14580963

5. Ottesen EA, Hooper PJ, Bradley M, Biswas G. *The global programme to eliminate lymphatic filariasis: Health impact after 8 years*. PLoS Negl Trop Dis. 2008;2. pmid:18841205

6. World Health Organization. *Global Programme to Eliminate Lymphatic Filariasis: Progress Report 2000–2009 and Strategic Plan 2010–2020*. 2010.

7. Chu BK, Hooper PJ, Bradley MH, McFarland DA, Ottesen EA. *The economic benefits resulting from the first 8 years of the Global Programme to eliminate Lymphatic Filariasis (2000–2007)*. PLoS Negl Trop Dis. 2010;4. pmid:20532228

8. Hoerauf A, Pfarr K, Mand S, Debrah AY, Specht S. *Filariasis in Africa-treatment challenges and prospects*. Clin Microbiol Infect. 2011;17: 977–985. pmid:21722251

9. Molyneux DH, Taylor MJ. *Current status and future prospects of the global lymphatic filariasis programme*. Curr Opin Infect Dis. 2001;14: 155–159. pmid:11979126

10. Molyneux DH, Hopkins A, Bradley MH, Kelly-Hope LA. *Multidimensional complexities of filariasis control in an era of large-scale mass drug administration programmes: a can of worms*. Parasit Vectors. 2014;7: 363. pmid:25128408

11. Turner HC, Walker M, Churcher TS, Osei-Atweneboana MY, Biritwum NK, Hopkins A, et al. *Reaching the London declaration on neglected tropical diseases goals for onchocerciasis: An economic evaluation of increasing the frequency of ivermectin treatment in Africa*. Clin Infect Dis. 2014;59: 923–932. pmid:24944228

12. Kim YE, Remme JHF, Steinmann P, Stolk WA, Roungou JB, Tediosi F. *Control, Elimination, and Eradication of River Blindness: Scenarios, Timelines, and Ivermectin Treatment Needs in Africa*. PLoS Negl Trop Dis. 2015;9: 1–19. pmid:25860569

13. Basáñez MG, Walker M, Hamley JI, Milton P, Fronterre C, de Vlas SJ, et al. *The World Health Organization 2030 goals for onchocerciasis: Insights and perspectives from mathematical modelling*. Gates Open Res. 2019;3. pmid:31723729

14. Davis EL, Vlas SJ de, Fronterre C, Hollingsworth TD, Kontoroupis P, Michael E, et al. *The roadmap towards elimination of lymphatic filariasis by 2030: insights from quantitative and mathematical modelling*. Gates Open Res. 2019;3. pmid:31728440

15. World Health Organization. WHO launches global consultations for a new roadmap on neglected tropical diseases. 2019.

16. Gardon J, Gardon-Wendel N, Demanga-Ngangue , Kamgno J, Chippaux JP, Boussinesq M. *Serious reactions after mass treatment of onchocerciasis with ivermectin in an area endemic for Loa loa infection*. Lancet. 1997;350: 18–22. pmid:9217715

17. Boussinesq M, Gardon J, Gardon-Wendel N, Chippaux J-P. *Clinical picture, epidemiology and outcome of Loa-associated serious adverse events related to mass ivermectin treatment of onchocerciasis in Cameroon*. Filaria J. 2003;2 Suppl 1: S4. pmid:14975061

18. Bandi C, Anderson TJ, Genchi C, Blaxter ML. *Phylogeny of Wolbachia in filarial nematodes*. Proc R Soc London Biol Sci. 1998;265: 2407–2413. pmid:9921679

19. Slatko BE, Taylor MJ, Foster JM. *The Wolbachia endosymbiont as an anti-filarial nematode target*. Symbiosis. 2010;51: 55–65. pmid:20730111

20. Slatko BE, Luck AN, Dobson SL, Foster JM. *Wolbachia endosymbionts and human disease control*. Mol Biochem Parasitol. 2014;195: 88–95. pmid:25046729

21. Hoerauf A, Volkmann L, Hamelmann C, Adjei O, Autenrieth IB, Fleischer B, et al. *Endosymbiotic bacteria in worms as targets for a novel chemotherapy in filariasis*. Lancet. 2000;355: 1242–1243. pmid:10770311

22. Taylor MJ, Hoerauf A, Townson S, Slatko BE, Ward SA. *Anti-Wolbachia drug discovery and development: safe macrofilaricides for onchocerciasis and lymphatic filariasis*. Parasitology. 2014;141: 119–127. pmid:23866958

23. Taylor MJ, Makunde WH, McGarry HF, Turner JD, Mand S, Hoerauf A. *Macrofilaricidal activity after doxycycline treatment of Wuchereria bancrofti: a double-blind, randomised placebo-controlled trial*. Lancet. 2005;365: 2116–2121. pmid:15964448

24. Debrah AY, Specht S, Klarmann-schulz U, Batsa L, Mand S, Marfo-Debrekyei Y, et al. *Doxycycline Leads to Sterility and Enhanced Killing of Female Onchocerca volvulus Worms in an Area With Persistent Microfilaridermia After Repeated Ivermectin Treatment: A Randomized, Placebo-Controlled, Double-Blind Trial*. Clin Infect Dis. 2015;61: 517–526. pmid:25948064

25. Aljayyoussi G, Tyrer HE, Ford L, Sjoberg H, Pionnier N, Waterhouse D, et al. *Short-course, high-dose rifampicin achieves Wolbachia depletion predictive of curative outcomes in preclinical models of lymphatic filariasis and onchocerciasis*. Sci Rep. 2017;7: 1–12.

26. Bakowski MA, Shiroodi RK, Liu R, Olejniczak J, Yang B, Gagaring K, et al. *Discovery of short-course antiwolbachial quinazolines for elimination of filarial worm infections*. Sci Transl Med. 2019;11. pmid:31068442

27. Hübner MP, Koschel M, Struever D, Nikolov V, Frohberger SJ, Ehrens A, et al. *In vivo kinetics of Wolbachia depletion by ABBV-4083 in L. sigmodontis adult worms and microfilariae*. PLoS Negl Trop Dis. 2019;13: 1–19. pmid:31381563

28. Turner JD, Sharma R, Al Jayoussi G, Tyrer HE, Gamble J, Hayward L, et al. *Albendazole and antibiotics synergize to deliver short-course anti-Wolbachia curative treatments in preclinical models of filariasis*. Proc Natl Acad Sci. 2017;114: E9712–E9721. pmid:29078351

29. Hübner MP, Gunderson E, Vogel I, Bulman CA, Lim KC, Koschel M, et al. *Short-course quinazoline drug treatments are effective in the Litomosoides sigmodontis and Brugia pahangi jird models*. Int J Parasitol Drugs Drug Resist. 2020;12: 18–27. pmid:31869759

30. Langworthy NG, Renz A, Mackenstedt U, Henkle-Dührsen K, De C Bronsvoort MB, Tanya VN, et al. *Macrofilaricidal activity of tetracycline against the filarial nematode Onchocerca ochengi: Elimination of Wolbachia precedes worm death and suggests a dependent relationship.* Proc R Soc B Biol Sci. 2000;267: 1063–1069. pmid:10885510

31. Trees AJ, Graham SP, Renz A, Bianco AE, Tanya V. *Onchocerca ochengi infections in cattle as a model for human onchocerciasis: Recent developments*. Parasitology. 2000;120: 133–142. pmid:10874716

32. Gilbert J, Nfon CK, Makepeace BL, Njongmeta LM, Hastings IM, Pfarr KM, et al. *Antibiotic Chemotherapy of Onchocerciasis: In a Bovine Model, Killing of Adult Parasites Requires a Sustained Depletion of Endosymbiotic Bacteria (Wolbachia Species)*. J Infect Dis. 2005;192: 1483–1493. pmid:16170768

33. Nfon CK, Makepeace BL, Njongmeta LM, Tanya VN, Bain O, Trees AJ. *Eosinophils contribute to killing of adult Onchocerca ochengi within onchocercomata following elimination of Wolbachia*. Microbes Infect. 2006;8: 2698–2705. pmid:16962357

34. Nfon CK, Makepeace BL, Njongmeta LM, Tanya VN, Trees AJ. *Lack of resistance after re-exposure of cattle cured of Onchocerca ochengi infection with oxytetracycline*. Am J Trop Med Hyg. 2007;76: 67–72. pmid:17255232

35. Bah GS, Ward EL, Srivastava A, Trees AJ, Tanya VN, Makepeace BL. *Efficacy of three-week oxytetracycline or rifampin monotherapy compared with a combination regimen against the filarial nematode Onchocerca ochengi*. Antimicrob Agents Chemother. 2014;58: 801–810. pmid:24247133

36. Bah GS, Tanya VN, Makepeace BL. *Immunotherapy with mutated onchocystatin fails to enhance the efficacy of a sub-lethal oxytetracycline regimen against Onchocerca ochengi*. Vet Parasitol. 2015;212: 25–34. pmid:26100152

37. McGarry HF, Egerton GL, Taylor MJ. *Population dynamics of Wolbachia bacterial endosymbionts in Brugia malayi*. Mol Biochem Parasitol. 2004;135: 57–67. pmid:15287587

38. Halliday A, Guimaraes AF, Tyrer HE, Metuge HM, Patrick CNW, Arnaud K-OJ, et al. *A murine macrofilaricide pre-clinical screening model for onchocerciasis and lymphatic filariasis*. Parasit Vectors. 2014;7: 472. pmid:25338621

39. Johnston KL, Ford L, Umareddy I, Townson S, Specht S, Pfarr K, et al. *Repurposing of approved drugs from the human pharmacopoeia to target Wolbachia endosymbionts of onchocerciasis and lymphatic filariasis*. Int J Parasitol Drugs Drug Resist. 2014;4: 278–286. pmid:25516838

40. Taylor MJ, Von Geldern TW, Ford L, Hubner MP, Marsh K, Johnston KL, et al. *Preclinical development of an oral anti-Wolbachia macrolide drug for the treatment of lymphatic filariasis and onchocerciasis*. Sci Transl Med. 2019;11: 1–11. pmid:30867321

41. Lefoulon E, Vaisman N, Frydman HM, Sun L, Foster JM, Slatko BE. *Large Enriched Fragment Targeted Sequencing (LEFT-SEQ) Applied to Capture of Wolbachia Genomes*. Sci Rep. 2019; 1–10.

42. Hotopp JCD, Slatko BE, Foster JM. *Targeted Enrichment and Sequencing of Recent Endosymbiont-Host Lateral Gene Transfers*. Sci Rep. 2017;7: 1–10.

43. Wernegreen JJ, Kauppinen SN, Degnan PH. *Slip into something more functional: Selection maintains ancient frameshifts in homopolymeric sequences*. Mol Biol Evol. 2010;27: 833–839. pmid:19955479

44. Fang H, Wu Y, Narzisi G, O'Rawe JA, Barrón LTJ, Rosenbaum J, et al. *Reducing INDEL calling errors in whole genome and exome sequencing data*. Genome Med. 2014;6: 1–17.

45. Landmann F, Foster JM, Slatko B, Sullivan W. *Asymmetric wolbachia segregation during Early Brugia malayi embryogenesis determines its distribution in adult host tissues*. PLoS Negl Trop Dis. 2010;4. pmid:20689574

46. Landmann F, Bain O, Martin C, Uni S, Taylor MJ, Sullivan W. Both asymmetric mitotic segregation and cell-to-cell invasion are required for stable germline transmission of Wolbachia in filarial nematodes. Biol Open. 2012;1: 536–547. pmid:23213446

47. Landmann F, Foster JM, Slatko BE, Sullivan W. *Efficient in vitro RNA interference and immunofluorescence-based phenotype analysis in a human parasitic nematode, Brugia malayi*. Parasites and Vectors. 2012;5: 1–8.

48. Serbus LR, Landmann F, Bray WM, White PM, Ruybal J, Lokey RS, et al. *A Cell-Based Screen Reveals that the Albendazole Metabolite, Albendazole Sulfone, Targets Wolbachia*. PLoS Pathog. 2012;8. pmid:23028321

49. Foray V, Pérez-Jiménez MM, Fattouh N, Landmann F. *Wolbachia Control Stem Cell Behavior and Stimulate Germline Proliferation in Filarial Nematodes*. Dev Cell. 2018;45: 198–211.e3. pmid:29689195

50. Hong WD, Benayoud F, Nixon GL, Ford L, Johnston KL, Clare RH, et al. *AWZ1066S, a highly specific anti-Wolbachia drug candidate for a short-course treatment of filariasis*. Proc Natl Acad Sci. 2019;116: 1414 LP– 1419. pmid:30617067

51. Klarmann-Schulz U, Specht S, Debrah AY, Batsa L, Ayisi-Boateng NK, Osei-Mensah J, et al. *Comparison of Doxycycline, Minocycline, Doxycycline plus Albendazole and Albendazole Alone in Their Efficacy against Onchocerciasis in a Randomized, Open-Label, Pilot Trial*. PLoS Negl Trop Dis. 2014;11: e0005156. pmid:28056021

52. Gayen P, Nayak A, Saini P, Mukherjee N, Maitra S, Sarkar P, et al. *A double-blind controlled field trial of doxycycline and albendazole in combination for the treatment of bancroftian filariasis in India*. Acta Trop. 2013;125: 150–156. pmid:23123345

53. Volkmann L, Fischer K, Taylor M, Hoerauf A. *Antibiotic therapy in murine filariasis (Litomosoides sigmodontis): Comparative effects of doxycycline and rifampicin on Wolbachia and filarial viability*. Trop Med Int Heal. 2003;8: 392–401. pmid:12753632

54. Hoerauf A, Nissen-Pähle K, Schmetz C, Henkle-Dührsen K, Blaxter ML, Büttner DW, et al. *Tetracycline therapy targets intracellular bacteria in the filarial nematode Litomosoides sigmodontis and results in filarial infertility*. J Clin Invest. 1999;103: 11–18. pmid:9884329

55. Townson S, Tagboto S, McGarry HF, Egerton GL, Taylor MJ. *Onchocerca parasites and Wolbachia endosymbionts: Evaluation of a spectrum of antibiotic types for activity against Onchocerca gutturosa in vitro*. Filaria J. 2006;5: 1–9.

56. Weiss LM, Kim K. *The development and biology of bradyzoites of Toxoplasma gondii*. Front Biosci. 2000;5. pmid:10762601

57. Sullivan WJ, Jeffers V. *Mechanisms of Toxoplasma gondii persistence and latency*. FEMS Microbiol Rev. 2012;36: 717–733. pmid:22091606

58. Torrey HL, Keren I, Via LE, Lee JS, Lewis K. *High persister mutants in mycobacterium tuberculosis*. PLoS One. 2016;11: 1–28. pmid:27176494

59. Cameron DR, Shan Y, Zalis EA, Isabella V, Lewis K. *A genetic determinant of persister cell formation in bacterial pathogens*. J Bacteriol. 2018;200: 1–11. pmid:29941425

60. Prasetyoputri A, Jarrad AM, Cooper MA, Blaskovich MAT. *The Eagle Effect and Antibiotic-Induced Persistence: Two Sides of the Same Coin?* Trends Microbiol. 2019;27: 339–354. pmid:30448198

61. Rittershaus E, Baek S, Sassetti C. *The normalcy of dormancy*. Cell Host Microbe. 2013;13: 643–651. pmid:23768489

62. Ehrt S, Schnappinger D, Rhee KY. *Metabolic principles of persistence and pathogenicity in Mycobacterium tuberculosis*. Nat Rev Microbiol. 2018;16: 496–507. pmid:29691481

63. Singh AE, Romanowski B. *Syphilis: Review with emphasis on clinical, epidemiologic, and some biologic features*. Clin Microbiol Rev. 1999;12: 187–209. pmid:10194456

64. Panzetta ME, Valdivia RH, Saka HA. *Chlamydia persistence: A survival strategy to evade antimicrobial effects in-vitro and in-vivo*. Front Microbiol. 2018;9: 1–11.

65. Monack DM, Mueller A, Falkow S. *Persistent bacterial infections: The interface of the pathogen and the host immune system*. Nat Rev Microbiol. 2004;2: 747–765. pmid:15372085

66. Fisher RA, Gollan B, Helaine S. *Persistent bacterial infections and persister cells*. Nat Rev Microbiol. 2017;15: 453–464. pmid:28529326

67. Singhal K, Mohanty S. *Comparative genomics reveals the presence of putative toxin–antitoxin system in Wolbachia genomes*. Mol Genet Genomics. 2018;293: 525–540. pmid:29214346

68. Helaine S, Cheverton AM, Watson KG, Faure LM, Matthews SA, Holden DW. *Internalization of Salmonella by Macrophages Induces Formation of Nonreplicating Persisters*. Science. 2014;343: 204–208. pmid:24408438

69. Harms A, Brodersen DE, Mitarai N, Gerdes K. *Toxins, Targets, and Triggers: An Overview of Toxin-Antitoxin Biology*. Mol Cell. 2018;70: 768–784. pmid:29398446

70. Fallon AM. *Computational evidence for antitoxins associated with RelE/ParE, RatA, Fic, and AbiEii-family toxins in Wolbachia genomes*. Mol Genet Genomics. 2020. pmid:32189066

71. Fischer K, Beatty WL, Weil GJ, Fischer PU. *High pressure freezing/freeze substitution fixation improves the ultrastructural assessment of Wolbachia endosymbiont—Filarial nematode host interaction*. PLoS One. 2014;9: 16–19. pmid:24466066

72. Geniez S, Foster JM, Kumar S, Moumen B, Leproust E, Hardy O, et al. *Targeted genome enrichment for efficient purification of endosymbiont DNA from host DNA. Symbiosis*. 2012;58: 201–207. pmid:23482460

73. Koren S, Walenz BP, Konstantin B, Miller JR, Bergman NH, Phillippy AM. *Canu: scalable and accurate long-read assembly via adaptive k-mer weighting and repeat separation*. Genome Res. 2017;27: 722–736. pmid:28298431

74. Li H. *Minimap2: Pairwise alignment for nucleotide sequences*. Bioinformatics. 2018;34: 3094–3100. pmid:29750242

75. Hunt M, Silva N De, Otto TD, Parkhill J, Keane JA, Harris SR. *Circlator: Automated circularization of genome assemblies using long sequencing reads*. Genome Biol. 2015;16: 1–10.

76. Walker BJ, Abeel T, Shea T, Priest M, Abouelliel A, Sakthikumar S, et al. *Pilon: An integrated tool for comprehensive microbial variant detection and genome assembly improvement*. PLoS One. 2014;9. pmid:25409509

77. Tatusova T, Dicuccio M, Badretdin A, Chetvernin V, Nawrocki EP, Zaslavsky L, et al. *NCBI prokaryotic genome annotation pipeline*. Nucleic Acids Res. 2016;44: 6614–6624. pmid:27342282

78. Tanizawa Y, Fujisawa T, Nakamura Y. *DFAST: A flexible prokaryotic genome annotation pipeline for faster genome publication*. Bioinformatics. 2018;34: 1037–1039. pmid:29106469

79. Poplin R, Chang PC, Alexander D, Schwartz S, Colthurst T, Ku A, et al. *A universal snp and small-indel variant caller using deep neural networks*. Nat Biotechnol. 2018;36: 983. pmid:30247488

80. Li H, Handsaker B, Wysoker A, Fennell T, Ruan J, Homer N, et al. *The Sequence Alignment/Map format and SAMtools*. Bioinformatics. 2009;25: 2078–2079. pmid:19505943

81. Desvillechabrol D, Bouchier C, Kennedy S, Cokelaer T. *Sequana coverage: Detection and characterization of genomic variations using running median and mixture models*. Gigascience. 2018;7: 1–13. pmid:30192951

82. Danecek P, Auton A, Abecasis G, Albers CA, Banks E, DePristo MA, et al. *The variant call format and VCFtools*. Bioinformatics. 2011;27: 2156–2158. pmid:21653522

83. Cingolani P, Platts A, Wang LLL, Coon M, Nguyen T, Wang LLL, et al. *A program for annotating and predicting the effects of single nucleotide polymorphisms, SnpEff: SNPs in the genome of Drosophila melanogaster strain w1118; iso-2; iso-3*. Fly (Austin). 2012;6: 80–92. pmid:22728672

Chapter 5: Fexinidazole and Corallopyronin A target antibiotic resistant *Wolbachia* bacteriocytes present in filarial nematodes

ABSTRACT

The discovery of the endosymbiotic bacteria *Wolbachia* as an obligate symbiont of filarial nematodes has led to antibiotic-based treatments of filarial disease. While lab and clinical studies have yielded promising results, recent studies reveal that *Wolbachia* levels rebound even after severe reductions following treatment with the antibiotic rifampicin. In addition to raising questions about the long-term efficacy of antibiotic-based therapies, this finding increases the concern regarding the development of drug resistance for mass drug administration programs. Previous work revealed that the likely source of the bacterial rebound were dense clusters of *Wolbachia* embedded in ovarian tissue bacteriocytes. The number, size, and *Wolbachia* density of these bacteriocytes are not diminished despite large doses of antibiotics. Here we define the cellular characteristics of the bacteriocytes and identify drugs that target them. We find *Wolbachia* clusters emerge after the L4 larval stage of the filarial nematode. Nascent bacteriocytes arise in newly formed sheath cells adjacent to the distal tip cell. They dramatically enlarge but do not appear to disrupt the integrity of the sheath cells. We determined that the *Wolbachia* within the bacteriocytes are either in a quiescent form or replicating at a very low rate. Wolbachia-based bacteriocytes are present in *Brugia malayi* as well as *B. pahangi*. Screens of known antibiotics and other drugs revealed two drugs, Fexinidazole and Corallopyronin A, have strong anti-bacteriocyte efficacy.

INTRODUCTION

The filarial nematodes *Onchocerca volvulus* and *Brugia malayi* are human parasites that cause Onchocerciasis (African River-blindness) and lymphatic filariasis (Elephantiasis, LF). Together these neglected diseases afflict over 175 million with many more at risk [1,2].

While drugs exist that efficiently target the microfilariae, identifying small-molecules that kill adults has been much more problematic. This is of particular concern because these adults live and remain fertile for 10 to 15 years. Thus, curing afflicted individuals requires a multiple-year drug regimen. In the late 1970s cytological studies revealed the presence of a bacteria in the nematode hypodermal chords and germline tissues [3-5]. Subsequent sequence analysis demonstrated that the bacteria is a streamlined version of *Wolbachia*, a bacteria widely distributed among a majority of insect species [6]. Unlike insects in which *Wolbachia* is a facultative endosymbiont, in nematodes *Wolbachia* is an obligate endosymbiont [7]. Loss of *Wolbachia* through antibiotic curing results in infertility and eventual death of the adults. This discovery led to the use of antibiotics as an effective macrofilaricidal treatment of Onchocerciasis and lymphatic filariasis [8]. Clinical trials show that an extended course of antibiotics is effective at *Wolbachia* elimination and eventual killing of the nematodes [9].

As antibiotic methods of treating filarial nematode-based diseases are becoming more widely applied, addressing concerns regarding resistance and recrudescence become necessary. Highlighting this concern, a recent study demonstrated that while a one-week treatment of the filarial nematode *Brugia pahangi* with rifampicin resulted in a 95% reduction in *Wolbachia* load, eight months later *Wolbachia* titers returned to normal [10]. Cellular analysis immediately following treatment revealed that, as expected, rifampicin eliminated virtually all of the *Wolbachia* in the oocytes. However, these studies revealed that within the ovarian tissue dense clusters of *Wolbachia,* strikingly similar to bacteriocytes, are present both in the untreated and antibiotic-treated nematodes. Dense clusters of endosymbionts that reside within and modify host cell morphology and gene expression profiles are known as bacteriocytes [11]. They are most commonly found in insects and to our knowledge have never been reported in a nematode lineage. As described below, we provide evidence that these *Wolbachia* clusters form bacteriocytes in filarial nematode oocytes. Significantly, the number, size, and bacterial density of these clusters remained unchanged in the treated

oocytes. Thus, these *Wolbachia*-based bacteriocytes proved resistant to the antibiotics and are the likely source of *Wolbachia* rebound [10].

Here we further characterize these bacteriocytes by examining the regions of the germline in which they are localized, their origin, whether they are inter- or intracellular, and if the latter, whether they reside in a particular cell type. We also determine whether species in addition to *B. pahangi* contain *Wolbachia*-based bacteriocytes. Finally, in an effort to develop the next generation of antibiotic-based treatment for Onchocerciasis and Lymphatic Filariasis, we have assayed a set of compounds for their ability to target these clusters. These studies have yielded two compounds, Fexinidazole and Corallopyronin A, that are particularly promising.

RESULTS

Wolbachia form dense clusters within and dramatically enlarge sheath cells

To determine whether the *Wolbachia* clusters were intra- or extracellular, dissected *B. pahangi* female germlines were stained with DAPI, Propidium Iodide (PI), and fluorescently-labeled phalloidin. The PI targets nucleic acids and preferentially stains *Wolbachia*. Unless otherwise noted, host nuclei are depicted in purple, *Wolbachia* puncta are red, and actin is green. Examples of *Wolbachia* clusters are in Figure 5.1A. The top left panel shows a cluster of *Wolbachia* encompassing a host nucleus. *Wolbachia* are also present in the surrounding cells but much less densely distributed (Figure 5.1A, bottom right panel). Previous work demonstrated that antibiotics target this latter class of bacteria, but not the clusters [10]. Ovaries often contain multiple clusters, some of which are juxtaposed (Figure 5.1A, bottom left panel). Each cluster is localized in a cell at the outer edge of the nematode oocyte containing a single flattened oblong nucleus (Figure 5.1A, white arrows). Based on studies in *C. elegans*, the position and flattened shape of the nucleus indicates that *Wolbachia* clusters are localized in sheath cells. In *C. elegans*, a single layer of sheath cells encompasses the germline during larval development and is maintained in the adults [12]. In

Figure 5.1 *Wolbachia* form dense clusters within and dramatically enlarge sheath cells. (A) *Wolbachia* clusters in *Brugia pahangi* germline tissue are nearly always associated with a single, oblong nucleus (white arrows). This indicates the clusters exist inside the sheath cells of the nematode. All panels represent single images except the bottom righthand panel, which is a maximum projection of five z-stack images (step size of 2µm, representing an 8µm thick section of tissue). (B) *Wolbachia* clusters greatly increase the volume of the sheath cells in the ovarian tissue of *Brugia pahangi*. Left, an uninfected sheath cell at the bottom surface of the ovary. Right, an infected sheath cell containing a dense cluster of *Wolbachia*. Below each image of sheath cells is a grayscale image of the actin channel. The yellow lines indicate the outline of each sheath cell. (C) Image of a *Wolbachia* cluster surrounding a sheath cell nucleus. This image is a maximum projection comprised of 24 individual z-stack images with a step size of 0.38 µm between stacks, representing a slice of tissue 8.74 µm thick. (D) Images of the *Wolbachia* cluster shown in Figure 1C separated into four sequential z-stacks. Each image is a max projection of four z-stacks with a step size of 0.38 µm. Nematodes are stained with Propidium Iodide (red), DAPI (blue), and Phalloidin 488 (green). All scale bars are 10µm.

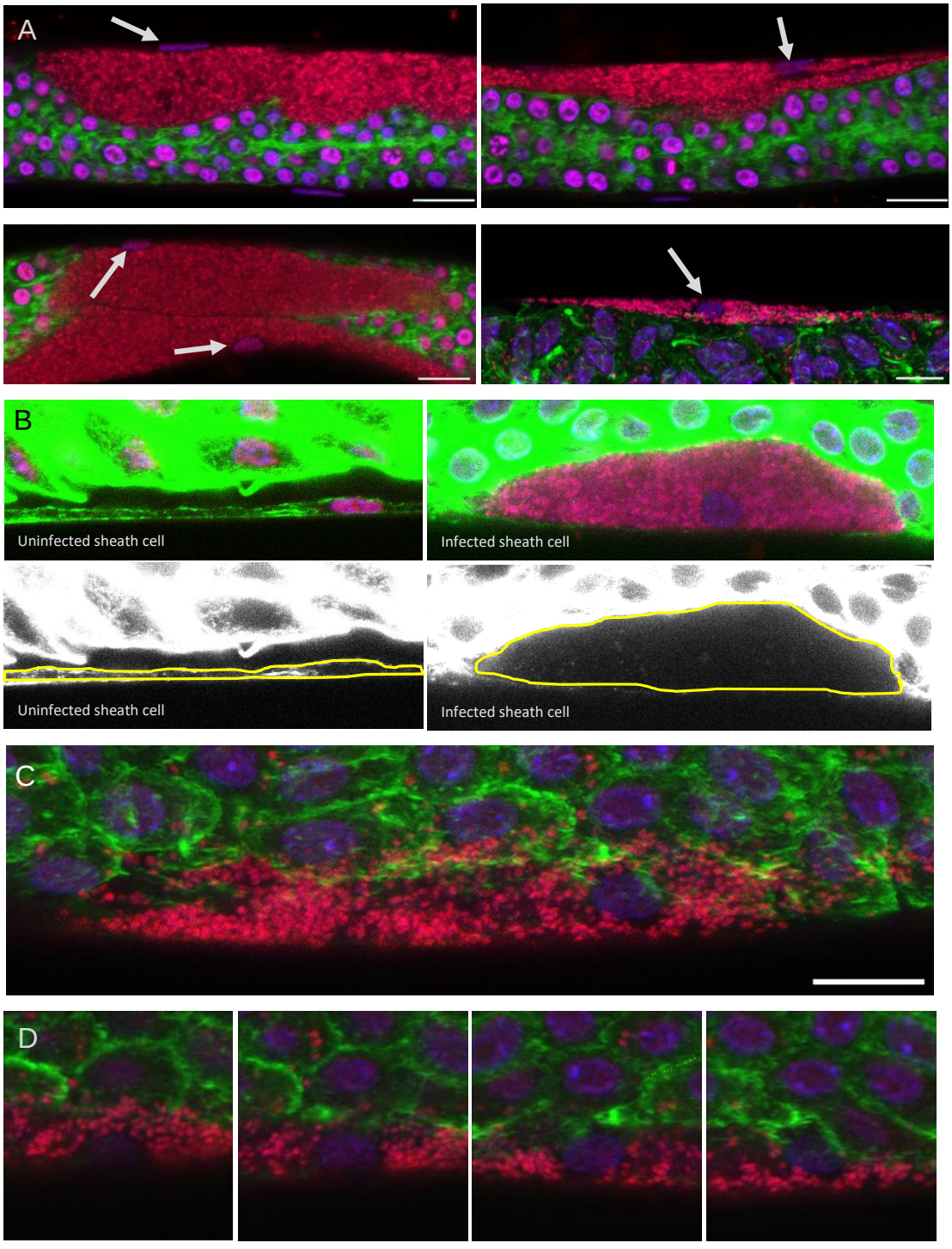
A
B
Uninfected sheath cell
Infected sheath cell
Uninfected sheath cell
Infected sheath cell
C
D

these *B. pahangi* infected sheath cells, the entire volume of the cytoplasm is occupied by *Wolbachia*, and the width of the cells is greatly expanded compared to uninfected cells (Figure 5.1B). Thus, pressure from the increased volume of *Wolbachia* likely results in the increased cell volume. We further characterized these infected sheath cells by constructing three-dimensional profiles of *Wolbachia* clusters. Z-plane stacks of these images revealed that the *Wolbachia* are closely associated with and encompass the host nucleus, clearly demonstrating their intracellular location (Figure 5.1C and 5.1D).

To determine if *Wolbachia* disrupt the integrity of the plasma membrane, we performed super-resolution confocal microscopy using the fluorescent marker Phalloidin 488 to mark the cortical actin. As shown in Figure 5.2, there are no obvious differences in the pattern of cortical actin staining between infected (panel A) and uninfected (panel B) sheath cells. However, this analysis was inconclusive regarding plasma membrane integrity as the staining in both cells is non-uniform. Evidence that membrane integrity is not disrupted comes from the analysis of juxtaposed infected sheath cells (Figure 5.2C and 5.2D). In the two examples, *Wolbachia* in the two cells remain separated, and over-exposure of the Phalloidin 488 channel reveals a continuous line of cortical actin between the two cells. We also performed EM analysis. Although there is evidence of tissue degradation, the images clearly revealed clusters of *Wolbachia* encompassed by an intact host membrane containing junctions (Supplemental Figure 5.1).

Given the *Wolbachia* clusters reside within and modify a specific host cell-type, the sheath cell, we conclude these are *Wolbachia*-based bacteriocytes and refer to them as such henceforth.

Wolbachia **bacteriocytes are present in** ***Brugia malayi*** **germline tissue**

To determine if the *Wolbachia* clusters in the sheath cells are unique to *B. pahangi,* we examined oocytes derived from *B. malayi*, one of three species that infects humans, causing lymphatic filariasis. The other two species, *Brugia timori* and *Wuchereria bancrofti*,

Figure 5.2 The integrity of the plasma membrane is not disrupted in infected sheath cells. (A) Actin staining of an uninfected sheath cell shows a patchy distribution of actin surrounding the cell. (B) Actin staining of a *Wolbachia*-infected sheath cell shows a similar patchy distribution of actin surrounding the bacterial cluster. The presence of *Wolbachia* does not appear to affect the integrity of the plasma membrane surrounding sheath cells. (C) and (D) Two *Wolbachia* bacteriocytes were discovered next to each other (top panels). When the actin channel (green) is overexposed, a clear bridge of actin can be seen between these two bacteriocytes (bottom panels, grayscale). Arrows point to actin boundaries between bacteriocytes. Tissues are stained with Propidium Iodide (red), DAPI (blue), and Phalloidin 488 (green).

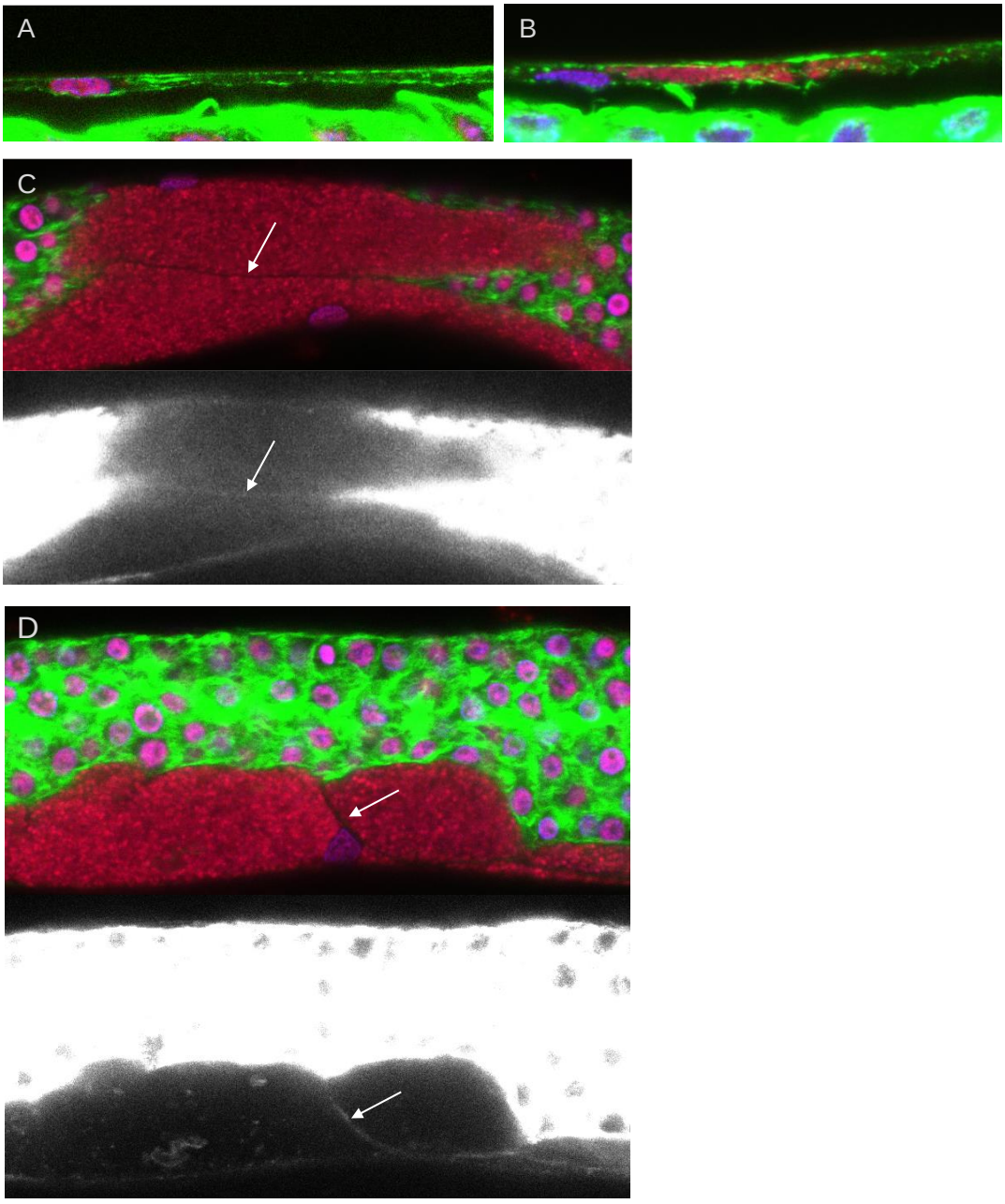
A
B
C
D

cannot be cultured as adults for laboratory experimentation. As shown in Figure 5.3, this analysis revealed that bacteriocytes containing densely packed *Wolbachia* are in *B. malayi* oocytes. As with *B. pahangi*, the *Wolbachia* clusters are observed closely associated with oblong flattened nuclei in the sheath cells that encompass the oocytes. Also like *B. pahangi*, the location of the clusters is similar to that found in *B. pahangi*. Also, the *Wolbachia* result in expansion of the *B. malayi* sheath cells, although not as dramatically as observed in *B. pahangi*. Given these similarities, it is likely that these bacteriocytes are also resistant to treatment with rifampicin.

Nascent bacteriocytes are located near the Distal Tip Cell

To determine the origin of the *Wolbachia* bacteriocytes, we reasoned that cells of origin would contain smaller clusters and not have undergone expansion. Analysis revealed that cells adjacent to the Distal Tip Cell (DTC) occasionally contained small *Wolbachia* clusters (Figure 5.4). In *C. elegans* the distal tip cell serves as the niche for the germline stem cells [13]. Neighboring the distal tip cell is the first of five pairs of sheath cells that divide, migrate, and elongate such that the entire gonad is encompassed by sheath cells [12]. We suspect that the cells with small *Wolbachia* clusters near the DTC are nascent sheath cells. Figure 5.4 depicts five Z-planes cutting through the DTC of a *B. pahangi* ovary. In the top panel, arrows highlight two small clusters of *Wolbachia* in cells adjacent to the DTC. Given their position within the germline tissue, we conclude it is a sheath cell. As one images deeper into the distal tip tissue, the cluster of *Wolbachia* is more apparent and can be seen extending along the length of the ovary at the bottom edge. These nascent *Wolbachia* bacteriocytes are commonly seen at the distal tip of *B. pahangi* germline tissue (Supplemental Figure 5.2).

Support for this conclusion comes from the fact that the nuclei in these cells tend to be oblong and flattened (Supplemental Figure 5.2A-C). Presumably as more sheath cells are

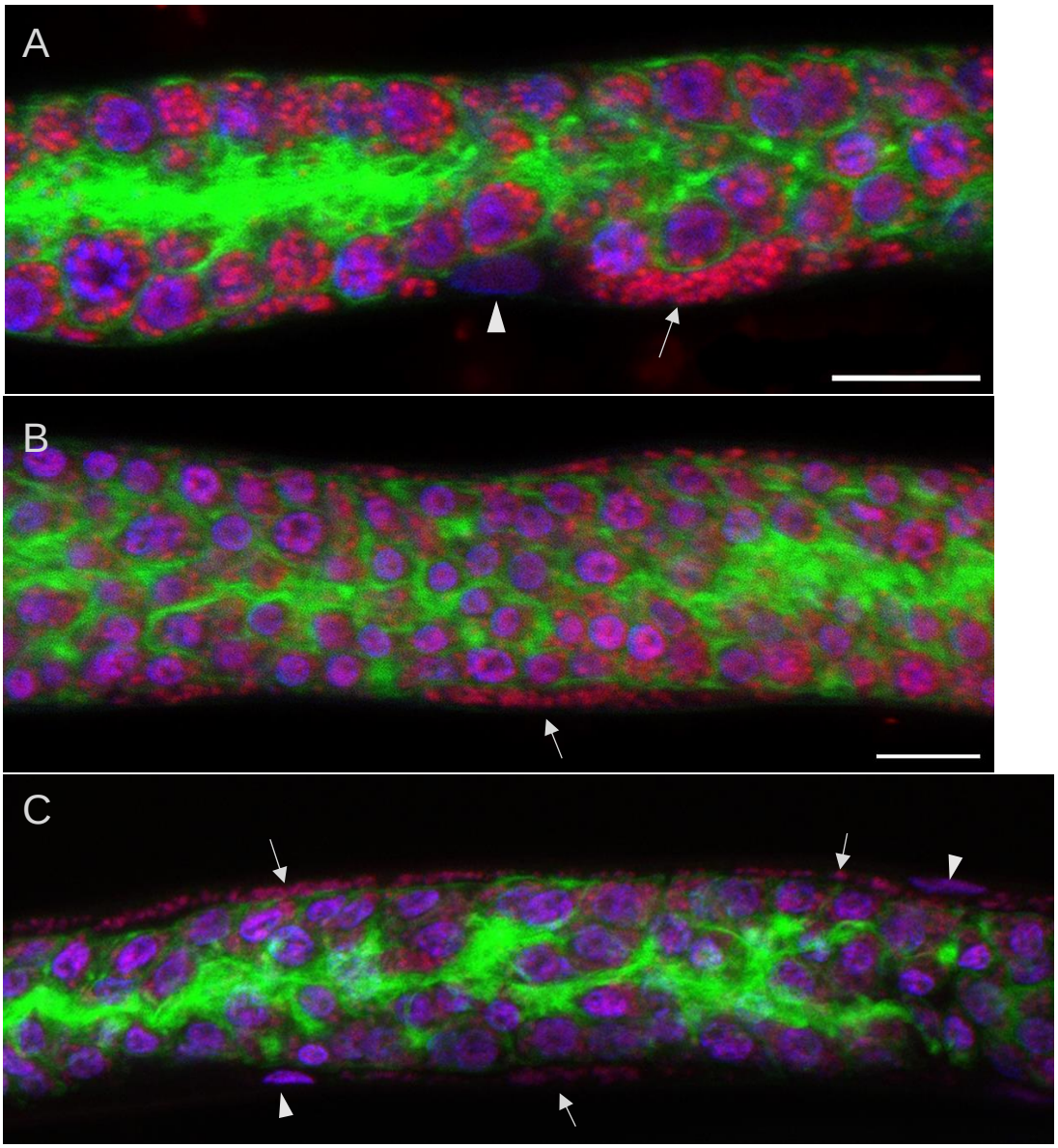

Figure 5.3 *Wolbachia* bacteriocytes are present in *Brugia malayi* germline tissue. A-C) *Wolbachia* clusters are also found in the species of filarial nematode that infects humans, *Brugia malayi*. Nematode germline tissue is stained with Propidium Iodide (red), DAPI (blue), and Phalloidin 488 (green). Arrows point to bacteriocytes of *Wolbachia.* Arrowheads point to sheath cell nuclei. All scale bars are 10µm.

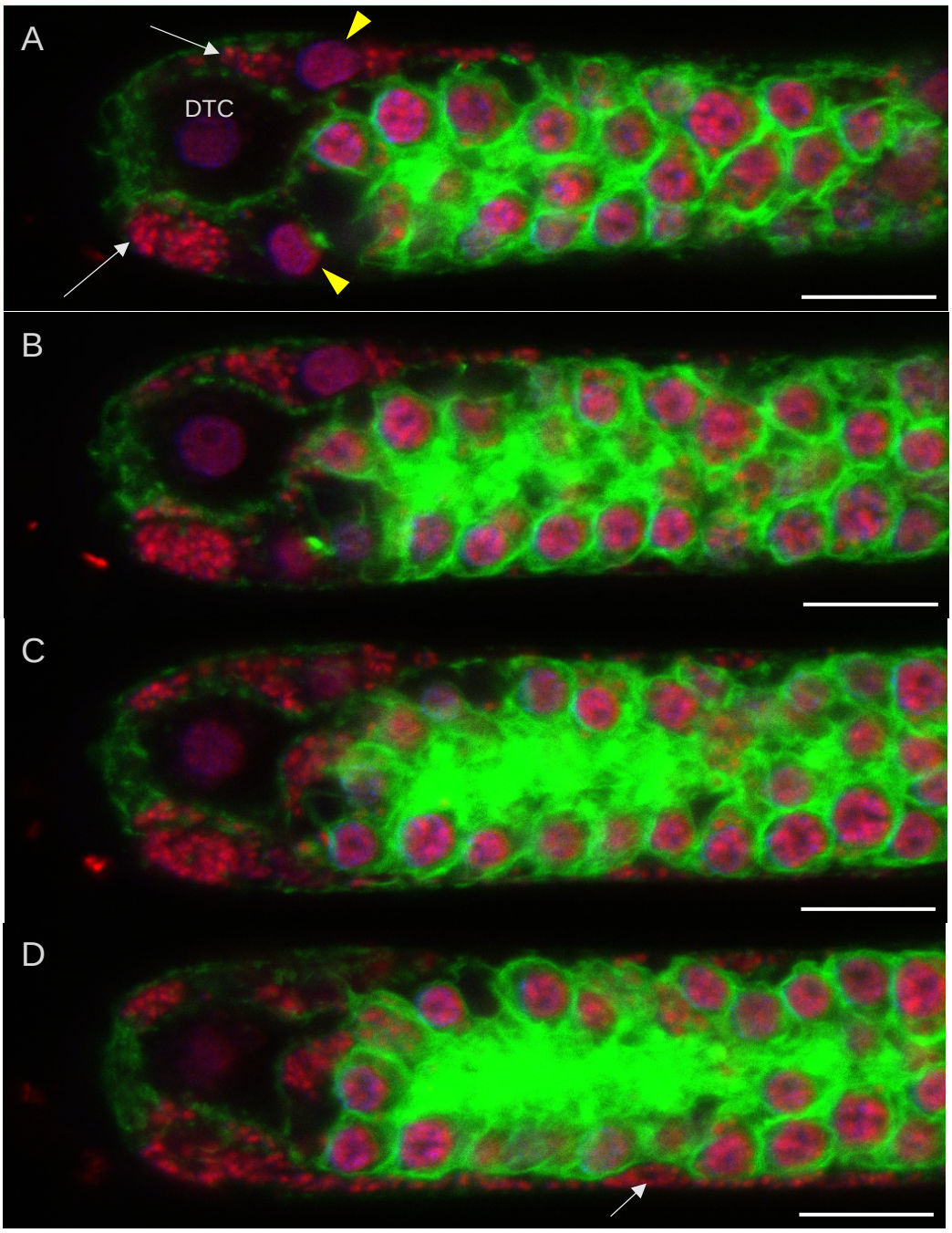

Figure 5.4 Nascent bacteriocytes are located near the Distal Tip Cell. (A-D) Small *Wolbachia* bacteriocytes are found near, and often surrounding, the distal tip cell (DTC) of the *Brugia pahangi* ovary. Images represent sequential z-stacks of the nematode ovary distal tip (step size = 1.32 µm). Tissue is stained with Propidium Iodide (red), DAPI (blue), and Phalloidin 488 (green). White arrows point to *Wolbachia* bacteriocytes. Yellow arrowheads point to sheath cell nuclei. For clarity, only panels A, D, and E are labeled. Scale bars are 10 µm.

produced these cells migrate away from the DTC and during this time *Wolbachia* replicate to fill and expand the cell forming a bacteriocyte.

No replicating *Wolbachia* are detected in enlarged infected sheath cells

To determine if the *Wolbachia* are actively replicating in the mature sheath cells, we incubated ovarian tissue of mature *Brugia pahangi* females with the nucleotide analog EdU for one to three days. Previous studies in *B. malayi* revealed that the germline stem cells adjacent to the DTC are quiescent [14]. However, their daughter cells, destined to form oocytes, migrate anteriorly and become mitotically active in a region known as the Proliferative Zone (PZ) as evidenced by EdU [14]. Figure 5.5A demonstrates that the EdU labeling protocol works in *B. pahangi*. Living nematodes were incubated for 24 or 72 hours in media containing EdU, then fixed and stained with PI and DAPI. The proliferative zones of the oocytes were imaged. The bottom panel depicts the subset of EdU-positive nuclei and the middle panel depicts all of the nuclei (PI and DAPI stained). The top panel depicts the merged image. About a third of the nuclei are EdU-positive, consistent with previously published studies [14]. The arrowheads highlight *Wolbachia*, none of which are EdU positive. We also analyzed EdU incorporation in the hypodermal chords (Figure 5.5B and Supplemental Figure 5.3). Nematode host nuclei are outline in white. EdU-positive *Wolbachia* are present in among the mass of *Wolbachia* in the hypodermal chords, indicating active replication. However, EdU incorporation was not observed in the *Wolbachia* clusters present in the oocyte after 24 hours (Figure 5.5C, seven total clusters analyzed). Even after 3 days of EdU incubation, no replicating *Wolbachia* could be detected (Supplemental Figure 5.4, seven total clusters analyzed), suggesting that these are in a quiescent state.

Examination of EdU incorporation of host nuclei in the distal region of germline tissue reveal 24% are highly labeled and 8% are weakly labeled. These findings are in accord with the previous studies performed in *B. malayi*. While we find clear evidence of host nuclei

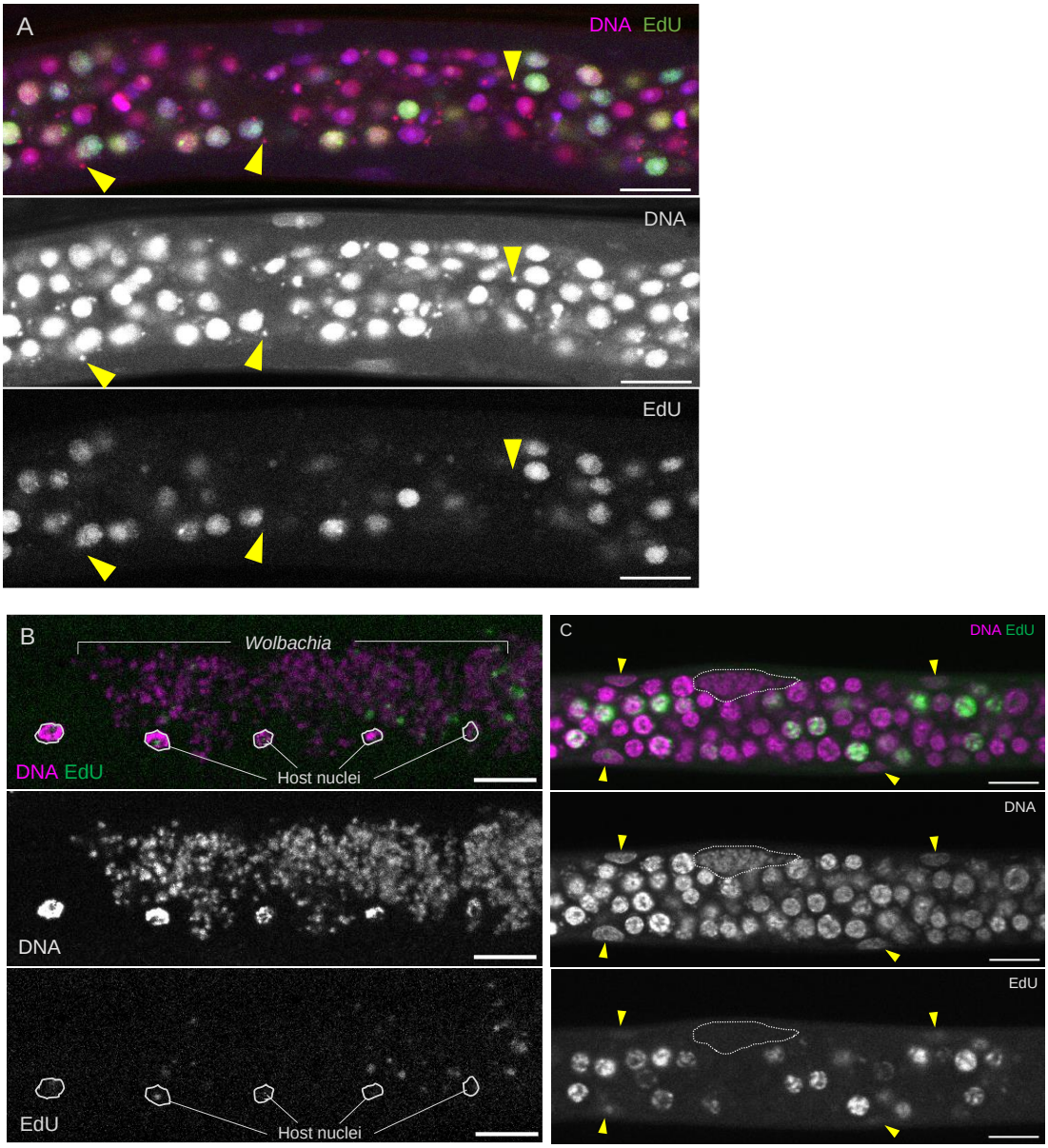

Figure 5.5 No replicating *Wolbachia* are detected in enlarged infected sheath cells. (A) Ovarian tissue of *Brugia pahangi* incubated with 200 µM EdU for 24 hours. Nematode host nuclei incorporate EdU, but *Wolbachia* puncta do not (yellow arrowheads point to three representative *Wolbachia* puncta). DNA is stained with Propidium Iodide and DAPI. (B) Hypodermal chords of *Brugia pahangi* incubated with 200 µM EdU for three days. Nematode host nuclei are outlined in white. All other blue puncta are *Wolbachia.* EdU incorporation can be seen amongst the *Wolbachia* puncta. Image represents a max projection of four z-stacks with a step size of 0.38 µm. DNA is stained with DAPI only. (C) EdU incorporation was not seen in *Wolbachia* bacteriocytes after 24 hours incubation at 200 µM concentration (7 bacteriocytes analyzed). White dotted line indicates the outline of the infected sheath cell. For all images, EdU is visualized with Invitrogen Click-iT EdU imaging kit, Alexa Fluor 488. All scale bars are 10 µm.

replication, all of the *Wolbachia* in this region remain unlabeled (Figure 5.5A, see arrows). However, images of the hypodermal chords revealed incorporation of EdU into *Wolbachia* after 3 days. The finding that *Wolbachia* replicate in the hypodermal chords is also in accord with previous studies [15,16]. Taken together, these results indicate that our 3-day incubation protocol is capable of detecting both host and *Wolbachia* DNA replication.

Finally, we examined *Wolbachia* clusters in the ovary for EdU incorporation (Figure 5.5C). After 24 hours there are no EdU-positive puncta in the *Wolbachia* clusters outlined in white. Similar results were obtained in an additional seven clusters analyzed. We suspected the bacteria may still be replicating in these clusters, but at a slower rate, so we repeated the EdU assay for a three-day long incubation. Even after this extended incubation period, no EdU incorporation could be seen in the seven additional clusters analyzed (Supplemental Figure 5.4). These results indicate that *Wolbachia* in the clusters are not actively replicating or are replicating at a severely reduced rate compared to *Wolbachia* in the hypodermal chords. That *Wolbachia* are in a non-replicating, perhaps quiescent state, may explain their resistance to extended rifampicin treatment.

Identification of small molecules that target *Wolbachia* bacteriocytes

While a short-course 7-day rifampicin treatment eliminates 95% of the *Wolbachia* in adult nematodes, this treatment had no effect on the number and size of the *Wolbachia* clusters [10]. Also, rifampicin treatment did not diminish the density of *Wolbachia* in the clusters. Further, 36 weeks after the 7-day rifampicin treatment, *Wolbachia* titer returned to normal levels. This observation led to the hypothesis that *Wolbachia* in the clusters are the source of the rebound. The finding that *Wolbachia* rebounds following withdrawal of antibiotics has key implications for developing effective anti-*Wolbachia* therapies. If these clusters serve as a protective niche for *Wolbachia* to elude current antibiotic treatment, targeting these protected bacteria will be a necessity to ensure a full elimination of *Wolbachia* from the filarial nematode and successful treatment of filarial disease by anti-

Wolbachia compounds. Thus, we were motivated to screen for small molecules that target *Wolbachia* within these clusters

To this end, *B. pahangi* females were incubated for three days in media containing small molecule inhibitors at a concentration of 5 μM. As described above, the ovaries of the nematodes were dissected, fixed with paraformaldehyde, and stained with DAPI and PI. The dissected ovaries were scanned and the number and size of *Wolbachia* clusters were counted. DMSO treated nematodes served as a control. As shown in Figure 5.6, this treatment exhibited the same number of ovarian clusters as untreated nematodes (data not shown). In addition, we examined the effect of rifampicin on cluster number, as previous studies revealed it had no effect. We also found rifampicin to have no effect on number of clusters in our *in vitro* assay.

Because screening for drugs that eliminate the clusters is labor-intensive, we could only screen a limited number of compounds. Therefore, our rationale was to select diverse compounds with a broad range of targets (Table 5.1). As a control, we retested the effects of rifampicin, a DNA-dependent RNA polymerase inhibitor, on the frequency and size of the *Wolbachia* clusters. Similar to our previous results [10], while this compound effectively eliminated *Wolbachia* from ovarian tissue, there was no effect on the frequency of *Wolbachia* clusters (Figure 5.6). The frequency and size of *Wolbachia* clusters in rifampicin-treated nematodes was similar to our DMSO-treated controls (Figure 5.6). We also tested another DNA-dependent RNA polymerase inhibitor, Corallopyronin A, a proven potent anti-*Wolbachia* compound [17,18]. In addition, we tested two pro-drugs, fexindazole and metronidazole [19,20]. The former is activated by nitroreductase and the latter by oxyreductase. Bioinformatics analysis reveals the reduced genomes of filarial *Wolbachia* maintain intact versions of both of these genes (unpublished, personal correspondence, Cooper Lab, University of Montana). We also tested Albendazole and its metabolic derivatives, Albendazole sulfone and Albendazole sulfoxide. Previous studies demonstrated that these compounds reduce *Wolbachia* titers in cell lines and *ex vivo* nematode studies [21].

Drug	Mechanism/Target	Reference
Rifampicin	DNA-dependent RNA polymerase	Mosaei, et al. 2019 [51]
Corallopyronin A	DNA-dependent RNA polymerase	Krome, et al. 2022 [18]
Fexinidazole	Prodrug: nitroreductase-activated	Deeks, 2019 [20]
Metronidazole	Prodrug: oxidoreductase-activated	Dingsdag and Hunter, 2018 [19]
Rapamycin	mTOR	Ballou and Lin, 2008 [26]
Pararosaniline pamoate	Heat Shock Protein 90	Shahinas, et al. 2015 [28]
Colistin sulfate	Phospholipid A, outer membrane	Velkov, et al. 2013 [29]
Albendazole	Nematode beta-tubulin	Borgers, et al. 1975 [53]
Albendazole sulfoxide	Nematode beta-tubulin	Marriner, et al. 1980 [52]
Albendazole sulfone	Nematode beta-tubulin	Marriner, et al. 1980 [52]
CBR417	Unknown	Bakowski, et al. 2019 [24]
CBR490	Unknown	Bakowski, et al. 2019 [24]

Table 5.1 List of small molecules screened for anti-bacteriocyte activity in *Brugia pahangi.*

Subsequent clinical studies revealed that they are particularly potent when used in combination with other antibiotics [22,23]. CBR417 and CBR490 are novel compounds discovered in high-throughput cell-based screens for anti-*Wolbachia* activity [24]. Animal studies reveal these compounds have robust anti-*Wolbachia* activity *in vivo* [24,25]. Rapamycin, an mTOR inhibitor and potential anti-*Wolbachia* compound [26,27]. Pamoate compounds were recovered in a cell-based anti-*Wolbachia* screens and Pararosaniline pamoate targets bacteria Heat Shock Protein 90 [21,28]. Colistin targets Phospholipid A of the outer membrane of gram-negative bacteria [29].

The results of our analysis are shown in Figure 5.6A. Of the compounds tested, CBR417, Corallopyronin A, CBR490, and Fexinidazole revealed a significant reduction in *Wolbachia* bacteriocyte number. Both Fexinidazole and CBR490 reduced frequency of

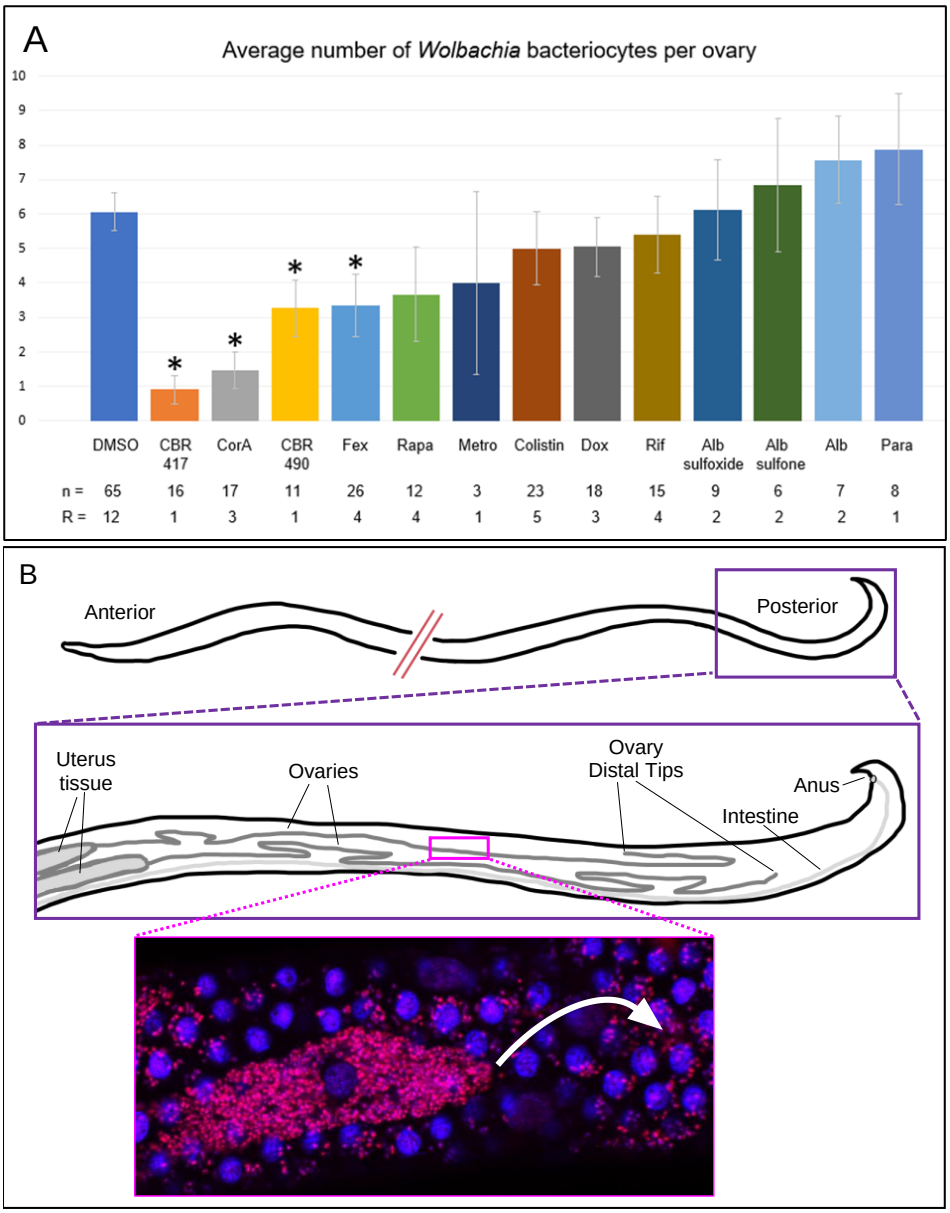

Figure 5.6 Identification of small molecules that target sheath cell *Wolbachia.* (A) Average number of *Wolbachia* bacteriocytes found per ovary in *Brugia pahangi* treated with various small molecule drug compounds. Error bars represent standard error. (***** = $p < 0.05$, n = number of ovaries analyzed, R = rounds of drug treatments performed) (B) A graphical depiction of our working model: *Wolbachia* bacteriocytes act as a protective niche for the bacteria and serve as a source of bacterial rebound after antibiotic treatment. Confocal image depicts an infected sheath cell at the surface of *B. pahangi* ovarian tissue. *Wolbachia* DNA is stained with PI (magenta) and nematode DNA is stained with DAPI (blue).

bacteriocytes by about 45% compared to the DMSO control. We believe Fexinidazole to have a more potent anti-bacteriocyte property than the data suggest, as this compound initially reduced bacteriocyte frequency by 67% (n=13). During the third round of treatment, frequency of clusters matched those of controls. We believe our stock solution of Fexinidazole had expired, rendering it inactive for this round. We repeated the drug treatment for a fourth time using freshly made drug solution, and the frequency of bacteriocytes reduced by 92% (n=8). Corallopyronin A was tested in our assay three separate times and, on average, reduced frequency of bacteriocytes by 76%. CBR417 reduced frequency by 85%, but did not have a chance to repeat drug treatments of CBR417 and CBR490, so this should be taken into consideration when analyzing the results.

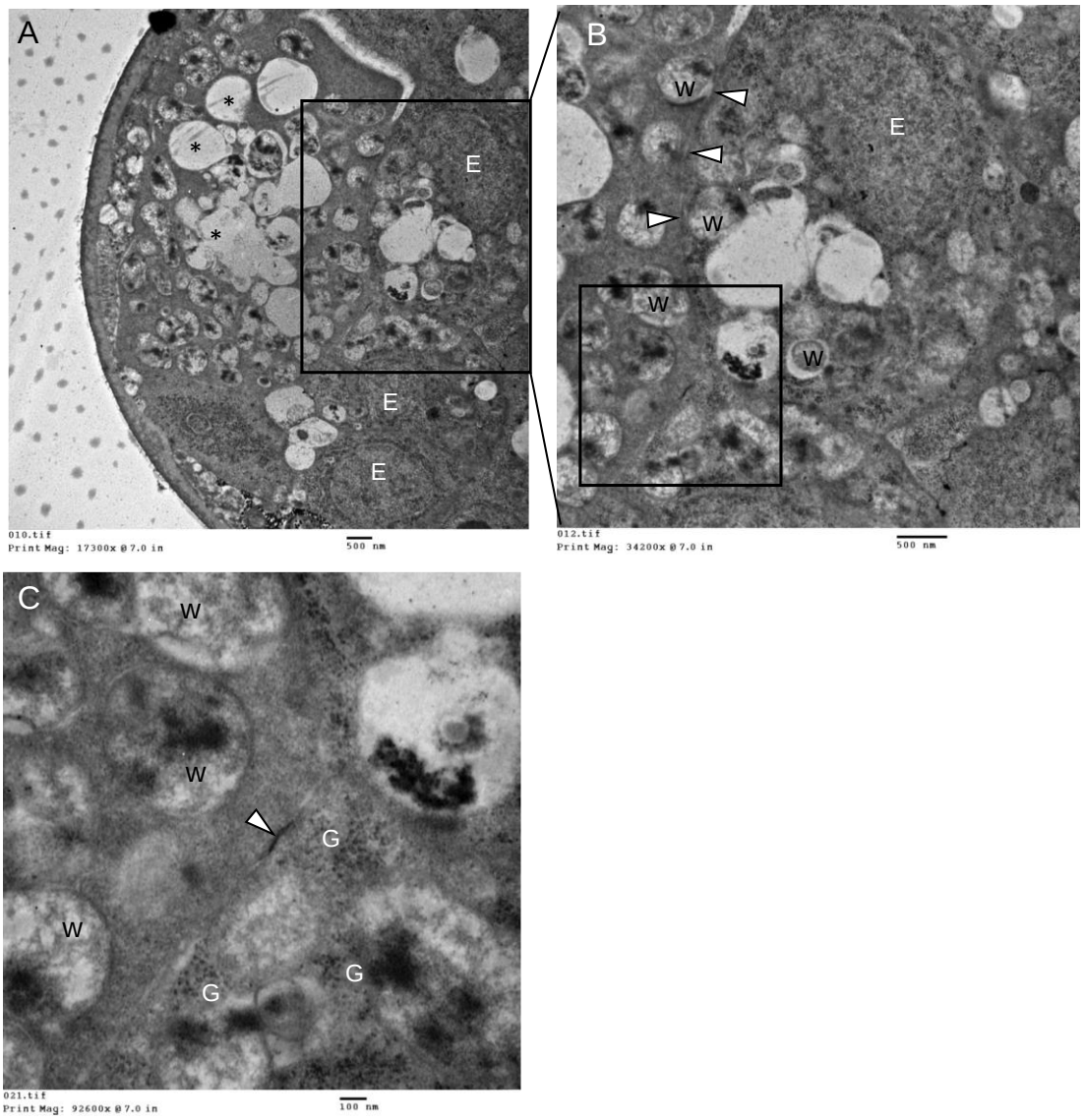

Supplemental Figure 5.1 EM analysis identifies host membrane surrounding *Wolbachia* clusters in *B. pahangi* germline tissue. (A) *B. pahangi* distal tip germline tissue exhibiting degenerative tissue (asterisks) surrounded by a large cluster of swollen *Wolbachia.* Eggs (E) are seen in proximity to the cluster. (B) A high magnification image of the black box in panel A, where *Wolbachia* (w) can be seen with abnormal chromatin. The membrane separating the *Wolbachia* cluster, and the surrounding tissue is clearly visible (arrowheads). Many *Wolbachia* appear closely associated with the membrane. (C) A high magnification image of the black box in panel B showing a very well-developed junction (arrowhead). At high magnifications, glycogen can also be seen in the surrounding area (G). EM images and analysis credited to Ricardo Peguero, New York Blood Center, NY, USA.

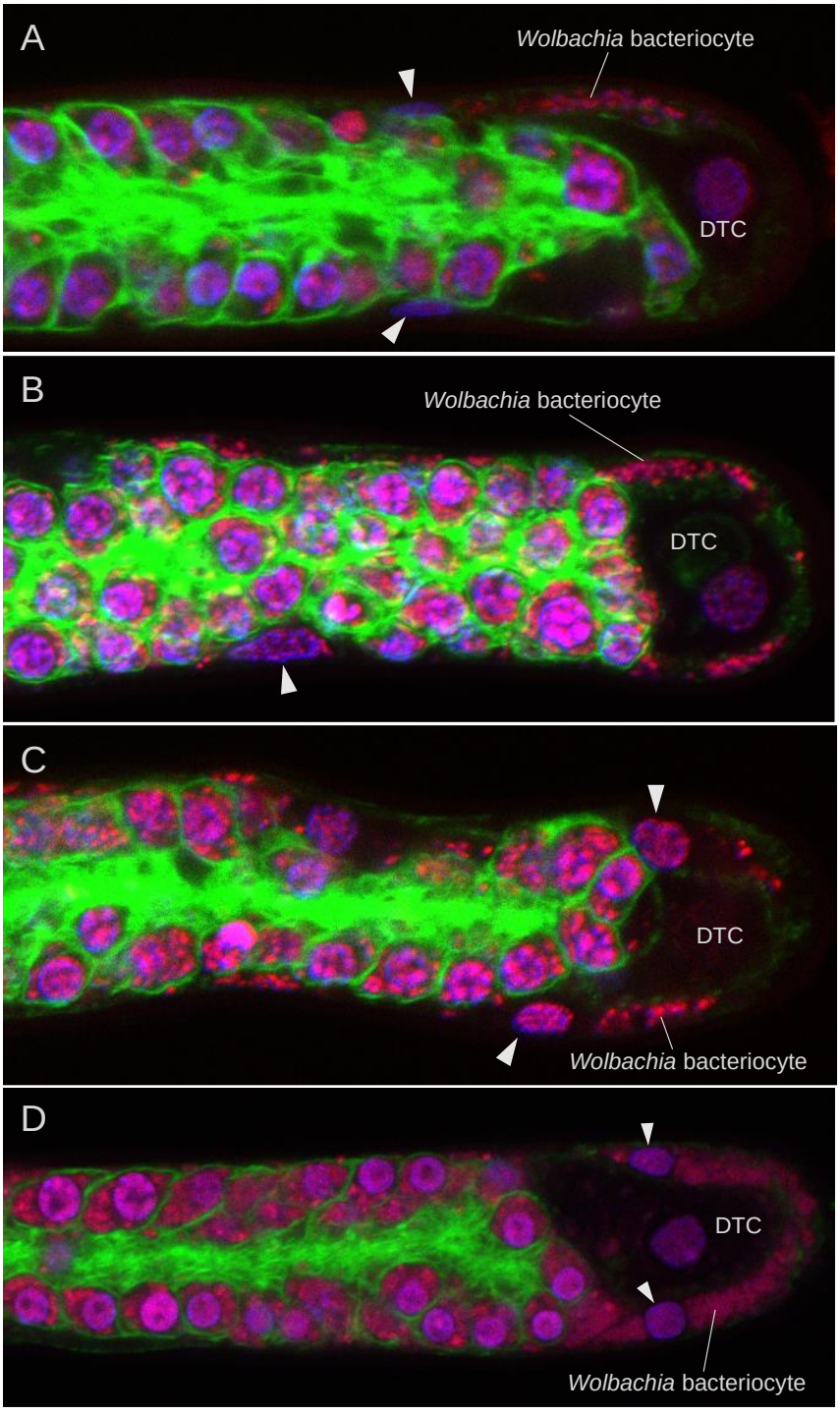

Supplemental Figure 5.2 Nascent bacteriocytes are located near the Distal Tip Cell. (A-D) Small *Wolbachia* clusters are found near, and often surrounding, the distal tip cell (DTC) of the *Brugia pahangi* ovary. Panel D shows two *Wolbachia* bacteriocytes at the DTC, but only one is labeled. Nematode tissues are stained with Propidium Iodide (red), DAPI (blue), and Phalloidin 488 (green). Arrowheads point to sheath cell nuclei.

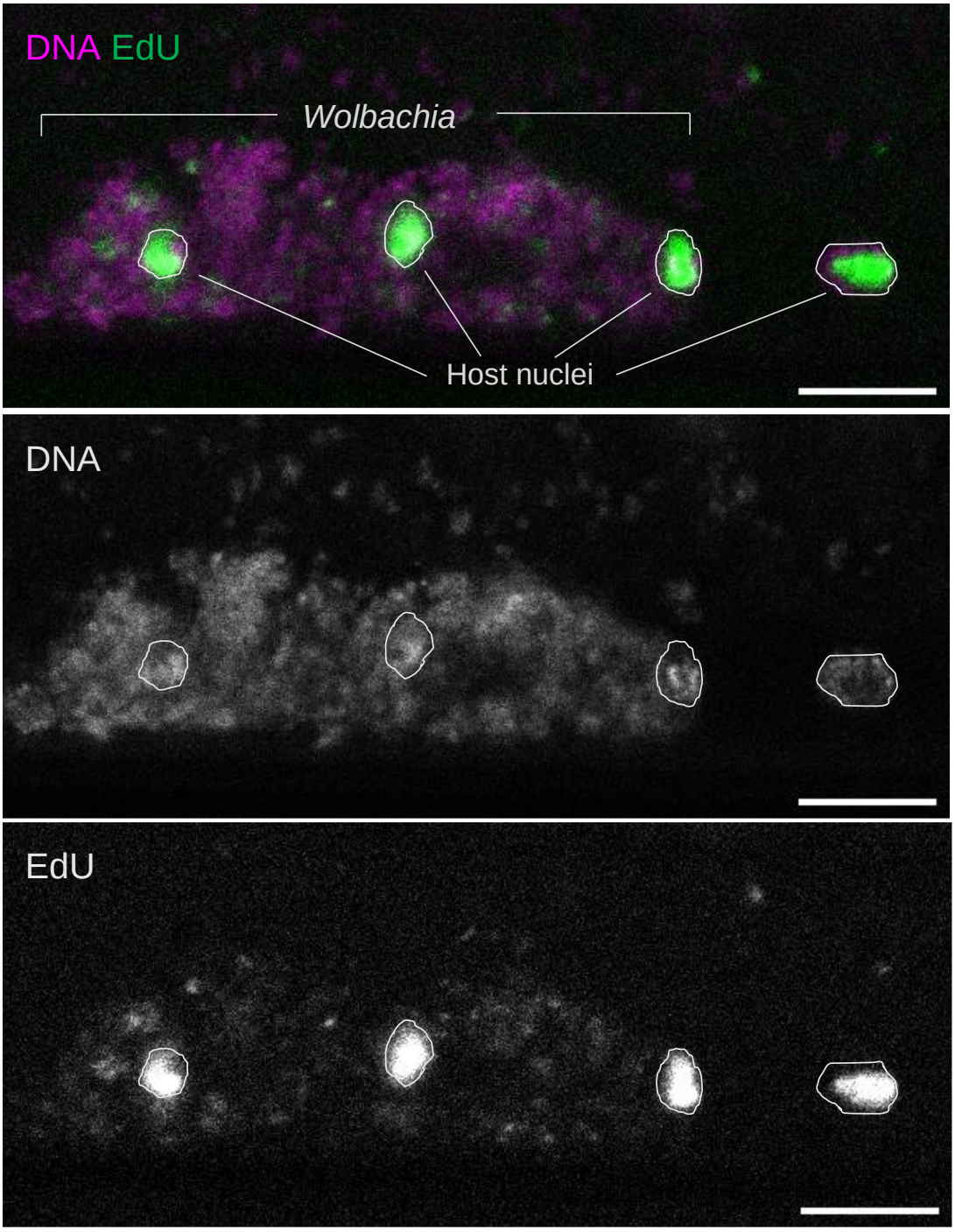

Supplementary Figure 5.3 Replicating bacteria are detected hypodermal chords after 3 days. EdU incorporation was seen in *Wolbachia* of the adult *B. pahangi* hypodermal chords after 3 days of incubation with 200 µM concentration (7 bacteriocytes analyzed). In this image, EdU incorporation can also be seen in the host nuclei (outlined in white). EdU is visualized with Invitrogen Click-iT EdU imaging kit, Alexa Fluor 488. DNA is visualized with DAPI. All scale bars are 10 µm.

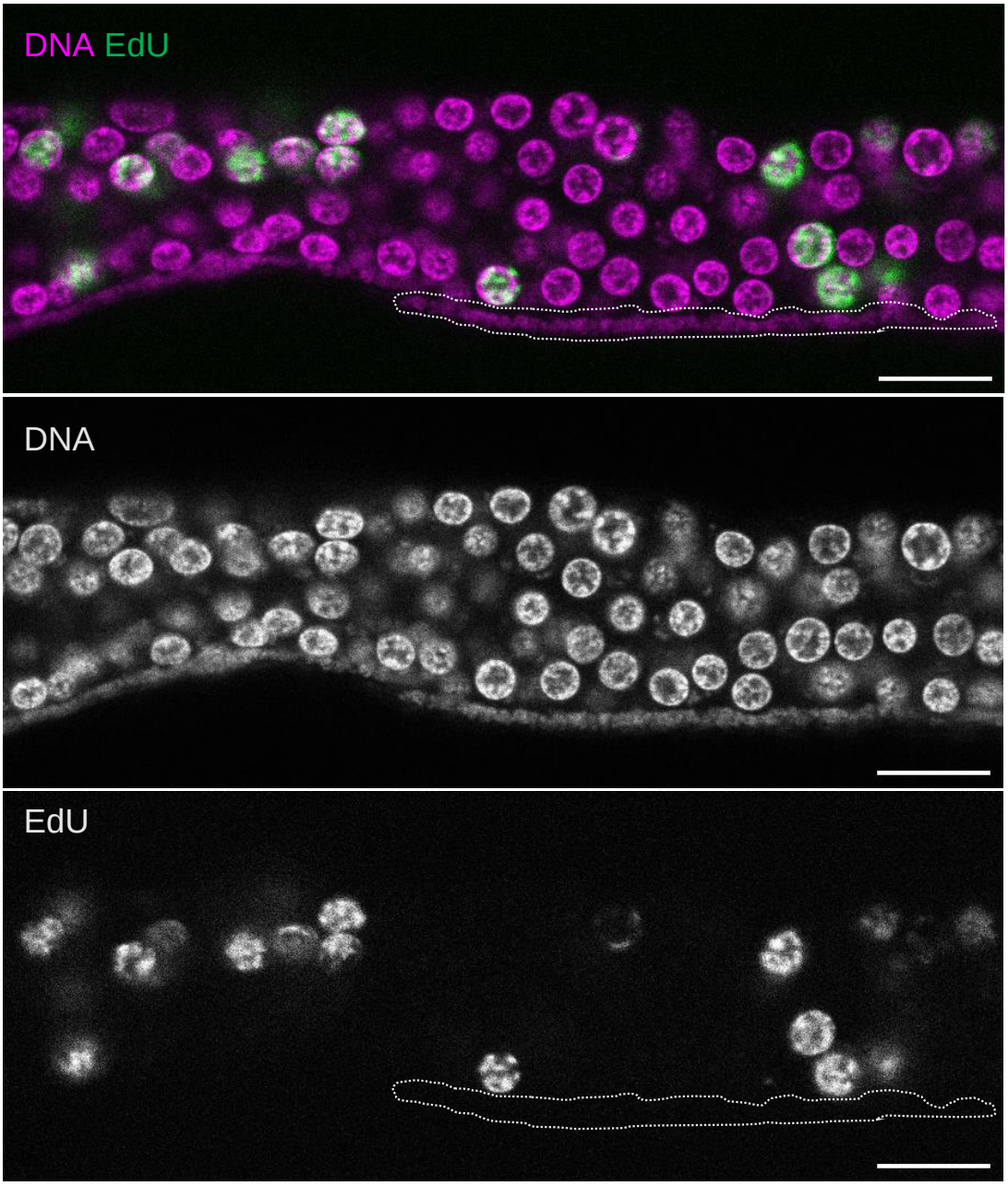

Supplementary Figure 5.4 No replicating bacteria are detected in infected sheath cells after 3 days. EdU incorporation was not seen in *Wolbachia* bacteriocytes after 3 days of incubation with 200 µM concentration (7 bacteriocytes analyzed). White dotted line indicates the outline of the infected sheath cell. EdU is visualized with Invitrogen Click-iT EdU imaging kit, Alexa Fluor 488. DNA is visualized with DAPI. All scale bars are 10 µm.

DISCUSSION

The fact that *Wolbachia* is an obligate endosymbiont has led to promising anti-*Wolbachia* based therapies for the treatment of filarial nematode diseases. Indeed, a number of *in vivo* animal and clinical studies demonstrate that antibiotic treatment is a promising macrofilaricidal therapy [30]. However, recent studies raise concerns that the reduced titers are not always maintained after withdrawal of anti-*Wolbachia* treatment. For example, sustained reduction of *Wolbachia* titer was not achieved using the doxycycline-based anti-*Wolbachia* treatment regimes in the *Litomosoides sigmodontis* infection model [31]. Subsequent studies using the *Brugia pahangi* jird model of infection produced similar results [10]. In spite of a 95% reduction in *Wolbachia* following a 7-day rifampicin treatment, after 36 weeks the *Wolbachia* titer returned to normal pretreatment levels.

Cellular analysis provided a compelling explanation for *Wolbachia* recrudescence after completion of this highly effective 7-day regime of antibiotic therapy. Analysis revealed the presence of dense clusters of *Wolbachia* with their size, number, and distribution unaffected by exposure to antibiotics [10]. The presence of these antibiotic-resistant *Wolbachia* clusters suggested that they were the source of the *Wolbachia* rebound. Therefore, these clusters merited a more detailed cellular characterization and the identification of compounds that specifically target them.

Here we provide evidence that the antibiotic-resistant *Wolbachia* clusters form bacteriocytes. Bacteriocytes are host cells in which endosymbionts reside and dramatically modify. They provide protection from the immune system and a safe cellular environment for endosymbiont replication and transmission [32,33]. Bacteriocytes are commonly found, and most extensively studied, in insects. In the Cereal Weevils, endosymbionts form distinct germline and somatic bacteriocytes [34]. Bacteriocytes often dramatically increase the volume of their host cell, influence a wide array of cellular functions including metabolism, the immune response, and cell cycle, and provide a protective environment for the endosymbiont [33]. Based on these properties, we conclude *Wolbachia* reside in and dramatically modify

sheath cells, forming bacteriocytes. Support for this conclusion comes from the fact that there are a number of reports demonstrating *Wolbachia* form bacteriocytes in insects [7]. *Wolbachia*-induced bacteriocytes have been identified in the bedbug, mealy bug, and in *Drosophila* [35-38]. Thus, it is not unexpected that *Wolbachia* bacteriocytes exist in filarial nematodes. As we propose for the filarial nematode *Wolbachia* clusters, endosymbionts in these bacteriocytes have been shown to escape, migrate, and repopulate other tissues in the insect [33].

In *C. elegans*, sheath cells form an outer monolayer of cells that encompass the oocyte. Each sheath cell contains a characteristic disc-shaped flattened nucleus [39]. *C. elegans* contains five pairs of sheath cells that provide structure to the oocyte [40] as well as regulating germline proliferation [41]. The *Wolbachia* clusters reside in this layer of cells. In addition, all of the *Wolbachia*-infected cells contain a single distinctive flattened host nucleus. As *Wolbachia*-infected sheath cells surround the germline, the bacteria are well positioned to invade and occupy the germline.

One of the most striking aspects of the clusters is that the packing of *Wolbachia* is so extensive that the volume of the sheath cell is enlarged many-fold. We conclude that the overwhelming majority of the clustered *Wolbachia* reside within expanded but intact sheath cells. This is supported by the fact that infected sheath cell cortical actin reveals no obvious breaks. Also, we occasionally observed two expanded infected sheath cells abutting one another, yet there is a distinct band of cortical actin maintaining separation (Figure 5.2C-D). Previous studies revealed clear evidence in female nematodes of *Wolbachia* invading the germline from neighboring somatic cells [42]. *Wolbachia* were observed exiting through distinct breaks in the cortical actin. In contrast, we did not find *Wolbachia* exiting through distinct breaks in the cortical actin of the infected sheath cells.

Finally, EM analysis revealed a continuous plasma membrane in the *Wolbachia*-containing sheath cells. It may be that *Wolbachia* exit through cellular junctions that are

below the resolution of light microscopy. Alternatively, *Wolbachia* may exit in mass via lysis of the infected sheath cells, or possibly hijack cellular exocytosis pathways.

In *C. elegans*, sheath cells engulf apoptotic cells and other debris, as well as residual bodies during spermatogenesis [43,54]. Therefore, it is possible that the Wolbachia accumulate in these cells through engulfment. This scenario also raises the possibility that these cells are engulfing dead Wolbachia. We do not believe this to be the case because antibiotics, such as rifampicin, that are clearly effective at targeting Wolbachia in the nematodes would be expected to produce vast amounts of dead bacteria which would be engulfed by the sheath cells. However, there is not an increase in cluster size or number upon antibiotic treatment [10]. In addition, we identified two compounds that dramatically reduced cluster number. If the Wolbachia were dead, this reduction would not be possible.

We find similar *Wolbachia*-based bacteriocytes in *B. malayi*, the filarial nematode that infects humans and is responsible for Lymphatic filariasis. Although smaller than those found in *B. pahangi*, based on their position at the surface of the tissue and their association with flattened host nuclei, these *Wolbachia*-based bacteriocytes are likely formed from sheath cells as well. The *Wolbachia* in these bacteriocytes also exhibit the same dense packing as found in *B. pahangi*. It is likely these *Wolbachia* clusters are a common feature among *Wolbachia*-infected filarial nematodes.

Examination of adult female gonads reveals nascent clusters in sheath cells near the Distal Tip Cell. In *C. elegans* and likely all nematodes, the Distal Tip Cell forms the niche for the germline stem cells relying on Notch signaling to control the decision between self-renewal and differentiation toward a meiotic fate [13]. As the nematode develops, sheath cells migrate to encompass the entire female germline [44]. Thus, *Wolbachia* are present in the sheath cells early in development and increase in number as the sheath cells migrate along the developing germline. To determine if *Wolbachia* was actively replicating in adult nematode bacteriocytes, we employed EdU incorporation. In spite of three-day incubations, we did not detect EdU incorporation. Thus, we conclude that the *Wolbachia* are either not

replicating, or are replicating very slowly in the adult bacteriocytes. Therefore, *Wolbachia* replication within the bacteriocytes may occur sometime between L4 and adulthood. Alternatively, *Wolbachia* may accumulate in the sheath cells via endocytic or related mechanisms.

It is unclear why the *Wolbachia* clusters in filarial nematodes are resistant to standard antibiotic treatment as other bacteriocytes are sensitive to antibiotics [45]. The bacteria *Mycobacterium tuberculosis* results in the formation of complex heterozygous cell compositions, called granulomas [46]. Granulomas alter the normal internal cellular environment, resulting in hypoxia and other changes. These changes are thought to diminish the efficacy of antibiotics that target the *Mycobacterium* [47]. Similar explanations may apply to the *Wolbachia*-based bacteriocytes we describe in the filarial nematodes.

We were motivated to identify compounds that targeted the bacteriocytes in an effort to prevent *Wolbachia* rebound following withdrawal of short-course antibiotic treatment regimes. Given that the basis for the resistance of the bacteriocytes to antibiotics were unknown, we screened a diverse set of drugs with a broad range of targets. As described, the screening is labor intensive and thus only 13 drugs were screened. Targets of the drugs tested include: DNA-dependent RNA polymerase, nitroreductase-activated prodrug, oxidoreductase-activated prodrug, mTOR, Heat Shock Protein 90, beta-tubulin. In addition, we tested drugs with unknown targets that have previously shown potent anti-*Wolbachia* effects. Our retest of rifampicin, a drug that has proved effective at reducing *Wolbachia* titer, was in accord with previous studies finding it had no effect on the number and size of *Wolbachia*-based bacteriocytes [10].

Two of the thirteen drugs tested, Corallopyronin A and Fexinidazole, resulted in a significant reduction in bacteriocyte number. Corallopyronin A targets bacterial DNA-dependent RNA polymerase in both gram-negative and gram-positive bacteria [18]. This compound has proven extremely effective at targeting *Wolbachia in vivo* [17] and is a preclinical candidate for anti-*Wolbachia* based treatment of filarial nematode-based diseases.

Thus, it may be preventing the transcription of *Wolbachia* genes necessary for its survival both within and outside of the bacteriocytes. It is puzzling that rifampicin, an FDA-approved drug that also targets DNA-dependent RNA polymerases, is ineffective at targeting the bacteriocytes but is effective at the other *Wolbachia* populations in the nematodes [10]. It may be Corallopyronin A is much more efficient at penetrating the bacteriocyte.

Fexinidazole is an FDA-approved drug that has been particularly effective against *Trypanosoma brucei*, a blood-borne parasite and the causative agent in sleeping sickness [48]. Known as a prodrug, it is inactive until internalized by the trypanosome. Once internalized, the trypanosome enzyme nitroreductase cleaves/modifies fexinidazole, producing toxic radicals that damage parasite DNA and protein [49]. It has been shown that all strains of *Wolbachia* possess an intact gene for this enzyme (personal correspondence, Cooper Lab, University of Montana). Analysis of *Wolbachia* in filarial nematode and insect hosts reveals all maintain at least one copy of the nitroreductase gene.

Anti-*Wolbachia* based therapies are proving to be one of the most effective macrofilaricidal strategies in combatting filarial nematode-based diseases. However, as with all antibiotic-based therapies, the emergence of resistant strains is a concern. For example, in insects, wild strains of *Wolbachia* differ significantly in their resistance to rifampicin [50]. As described, *Wolbachia* populations rebound in filarial nematodes following withdrawal of the antibiotic, a situation ripe for the selection of resistant strains. *Wolbachia* bacteriocytes are a likely source of the rebound and new resistant strains. Thus, further exploration of Corallopyronin A, Fexinidazole and other compounds for their ability to target *Wolbachia*-based bacteriocytes is warranted.

MATERIALS AND METHODS

Parasite Material

Live *B. pahangi* and frozen *B. malayi* worms, harvested from infected jirds (*Meriones unguiculatus*), were supplied by the NIAID/NIH Filariasis Research Reagent Resource Center (FR3, Athens, GA, USA, www.filariasiscenter.org) via the Biodefense and Emerging Infections Research Resources Repository (BEI Resources, Manassas, VA, USA). Upon delivery, live worms were placed in an incubator at 37˚C with 5% CO_2 to recover overnight from shipping. Drug treatments or EdU incubations were performed the following day.

Drug Treatments

Stock concentrations of 10 mM were created for all drug solutions using DMSO solvent (Sigma-Aldrich). Drugs used and their manufacturer information can be found in the table below. Corallopyronin A is a natural product purified by liquid chromatography from extracts of *Myxococcus xanthus*, a soil bacterium, and was generously gifted to us for drug screening by Kenneth Pfarr, Institute for Medical Microbiology, Immunology & Parasitology, University Hospital Bonn, Bonn, Germany. CBR417 and CBR490 are synthetic compounds provided by Calibr at Scripps Research, La Jolla, CA, USA.

Drug	**Manufacturer**	**Catalog No.**
Albendazole	Thermo Scientific	H25925-22
Albendazole sulfone	Fisher Scientific	501454432
Albendazole sulfoxide	Fisher Scientific	501415383
CBR417	Calibr	N/A
CBR490	Calibr	N/A
Colistin sulfate	Fisher Scientific	50247446
Corallopyronin A	Kenneth Pfarr	N/A
Doxycycline hydrochloride	Fisher BioReagents	BP26531
Fexinidazole	Med Chem Express	HY-13801
Metronidazole	WW Grainger Inc.	30TZ38
Pararosaniline pamoate	Sigma-Aldrich	SIAL-P3750
Rapamycin	Fisher Scientific	507513705
Rifampicin	TCI America	R007925G

Stock concentrations of drugs were diluted to a working concentration of 5 µM in worm media created from 80% RPMI 1640 (Gibco), 10% FBS (Life Technologies), and 10% DMEM (Corning). Worms were treated for 72 hours in 8 mL of drug-media or control media (equivalent amounts of DMSO) in 6-well plates at 37˚C and 5% CO_2. Media was refreshed daily until the final day when worms were collected in 1.5 mL of drug-media and immediately frozen at -80˚C for later immunostaining.

Tissue Collection

For confocal analysis of germline tissue, frozen worms were thawed at room temperature and immediately fixed in 3.2% paraformaldehyde (Electron Microscopy Sciences, 15714) in PBS for 25 minutes. Worms were rinsed twice with PBS and ovaries were dissected in PBS using dissection tweezers. Briefly, cuticles of each worm were cut about a third of the length from the posterior end by gently pulling with the tweezers until the cuticle broke. Holding the tissue anterior to the cut with one tweezer, the very posterior end of the tail was pulled with the other tweezer until the cuticle was pulled off, exposing the two germlines and the intestine of the worm. Dissected germlines were collected in PBS-T (1X PBS with 0.1% Triton X-100) for subsequent immunostaining.

For electron microscopy analysis of germline tissue, live worms were immediately plunged into fixative made of 2% glutaraldehyde (VWR International, 16019) and 2.5% paraformaldehyde (Electron Microscopy Sciences, 15714) buffered with 0.1M sodium cacodylate (Electron Microscopy Sciences, 11654). Worms were fixed at room temperature for 2 hours, dissected in fixative during this incubation time. Dissections involved cutting 1mm posterior sections of the worm containing ovarian distal tips with attached cuticle tissue using a razor blade. Dissected sections, still in fixative, were placed in 4˚C until shipped on ice to collaborators at New York Blood Center, NY, USA.

Immunostaining

Dissected germline tissue was incubated with RNAse A (10 mg/mL in PBS) overnight at room temperature. Tissue was rinsed twice with PBS-T, then incubated with 1X Phalloidin 488 (Thermo Fisher) in PBS-T overnight at room temperature, protected from light. Tissue was rinsed twice with PBS-T, then stained with Propidium Iodide (Thermo Fisher) at a dilution of 1:100 in PBS-T (stock concentration of 1 mg/mL) for 25-30 seconds, and immediately rinsed twice with PBS-T. Samples were mounted on glass slides with Vectashield Mounting Media with DAPI (Vector Labs) and imaged via confocal microscopy.

EdU Assay

5-ethynyl-2'-deoxyuridine (EdU) is a thymidine analog that incorporates into actively replicating DNA. We used the Click-iT® EdU Imaging Kit with Alexa Fluor® 488 from Invitrogen to perform our EdU assays. Adult female *Brugia pahangi* were incubated in 200 µM of EdU in media (see Drug Treatments above) for 24 hours or 72 hours (denoted in text where applicable). Live worms were frozen at -80˚C to be processed at a later date. Frozen worms were thawed at room temperature and immediately fixed, dissected, and stained according to Invitrogen's protocol. Briefly, worms were fixed with 3.7% formaldehyde (Electron Microscopy Sciences) in PBS for 25 minutes. Worms were rinsed twice in PBS, and germline tissue was dissected as described above in PBS. Germline tissue was collected in 0.5 mL Eppendorf tubes and washed with 3% BSA in PBS. To permeabilize membranes, tissue was incubated in 0.5% Triton X-100 in PBS for 20 minutes at room temperature. After two rinses with 3% BSA, tissue was incubated in Click-iT® reaction cocktail made fresh according to protocol for 30 minutes. After two rinses with 3% BSA, tissue was mounted onto glass slides with Vectashield Mounting Media with DAPI (Vector Labs) and imaged via confocal microscopy.

Confocal Microscopy Analysis

Images were obtained with an inverted laser scanning Leica SP5 confocal microscope using a 63x/1.4-0.6 NA oil objective and a resonant scanner (8000 Hz). For bacteriocyte analysis, ovaries were scanned in search of *Wolbachia* clusters via direct observation through eyepieces using a DAPI filter. Tissue was scanned from top surface to bottom surface and from distal tip to uterus. Due to the differential staining of PI and DAPI, *Wolbachia* can be seen as red puncta through the eyepiece, making identification of clustering bacteria possible. Number of bacteriocytes per ovary were scored manually. Digital images were processed and analyzed using ImageJ 1.54d software.

Electron Microscopy Analysis

Six *Brugia* distal tips were received in 2% glutaraldehyde/2.5% paraformaldehyde buffered with 0.1 M sodium cacodylate. Samples were washed in buffer, and post-fixed with 1% osmium tetroxide. Samples were washed in buffer again before dehydration in an increasing ethanol series that included *en bloc* uranyl acetate staining at 70% ethanol. Following dehydration, samples were desiccated with propylene oxide and infiltrated in a 1:1 propylene oxide:epoxy resin mixture. Infiltration was continued in pure epoxy resin before embedment in pure epoxy resin at 60˚C for 48 hours. Polymerized blocks were trimmed with a razor blade and ultrathin sections were collected on formvar/carbon-coated 100 mesh grids using an RMC Boeckler Powertome and a Diatome diamond knife. Sections were contrasted with uranyl acetate and Reynolds' lead citrate and imaged in a Tecnai G2 Spirit TEM equipped with an AMT camera and imaging software. Micrograph contrast and brightness was balanced using ImageJ software.

REFERENCES

1. Greenstein D. *Control of oocyte meiotic maturation and fertilization: The C. elegans Research Community.* Wormbook, 2005.

2. Mathew CG, Bettis AA, Chu BK, English M, Ottesen EA, Bradley MH, and Turner HC. *The Health and Economic Burdens of Lymphatic Filariasis Prior to Mass Drug Administration Programs*. Clin Infect Dis. 2020. 70: 2561-2567.

3. Kozek WJ. *Transovarially-transmitted intracellular microorganisms in adult and larval stages of Brugia malayi*. J Parasitol, 1977. 63: 992-1000.

4. Kozek WJ, and Marroquin HF. *Intracytoplasmic bacteria in Onchocerca volvulus*. Am J Trop Med Hyg, 1977. 26: 663-678.

5. Sixl-voigt B, Roshdy MA, Nosek J, and Sixl W. *Electronmicroscopic investigations of Wolbachia-like microorganisms in Haemaphysalis inermis*. Mikroskopie, 1977. 33: 255-257.

6. Sironi M, Bandi C, Sacchi L, Di Sacco B, Damiani G, and Genchi C. *Molecular evidence for a close relative of the arthropod endosymbiont Wolbachia in a filarial worm*. Mol Biochem Parasitol, 1995. 74: 223-227.

7. Porter J and Sullivan W. *The cellular lives of Wolbachia*. Nat Rev Microbiol, 2023. doi: 10.1038/s41579-023-00918-x.

8. Wan Sulaiman WA, Kamtchum-Tatuene J, Mohamed MH, Ramachandran V, Ching SM, Sazlly Lim SM, Hashim HZ, Inche Mat LN, Hoo FK, and Basri H. *Anti-Wolbachia therapy for onchocerciasis and lymphatic filariasis*. Current perspectives: Indian J Med Res, 2019. 149: 706-714.

9. Ngwewondo A, Scandale I, and Specht S. *Onchocerciasis drug development: from preclinical models to humans*. Parasitol Res, 2021. 120: 3939-3964.

10. Gunderson EL, Vogel I, Chappell L, Bulman CA, Lim KC, Luo M, Whitman JD, Franklin C, Choi YJ, Lefoulon E, Clark T, Beerntsen B, Slatko B, Mitreva M, Sullivan W, and Sakanari JA. *The endosymbiont Wolbachia rebounds following antibiotic treatment*. PLoS Pathog, 2020. 16: e1008623.

11. Luan JB. *Insect Bacteriocytes: Adaptation, Development, and Evolution*. Annu Rev Entomol, 2024. 69: 81-98.

12. Kelley CA and Cram EJ. *Regulation of Actin Dynamics in the C. elegans Somatic Gonad*. J Dev Biol, 2019. 7, doi: 10.3390/jdb7010006.

13. Byrd DT and Kimble J. *Scratching the niche that controls Caenorhabditis elegans germline stem cells*. Semin Cell Dev Biol, 2009. 20: 1107-1113.

14. Foray V, Pérez-Jiménez MM, Fattouh N, and Landmann F. *Wolbachia Control Stem Cell Behavior and Stimulate Germline Proliferation in Filarial Nematodes*. Dev Cell, 2018. 45: 198-211.e3.

15. McGarry HF, Egerton GL, and Taylor MJ. *Population dynamics of Wolbachia bacterial endosymbionts in Brugia malayi*. Mol Biochem Parasitol, 2004. 135: 57-67.

16. Fischer K, Beatty WL, Jiang D, Weil GJ, Fischer PU. *Tissue and stage-specific distribution of Wolbachia in Brugia malayi*. PLoS Negl Trop Dis, 2011. 5: e1174.

17. Schiefer A, Hübner MP, Krome A, Lämmer C, Ehrens A, Aden T, Koschel M, Neufeld H, Chaverra-Muñoz L, Jansen R, Kehraus S, König GM, Pogorevc D, et al. *Corallopyronin A for short-course anti-wolbachial, macrofilaricidal treatment of filarial infections*. PLoS Negl Trop Dis, 2020. 14: e0008930.

18. Krome AK, Becker T, Kehraus S, Schiefer A, Gütschow M, Chaverra-Muñoz L, Hüttel S, Jansen R, Stadler M, Ehrens A, Pogorevc D, Müller R, Hübner MP, et al. *Corallopyronin A: antimicrobial discovery to preclinical development*. Nat Prod Rep, 2022. 39: 1705-1720.

19. Dingsdag SA and Hunter N. *Metronidazole: an update on metabolism, structure-cytotoxicity and resistance mechanisms*. J Antimicrob Chemother, 2018. 73: 265-279.

20. Deeks ED. *Fexinidazole: First Global Approval*. Drugs, 2019. 79: 215-220.

21. Serbus LR, Landmann F, Bray WM, White PM, Ruybal J, Lokey RS, Debec A, and Sullivan W. *A cell-based screen reveals that the albendazole metabolite, albendazole sulfone, targets Wolbachia*. PLoS Pathog, 2012. 8: e1002922.

22. Gayen P, Nayak A, Saini P, Mukherjee N, Maitra S, Sarkar P, and Sinha Babu SP. *A double-blind controlled field trial of doxycycline and albendazole in combination for the treatment of bancroftian filariasis in India*. Acta Trop, 2013. 125: 150-156.

23. Turner JD, Sharma R, Al Jayoussi G, Tyrer HE, Gamble J, Hayward L, Priestley RS, Murphy EA, Davies J, Waterhouse D, Cook DAN, Clare RH, Cassidy A, Steven A, Johnston KL, McCall J, Ford L, Hemingway J, Ward SA, and Taylor MJ. *Albendazole and antibiotics synergize to deliver short-course anti-Wolbachia curative treatments in preclinical models of filariasis*. Proc Natl Acad Sci USA, 2017. 114: E9712-E9721.

24. Bakowski MA, Shiroodi RK, Liu R, Olejniczak J, Yang B, Gagaring K, Guo H, White PM, Chappell L, Debec A, Landmann F, Dubben B, Lenz F, Struever D, Ehrens A, Frohberger SJ, Sjoberg H, Pionnier N, Murphy E, Archer J, Steven A, et al. *Discovery of short-course antiwolbachial quinazolines for elimination of filarial worm infections*. Sci Transl Med, 2019. 11, doi: 10.1126/scitranslmed.aav3523.

25. Hübner MP, Gunderson E, Vogel I, Bulman CA, Lim KC, Koschel M, Ehrens A, Frohberger SJ, Fendler M, Tricoche N, Voronin D, Steven A, Chi V, Bakowski MA, Woods AK, Petrassi HM, McNamara CW, Beernsten B, Chappell L, Sullivan W, Taylor MJ, Turner JD, Hoerauf A, Lustigman S, and Sakanari JA. *Short-course quinazoline drug treatments are effective in the Litomosoides sigmodontis and Brugia pahangi jird models*. Int J Parasitol Drugs Drug Resist, 2020. 12: 18-27.

26. Ballou LM and Lin RZ. *Rapamycin and mTOR kinase inhibitors*. J Chem Biol, 2008. 1: 27-36.

27. Voronin D, Cook DA, Steven A, and Taylor MJ. *Autophagy regulates Wolbachia populations across diverse symbiotic associations*. Proc Natl Acad Sci USA, 2012. 109: E1638-1646.

28. Shahinas D, Debnath A, Benedict C, McKerrow JH, and Pillai DR. *Heat shock protein 90 inhibitors repurposed against Entamoeba histolytica*. Front Microbiol, 2015. 6: 368.

29. Velkov T, Roberts KD, Nation RL, Thompson PE and Li J. *Pharmacology of polymyxins: new insights into an 'old' class of antibiotics*. Future Microbiol, 2013. 8: 711-724.

30. Fordjour FA and Kwarteng A. *The filarial and the antibiotics: Single or combination therapy using antibiotics for filariasis*. Front Cell Infect Microbiol, 2022. 12: 1044412.

31. Hübner MP, Koschel M, Struever D, Nikolov V, Frohberger SJ, Ehrens A, Fendler M, Johannes I, Von Geldern TW, Marsh K, Turner JD, Taylor MJ, Ward SA, Pfarr K, Kempf DJ, and Hoerauf A. *In vivo kinetics of Wolbachia depletion by ABBV-4083 in L. sigmodontis adult worms and microfilariae*. PLoS Negl Trop Dis, 2019. 13: e0007636.

32. Buchner P. *Endosymbiosis of animals with plant microorganisms*. 1965. New York, NY: Interscience Publishers.

33. Alarcón ME, Polo PG, Akyüz SN, and Rafiqi AM. *Evolution and ontogeny of bacteriocytes in insects*. Front Physiol, 2022. 13, 1034066.

34. Vigneron A, Masson F, Vallier A, Balmand S, Rey M, Vincent-Monégat C, Aksoy E, Aubailly-Giraud E, Zaidman-Rémy A, and Heddi A. *Insects recycle endosymbionts when the benefit is over*. Curr Biol, 2014. 24: 2267-2273.

35. Hosokawa T, Koga R, Kikuchi Y, Meng XY, and Fukatsu T. *Wolbachia as a bacteriocyte-associated nutritional mutualist*. Proc Natl Acad Sci USA, 2010. 107: 769-774.

36. Szklarzewicz T, Kalandyk-Kolodziejczyk M, and Michalik A. *Ovary structure and symbiotic associates of a ground mealybug, Rhizoecus albidus (Hemiptera, Coccomorpha: Rhizoecidae) and their phylogenetic implications*. J Anat, 2022. 241: 860-872.

37. Sacchi L, Genchi M, Clementi E, Negri I, Alma A, Ohler S, Sassera D, Bourtzis K, and Bandi C. *Bacteriocyte-like cells harbour Wolbachia in the ovary of Drosophila melanogaster (Insecta, Diptera) and Zyginidia pullula (Insecta, Hemiptera)*. Tissue Cell, 2010. 42: 328-333.

38. Strunov A, Schneider DI, Albertson R, and Miller WJ. *Restricted distribution and lateralization of mutualistic Wolbachia in the Drosophila brain*. Cell Microbiol, 2017. 19: doi: 10.1111/cmi.12639.

39. Hall DH, Winfrey VP, Blaeuer G, Hoffman LH, Furuta T, Rose KL, Hobert O, and Greenstein D. *Ultrastructural features of the adult hermaphrodite gonad of Caenorhabditis elegans: relations between the germ line and soma*. Dev Biol, 1999. 212: 101-123.

40. McCarter J, Bartlett B, Dang T, and Schedl T. *Soma-germ cell interactions in Caenorhabditis elegans: multiple events of hermaphrodite germline development require the somatic sheath and spermathecal lineages*. Dev Biol, 1997. 181: 121-143.

41. McCarter J, Bartlett B, Dang T, and Schedl T. *On the control of oocyte meiotic maturation and ovulation in Caenorhabditis elegans*. Dev Biol, 1999. 205: 111-128.

42. Landmann F, Foster JM, Slatko B, and Sullivan W. *Asymmetric Wolbachia segregation during early Brugia malayi embryogenesis determines its distribution in adult host tissues*. PLoS Negl Trop Dis, 2010. 4: e758.

43. Gumienny TL and Hengartner MO. *How the worm removes corpses: the nematode C. elegans as a model system to study engulfment*. Cell Death Differ, 2001. 8: 564-568.

44. Li X, Singh N, Miller C, Washington I, Sosseh B, Gordon KL. *The C. elegans gonadal sheath Sh1 cells extend asymmetrically over a differentiating germ cell population in the proliferative zone*. eLife, 2022. 11: e75497.

45. Sangaré AK, Rolain JM, Gaudart J, Weber P, and Raoult D. *Synergistic activity of antibiotics combined with ivermectin to kill body lice*. Int J Antimicrob Agents, 2016. 47: 217-223.

46. Weeratunga P, Moller DR, and Ho LP. *Immune mechanisms of granuloma formation in sarcoidosis and tuberculosis*. J Clin Invest, 2024. 134: doi: 10.1172/JCI175264.

47. Day NJ, Santucci P, and Gutierrez MG. *Host cell environments and antibiotic efficacy in tuberculosis*. Trends Microbiol, 2023. doi: 10.1016/j.tim.2023.08.009.

48. Jamabo M, Mahlalela M, Edkins AL, and Boshoff A. *Tackling Sleeping Sickness: Current and Promising Therapeutics and Treatment Strategies*. Int J Mol Sci, 2023. 24: doi: 10.3390/ijms241512529.

49. Wittlin S and Mäser P. *From Magic Bullet to Magic Bomb: Reductive Bioactivation of Antiparasitic Agents*. ACS Infect Dis, 2021. 7: 2777-2786.

50. Liu HY, Wang YK, Zhi CC, Xiao JH, and Huang DW. *A novel approach to eliminate Wolbachia infections in Nasonia vitripennis revealed different antibiotic resistance between two bacterial strains*. FEMS Microbiol Lett, 2014. 355: 163-169.

51. Mosaei H and Harbottle J. *Mechanisms of antibiotics inhibiting bacterial RNA polymerase.* Biochem Soc Trans, 2019. 47: 339-350.

52. Marriner SE and Bogan JA. *Pharmacokinetics of albendazole in sheep*. Am J Vet Res, 1980. 41: 1126-1129.

53. Borgers M, De Nollin S, De Brabander M, and Thienpont D. *Influence of the anthelmintic mebendazole on microtubules and intracellular organelle movement in nematode intestinal cells*. Am J Vet Rs, 1975. 36: 1126-1129.

54. Huang J, Wang H, Chen Y, Wang X, Zhang H. *Residual body removal during spermatogenesis in C. elegans requires genes that mediate cell corpse clearance*. Development, 2012. 139(24): 4613-4622.

Chapter 6: A novel "lasso" assay reveals *Brugia pahangi* is capable of both ingestion of drugs and absorption through their cuticle

ABSTRACT

Filarial nematodes are the causative agent of the neglected tropical diseases elephantiasis and African river blindness. Mass drug administration programs of microfilaricidal compounds have proven to be a promising means of limiting the spread of these diseases in afflicted regions of the world. However, because these worms can reside in their human host for up to 8 to 15 years, people infected with these parasites must continually take microfilaricidal drugs for the duration of the lifespan of the parasite. Many research groups across the globe are implementing drug discovery efforts to identify macrofilaricidal compounds to fully eliminate adult worms from infected patients. These efforts invariably utilize *in vitro* drug treatment assays that incubate *Brugia* species of nematodes in drug-treated media. Despite the widespread use of these *in vitro* incubation assays, it remains unclear if worms are consuming drugs through ingesting the media, or if they absorb the drugs through their cuticles. Here we examine a novel "lasso" experiment that incorporates suspending the anterior feeding end of the worm out of rhodamine-labeled media in an attempt to determine if ingestion or absorption is favored in the nematode system. We find that rhodamine incorporation in *Brugia pahangi* tissues, predominantly the intestinal tissues, occurred regardless of suspension of the head. We conclude that *Brugia pahangi* are capable of both ingesting and absorbing chemical compounds.

INTRODUCTION

Parasitic nematodes cause devastating filarial diseases such as Lymphatic filariasis (Elephantiasis) and Onchocerciasis (African River Blindness). These Neglected Tropical Diseases (NTDs) cause debilitating symptoms for those infected by these parasitic nematodes. Three species of filarial nematodes cause Elephantiasis in humans: *Brugia*

malayi, *Brugia timori*, and *Wuchereria bancrofti*. The adult worms of these species reside within the lymphatic system of their human host and have a lifespan of 6-8 years. Due to this longstanding blockage of the lymphatic system, improper drainage of lymphatic and interstitial fluids can lead to painful swelling of the extremities known as lymphedema, thickening of the skin known as elephantiasis, and scrotal swelling known as hydrocele. In severe cases, people with these disfiguring symptoms cannot walk and may not be able to work and provide for their families, or may be socially outcast within their communities [1].

African River Blindness is caused by a single species of filarial nematode, *Onchocerca ochengi*, which has a lifespan of 12-15 years. The larval stages of this species reside in and move throughout the subcutaneous tissues of the skin. This causes intense and often painful itching in people infected by these parasites. In many cases, the larval worms invade ocular tissues of the human host, causing inflammation and irreversible damage, leading to permanent blindness [2,3]. Together, these two NTDs affect over 65 million people in tropical areas of the world. Over 1 billion people are at risk of infection and require preventative chemotherapy in the form of mass drug administration (MDA) programs [1,3]. Currently, there are no cures for these diseases, only treatment of symptoms and preventative measures such as MDAs and vector control strategies.

One of the most successful preventative measures for reducing the spread of filarial diseases has been the implementation of mass drug administration programs. Largescale annual and biannual distributions of the drugs Ivermectin, Albendazole, and Diethylcarbamazine (DEC) have successfully reduced the infection status of people in affected countries. These drugs specifically target the larval stages of the filarial parasites, helping to reduce transmission of these diseases [4,5]. However, since the adult stages of these worms can live inside the human host for up to 8 to 15 years, massive efforts to continually distribute these microfilaricidal drugs must be maintained each year. In order to rid worms from an infected patient and cure these filarial diseases, the world needs drugs that can specifically target the adult nematodes. For decades now, research groups across the

globe have participated in drug discovery efforts to identify small molecule compounds capable of targeting the adult parasite. This includes the many efforts to identify drugs that will target the natural bacterial endosymbiont of these filarial worms, *Wolbachia* [6-8]. *Wolbachia* is an attractive target for macrofilaricidal compounds because the adult worms rely on this bacterial symbiont for proper reproduction and survival [9,10]. Killing *Wolbachia* prevents transmission of these diseases by disrupting reproduction, and by eventually killing the parasite.

Despite these widespread efforts to screen for macrofilaricidal compounds, the mechanisms by which filarial nematodes take up chemical compounds remains unclear. Nematodes are roundworms of the phylum Nematoda, and constitute one of the most successfully adaptive species on the planet, populating nearly every ecosystem from salt and freshwater marine systems, to tropical and polar terrestrial environments [11]. One study even estimates that nematodes make up 80% of all individual animals on earth [11]. True to the phylum's astounding diversity, Nematodes have a wide variety of evolutionarily adapted feeding mechanisms. Soil nematodes contain mouth parts that form simple tubes and feed on bacteria within the soil [12]. Plant parasitic nematodes contain more complex features at their anterior end, such as the piercing stylet structure that allows the worm to puncture through and feed from plant tissues like a straw [12]. Filarial nematodes, including the species utilized in this study, *Brugia pahangi*, contain the more simplistic version of these feeding structures. The nematode species responsible for lymphatic filariasis and African river blindness are known to feed on blood and lymphatic fluids of their human hosts [13].

While there is evidence that the nematode model organism *C. elegans* can absorb drug compounds via absorption through their cuticle, it is still a topic of debate whether absorption or ingestion play a major role in nematode consumption [14]. We wanted to know if the *Brugia* species that are often used in macrofilaricidal drug screening efforts are capable of the same chemical absorption, or if their modality of consumption is strictly limited to ingestion. Here we describe a novel "lasso" assay that identifies the dual mode of drug

consumption by both ingestion and absorption in the nematode species *B. pahangi*. These results can inform both drug screening assays and medicinal chemistry efforts to discover or design macrofilaricidal compounds that target filarial parasites.

RESULTS

To identify if *Brugia pahangi* are capable of absorbing chemical compounds through their cuticle as a direct mode of consumption, we developed a novel “lasso” assay. This assay allows the worm to be submerged in media while its head stays suspended outside of the media. Fluorescent rhodamine was added to the media to identify any fluorescent incorporation within the nematode tissues through confocal microscopy analysis. We chose fluorescent rhodamine due to its similar molecular size and weight as doxycycline, a common antibiotic often used as positive controls in drug treatment regimens [15,16]. In addition, rhodamine labeling has long been used as a biomarker in wildlife rabies vaccination programs to identify animals that have successfully eaten bait laced with rabies vaccine [17]. Due to the similar chemical sizes and characteristics of doxycycline and rhodamine, we reason that incorporation of rhodamine into worm tissues can be extrapolated to doxycycline and potentially any other chemical compounds of similar size and structure. We used a concentration of rhodamine equivalent to that used for doxycycline in other drug screening experiments of *Brugia pahangi*, 5 µM [15,16].

The experimental design called for suspending the nematode’s head above the rhodamine-labeled media to ensure the worms were not feeding on the fluorescent media. To do this, we needed a material thin enough and malleable enough to tie around the head of the adult worm, and which was readily available and easy to sterilize. We chose to use human hair provided by researchers in the lab. Through careful manipulation, a slip knot was created in the strand of hair, nematode heads were gently pulled through the loop, and the lasso was tightened just enough to hold the worm without risk of decapitation. The strand of hair was then placed in a slit created in sterilized card stock and adjusted to allow for the

majority of the worm's body to be submerged in rhodamine-labeled media while suspending the mouth above the surface of the solution. Figure 6.1 illustrates the procedure of "lassoing" the *Brugia* nematodes.

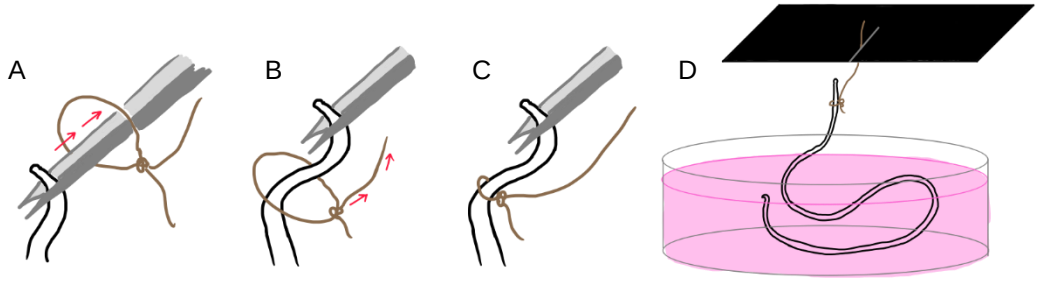

Fig 6.1 *Brugia pahangi* heads were suspended above fluorescently-labeled media using a novel lasso procedure. A graphical depiction of this lasso procedure can be seen in panels A-D. Microdissection tweezers were used to gently pull the head of each worm through a loop made from creating a slip knot in human hair, and suspended above rhodamine-labeled media. The lasso was held in place by a slit cut into sterilized card stock resting against the top of the 6-well plate in which worms were incubated. Worms were incubated overnight (20 hours) in 5 µM rhodamine and analyzed for fluorescence with confocal microscopy.

To see how rhodamine is incorporated into worm tissues when the worms are allowed to feed, a group of worms completely submerged in rhodamine-media served as a control. To identify any potential autofluorescence of the nematode tissues that may exist in the emission spectra of rhodamine, we included a group of worms submerged in media without rhodamine added. Confocal microscopy analysis of these three experimental groups showed rhodamine fluorescence in both the lasso and submerged groups, but not the unlabeled control group (Figure 6.2). In the lasso group, fluorescence was seen in both the intestinal and germline tissues of the worm, indicating rhodamine's ability to enter tissues of the worm without being ingested via the mouth. In the submerged group, fluorescence appeared brighter in the intestinal tissue, indicating rhodamine incorporation is probably predominantly attributed to ingestion. But the strong fluorescence also seen in the intestine

of lassoed worms show that *Brugia pahangi* are clearly capable of absorbing chemicals through their cuticle as well.

Brugia pahangi worms are about 2 cm to 3 cm in length, and it is virtually impossible to distinguish the head from the tail by eye. While attempting to lasso the heads of each worm, it is inevitable that one will lasso the tail by accident. Fortunately, this serves as an additional control to our study. Perhaps *Brugia* nematodes are capable of incorporating rhodamine-labeled media through the anus at the posterior end of the worm. This seems highly unlikely as the digestive systems of most animals have strong mechanisms in place to only allow for one-way movement of digested food, but the strong fluorescence seen in the intestinal tract of our lassoed worms calls for this consideration. In fact, there are reports of some animals being capable of feeding from their anus. A 2013 study showed the Giant California Sea Cucumber, *Parastichopus californicus*, was capable of this "bipolar feeding," incorporating radioactive algae through their cloaca [18].

Of the five worms we attempted to lasso, only two were successfully suspended above the media by their heads. Two were accidentally decapitated, and one was lassoed by the tail. This tail-lassoed worm incorporated rhodamine in its intestinal tissue throughout the body but not at the tail end (Figure 6.2, bottom panel). This indicates that submerging the tail portion of the filarial nematode in media is not necessary for rhodamine incorporation into its tissues. However, we did not perform an experiment in which both head and tail are suspended simultaneously outside of media. This experiment would be necessary to determine if cuticle absorption can serve as the sole means of rhodamine consumption from the worm's environment.

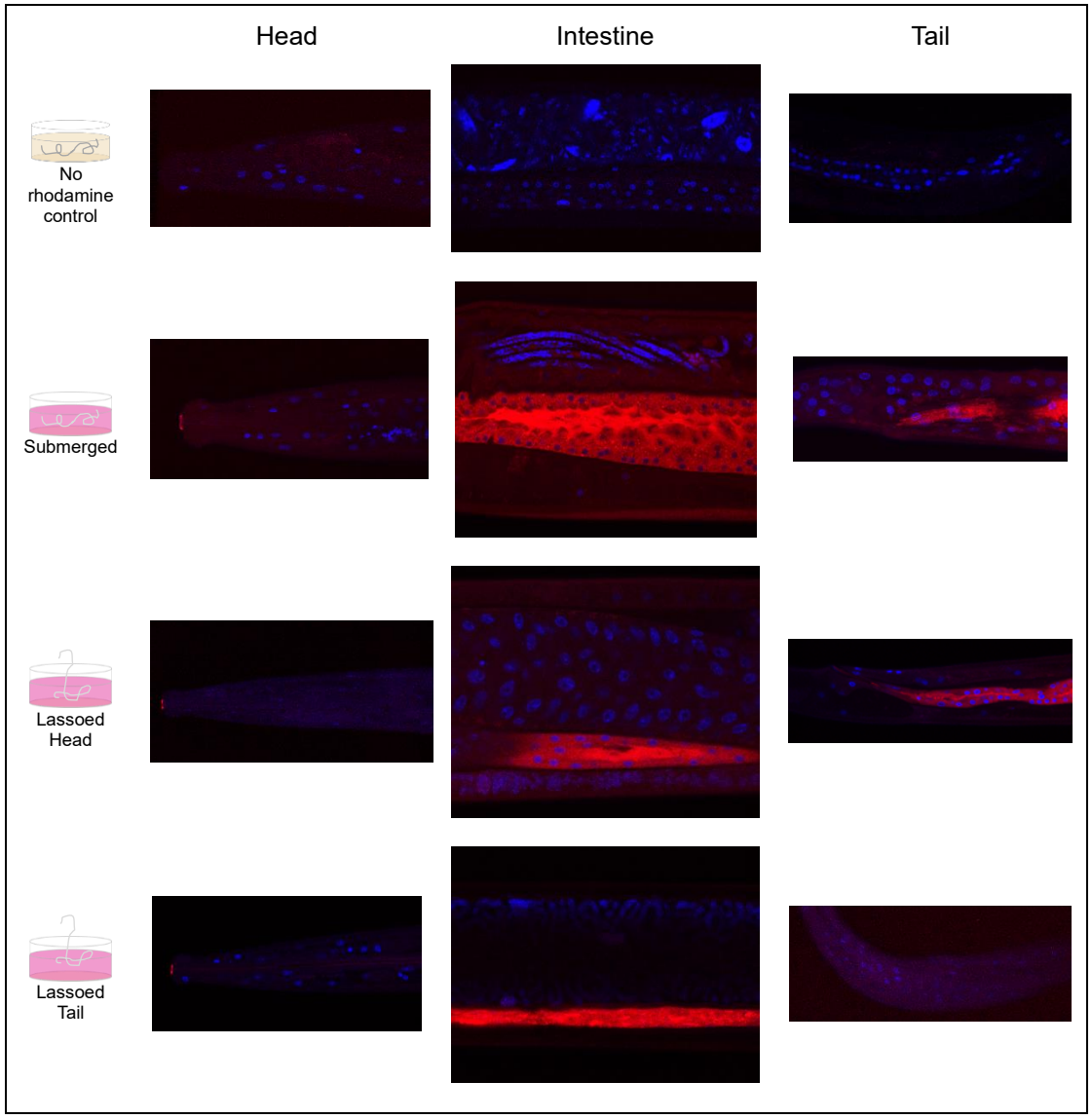

Figure 6.2 Rhodamine incorporation of *Brugia pahangi* tissues is independent of the head being submerged in media. Worms were incubated in media consisting of 5 µM rhodamine or no rhodamine control for 20 hours. Images were taken of the head, midbody intestine, and tail portions of the worms to trace rhodamine incorporation. Rhodamine fluorescence can be seen clearly in the intestine and tail regions of the worms regardless of their heads being submerged. Tail-lassoed worms also showed fluorescence in their intestinal tissue, but not at the suspended tail end. The same laser settings were used across all conditions for the rhodamine emission channel. This was to ensure the fluorescence we saw was not due to tissue autofluorescence.

DISCUSSION

Understanding the mode of consumption of drug compounds in *Brugia* filarial nematodes is important for drug discovery efforts in the fight against filarial diseases. *In vitro* drug screening assays of *Brugia* nematodes must consider how nematode tissues are exposed to the chemical compound. Ingestion through the mouth may result in metabolism of the drug, potentially exposing other tissues of the worm to different chemical variations of the drug, whereas absorption directly through the cuticle will result in no such metabolite exposures.

Through our lasso assay experiments, we showed that *Brugia pahangi* worms are capable of consuming fluorescent rhodamine even with their heads suspended above the media. This suggests they are absorbing chemicals through their cuticles. However, these results are preliminary and further experimentation must be performed to eliminate the possibility that drugs can enter through other cavities of the worm. In our experiment, we lassoed and suspended worms by either the head or the tail. In each of these worms, rhodamine incorporation was visualized in the intestinal tissues through confocal microscopy analysis. However, it is possible that this rhodamine incorporation could have entered via the other end of the digestive tract (the anus in the case of the suspended head trial, and the mouth in the case of the suspended tail trial). It would be prudent to repeat this experiment by suspending both head and tail out of the media simultaneously. This would verify that rhodamine incorporation is occurring strictly through cuticle absorption rather than entering through body cavities of the worm.

MATERIALS AND METHODS

Reagents

Rhodamine B (Fisher Scietific, #S25785) was dissolved in deionized water to a stock concentration of 10 mM. This solution was further diluted in *Brugia* media (80% RPMI 1640 [Gibco], 10% FBS [Life Technologies], and 10% DMEM [Corning]) to a final concentration of 5 µM.

Live *B. pahangi* worms, harvested from infected jirds (*Meriones unguiculatus*), were supplied by the NIAID/NIH Filariasis Research Reagent Resource Center (FR3, Athens, GA, USA, www.filariasiscenter.org) via the Biodefense and Emerging Infections Research Resources Repository (BEI Resources, Manassas, VA, USA). Upon delivery, live worms were placed in an incubator at 37˚C with 5% CO_2 to recover overnight from shipping. Lasso experiments were performed the following day.

Lassos

Human hair was generously donated by Sommer Fowler. Each strand of hair was tied into a loop using a simple slip knot to allow for adjustment of the size of the loop. Lassos were placed between two Kimwipe® laboratory task wipers, and doused in 70% ethanol to sterilize. To lasso the nematodes, nematode heads were gently pulled through the loop of each lasso using microdissection tweezers. Then the lasso was tightened just enough to hold the worm in place and not decapitate it. The strand of hair was then placed in a slit created in sterilized card stock and adjusted to allow for the majority of the worm's body to be submerged in rhodamine-labeled media while suspending the mouth above the surface of the solution. See Figure 6.1 for a graphical depiction of this process. Lassoed worms were placed in single wells of a 6-well dish in 10 mL of labeled or un-labeled media. The card stock holding the lasso in place rested on top of the edges of the well. Worms were allowed to incubate in media for 20 hours, then transferred to 1.5 mL collection tubes and frozen at -80˚C for later immunostaining.

Immunostaining

Frozen worms were thawed at room temperature and immediately fixed in 3.2% paraformaldehyde (Electron Microscopy Sciences, 15714) in PBS for 25 minutes. Worms were rinsed twice with PBS and submerged in Vectashield Mounting Media with DAPI (Vector Labs) for two hours before mounting on a glass slide for confocal imaging.

Confocal Microscopy Analysis

Images were obtained with an inverted laser scanning Leica SP5 confocal microscope using a 63x/1.4-0.6 NA oil objective and a resonant scanner (8000 Hz). Rhodamine-labeled worms were imaged first and the laser settings were set based on these samples. The same exact settings established for the rhodamine channel were kept for imaging the unlabeled control worms to assess for tissue autofluorescence in the emission spectra for rhodamine. Very little autofluorescence was detected in these tissues. Digital images were processed and analyzed using ImageJ 1.54d software.

REFERENCES

1. World Health Organization. “Lymphatic filariasis.” (2023) Available from: https://www.who.int/news-room/fact-sheets/detail/lymphatic-filariasis (Accessed March 2024).

2. Institute for Health Metrics and Evaluation (IHME). “GBD Results.” (2020) Seattle, WA: IHME, University of Washington. Available from: https://vizhub.healthdata.org/gbd-results (Accessed March 2024).

3. World Health Organization. “Onchocerciasis.” (2022) Available from: https://www.who.int/news-room/fact-sheets/detail/onchocerciasis (Accessed March 2024).

4. Taylor MJ, Hoerauf A, Bockarie M. *Lymphatic filariasis and onchocerciasis*. The Lancet, 2010. **376**(9747): 1175–1185.

5. Molyneux DH, Bradley M, Hoerauf A, Kyelem D, Taylor MJ. *Mass drug treatment for lymphatic filariasis and onchocerciasis*. Trends Parasitol, 2003. **19**: 516–522

6. Slatko BE, Luck AN, Dobson SL, Foster JM. *Wolbachia endosymbionts and human disease control*. Mol Biochem Parasitol, 2014. **195**: 88–95.

7. Hoerauf A, Volkmann L, Hamelmann C, Adjei O, Autenrieth IB, Fleischer B, et al. *Endosymbiotic bacteria in worms as targets for a novel chemotherapy in filariasis*. Lancet, 2000. **355**: 1242–1243.

8. Taylor MJ, Hoerauf A, Townson S, Slatko BE, Ward SA. *Anti-Wolbachia drug discovery and development: safe macrofilaricides for onchocerciasis and lymphatic filariasis*. Parasitology, 2014. **141**: 119–127.

9. Taylor MJ, Makunde WH, McGarry HF, Turner JD, Mand S, Hoerauf A. *Macrofilaricidal activity after doxycycline treatment of Wuchereria bancrofti: a double-blind, randomised placebo-controlled trial*. Lancet, 2005. **365**: 2116–2121.

10. Debrah AY, Specht S, Klarmann-schulz U, Batsa L, Mand S, Marfo-Debrekyei Y, et al. *Doxycycline Leads to Sterility and Enhanced Killing of Female Onchocerca volvulus Worms in an Area With Persistent Microfilaridermia After Repeated Ivermectin Treatment: A Randomized, Placebo-Controlled, Double-Blind Trial*. Clin Infect Dis, 2015. **61**: 517–526.

11. van den Hoogen J, Geisen S, Routh D, Ferris H, Traunspurger W, Wardle DA, de Goede RGM, Adams BJ, Ahmad W, Andriuzzi WS, et al. *Soil nematode abundance and functional group composition at a global scale*. Nature, 2019. **572**(7768): 194-198.

12. Kiontke K and Fitch DHA. *Nematodes*. Curr Biol, 2013. **23**(19): R862-R864.

13. Baron S, editor. Medical Microbiology. 4th ed. Galveston (TX): University of Texas Medical Branch at Galveston; 1996. PMID: 21413252.

14. Höss S, Sanders D, van Egmond R. *Determining the toxicity of organic compounds to the nematode Caenorhabditis elegans based on aqueous concentrations*. Environ Sci Pollut Res Int, 2023. **30**(42):96290-96300.

15. Serbus LR, Landmann F, Bray WM, White PM, Ruybal J, Lokey RS, Debec A, and Sullivan W. *A cell-based screen reveals that the albendazole metabolite, albendazole sulfone, targets Wolbachia*. PLoS Pathogens, 2012. 8(9): e1002922.

16. Bulman CA, Chappell L, Gunderson E, Vogel I, Beerntsen B, Slatko BE, Sullivan W, Sakanari JA. *The Eagle effect in the Wolbachia-worm symbiosis*. Parasit Vectors, 2021. **14**(1):118.

17. Slate D, Algeo TP, Nelson KM, Chipman RB, Donovan D, Blanton JD, Niezgoda M, Rupprecht CE*. Oral rabies vaccination in North America: opportunities, complexities, and challenges*. PLoS Negl Trop Dis, 2009. **3**(12): e549.

18. Jaeckle WB and Strathmann RR. *The anus as a second mouth: anal suspension feeding by an oral deposit-feeding sea cucumber*. Invertebrate Biology, 2013. **132**(1): 62-68. doi: 10.1111/ivb.12009.

Chapter 7: Unpublished Screening Data

This chapter contains unpublished screening data from secondary and tertiary screening assays identifying anti-*Wolbachia* effects of small molecules from a primary high-throughput cell screen. High-throughput cell screening assays were performed by a previous lab member, Dr. Pamela White. With the help of the UCSC Chemical Screening Center, Dr. White's initial drug screen tested 4,926 compounds from two separate drug compound libraries, and identified 40 candidate hits which significantly reduced *Wolbachia* titer in the JW18 cells.

Hits from this screen were then tested in the *Drosophila melanogaster* secondary screen. Briefly, newly eclosed *D. melanogaster* females were fed drug-treated food (at a concentration of 50 μM) for three days. Then, ovaries were dissected, fixed and stained, and imaged using confocal microscopy to analyze the number of *Wolbachia* in mature oocytes.

Hits from the secondary *D. melanogaster* screen were tested in a tertiary filarial nematode screen. Briefly, *B. pahangi* females were incubated with drug-treated media (at a concentration of 5 μM) for three days. Then, ovaries were dissected, fixed and stained, and imaged using confocal microscopy to analyze the number of *Wolbachia* in the distal tip region of the germline.

I found that while some hit compounds were successful at reducing *Wolbachia* in the secondary assay, these results were not always parallelled in the tertiary assay. This could be due in part to the different strains of *Wolbachia* present in the fruit fly versus nematode hosts. The strain of *Wolbachia* found in *D. melanogaster* is different from the strain found in *Brugia* species of filarial nematodes, and show different patterns of gene expression. The *Wolbachia* strain found in our *Drosophila*-derived immortal cell lines is wMel, a member of the *Wolbachia* Supergroup A. These *Wolbachia* strains are characterized as reproductive parasites, and are facultative in nature with their arthropod hosts, meaning hosts do not require *Wolbachia* infections to survive. The *Wolbachia* strain found in our tertiary screening

nematode model is wBp, a member of the *Wolbachia* Supergroup D. These *Wolbachia* strains are characterized as obligate mutualists, in which the filarial nematode relies on the bacterial endosymbiont for reproduction and survival. Results of the secondary and tertiary drug screens can be seen below in Figure 7.1.

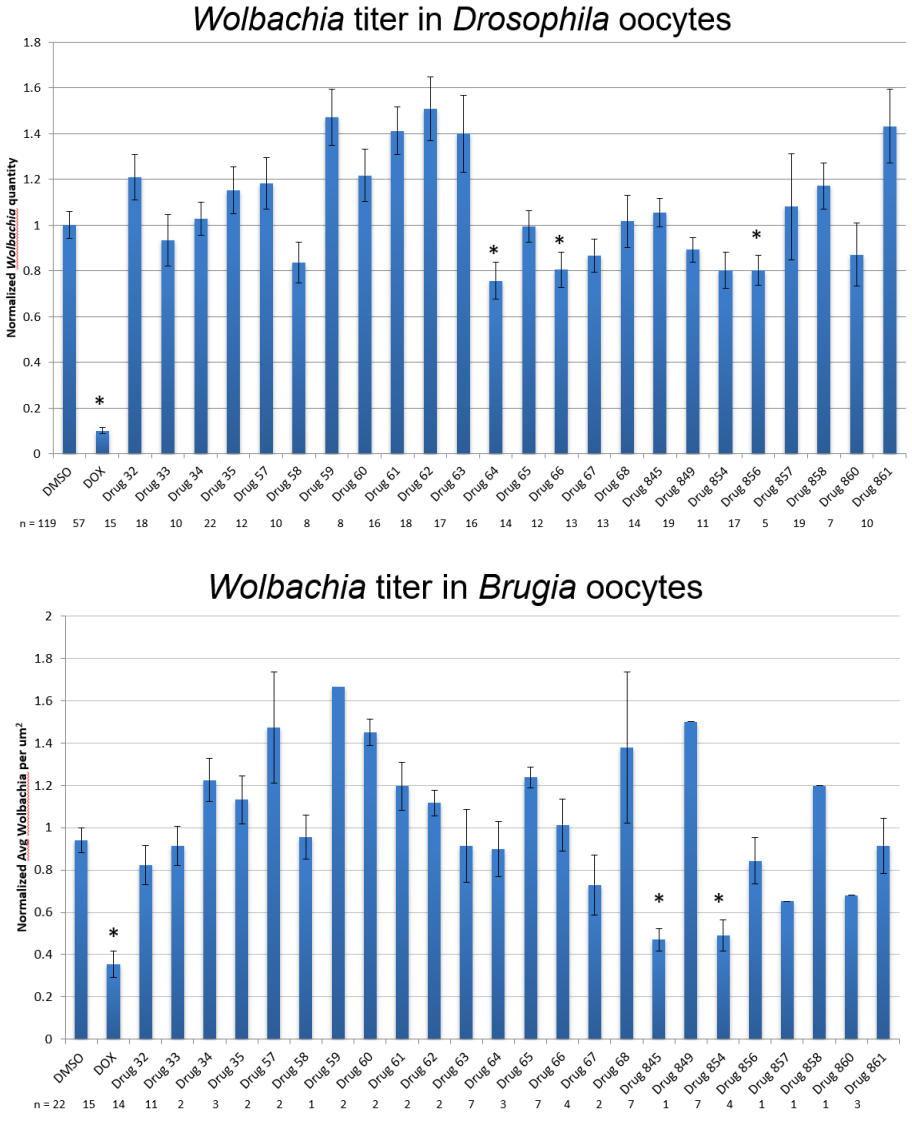

Figure 7.1 Unpublished secondary and tertiary screening data. Hit drug compounds from a primary high-throughput cell culture screen were tested in secondary *Drosophila* (top) and tertiary *Brugia* (bottom) screening assays to assess for anti-*Wolbachia* properties.

Chapter 8: Discussion

Throughout my dissertation work, I addressed a number of questions regarding antibiotic and small molecule effects on *Wolbachia* titer and clustering morphology in parasitic nematodes. However, many questions were raised as well, and further research is necessary to advance the work performed in my thesis project. Here, I summarize the key findings in my dissertation project and discuss future avenues of research for this endosymbiont-host system and its implications in finding cures for filarial diseases.

In Chapter 2, I addressed the efficacy of utilizing a high-throughput cell culture screen to identify anti-*Wolbachia* drugs. Two separate primary cell screens were performed before I joined the lab, and these resulted in separate lists of hit compounds that significantly reduced *Wolbachia* titer in naturally infected *Drosophila melanogaster* JW18 and LDW1 cell lines. For the beginning of my thesis work, I took the top hit compounds from these screens and tested them in both a secondary *in vivo D. melanogaster* assay and a tertiary *in vitro Brugia pahangi* nematode assay.

For the secondary assay, newly eclosed *D. melanogaster* females were fed drug-treated food for three days. Then, the ovaries were dissected, fixed and stained, and imaged using confocal microscopy to analyze the number of *Wolbachia* in mature oocytes. For the tertiary assay, *B. pahangi* females were incubated with drug-treated media for three days. Then, the ovaries were dissected, fixed and stained, and imaged using confocal microscopy to analyze the number of *Wolbachia* in the distal tip region of the germline. I found that while some hit compounds were successful at reducing *Wolbachia* in the secondary assay, these results were not always parallelled in the tertiary assay. This could be due in part to the different strains of *Wolbachia* present in the fruit fly versus nematode hosts. The strain of *Wolbachia* found in *D. melanogaster* is different from the strain found in *Brugia* species of filarial nematodes, and show different patterns of gene expression. The *Wolbachia* strain found in our *Drosophila*-derived immortal cell lines is wMel, a member of the *Wolbachia*

Supergroup A. These *Wolbachia* strains are characterized as reproductive parasites, and are facultative in nature with their arthropod hosts, meaning hosts do not require *Wolbachia* infections to survive. The *Wolbachia* strain found in our tertiary screening nematode model is wBp, a member of the *Wolbachia* Supergroup D. These *Wolbachia* strains are characterized as obligate mutualists, in which the filarial nematode relies on the bacterial endosymbiont for reproduction and survival. *Wolbachia* of Supergroup D are capable of supplying essential nutrients to their host, such as riboflavin, biotin, thiamine, and more, while *Wolbachia* of supergroup A do not generally have these capabilities [1]. These differences between the wMel strain in both our primary and secondary assays versus the wBp strain in our tertiary nematode assay could be the reason we saw differential effects of drug treatment between the assays.

Additionally, one must consider the different modes of ingestion between the secondary and tertiary assays. The fruit fly secondary assay incorporates drug compounds in the fly's diet, so the role of metabolism on the drug's mechanism of action must be considered. The nematode assay involves submerging the worm in drug-treated media. Supplemental experiments indicated that the nematodes in these assays both ingest media and absorb media through their cuticle. The mode of transmission of these drug compounds differs between hosts, and could be the source of differential drug effects on *Wolbachia* titers.

Continual drug screening for anti-*Wolbachia* compounds will be crucial in the coming years, as drug resistance is an ever-present issue that must be monitored and addressed. Therefore, it will be necessary to establish a high-throughput cell culture screen utilizing the specific strains of *Wolbachia* found in filarial nematodes. Collaborator Dr. Alain Debec, who created our JW18 and LDW1 cell lines, attempted to create a *Brugia*-derived cell line as well, with no success (data not published). This is clearly a challenging feat, and to date no nematode cell line (filarial or other) has been created. Dr. Pamela White, a former graduate student of the Sullivan lab, showed that horizontal transfer of *Wolbachia* occurs between cell lines when infected and uninfected cells are cultured together [2]. In fact, a 2023 report by

Manoj et al. successfully created a line of S2 *Drosophila* cells that stably house *Wolbachia* of the roundworm canine parasite *Dirofilarial immitis*, or heartworm [3]. Although these cell lines had not been around long enough to be deemed “immortal” at the time of publishing, it their results show a promising ability to infect *Drosophila* cells with a filarial nematode strain of *Wolbachia*. In addition, a post-doctoral researcher in the Sullivan lab, Shelbi Russell, showed that S2 *D. melanogaster* cells may be artificially infected with crude *Wolbachia* isolate. These macrophage-like S2 cells take up the *Wolbachia* in endocytic vesicles that evade degradation—possibly through key effectors of the bacteria themselves—and stably infect the cell lines indefinitely (personal correspondence). Dr. Russell has created S2 cell lines housing *Wolbachia* strains of the *D. simulans* host, wRi (unpublished data). Time will tell if these cell lines remain immortal, but if they do, one could repeat the experiment using crude *Wolbachia* isolate from *Brugia malayi* nematodes. This cell line can then be used for future high-throughput drug screening assays as a means to identify small molecules capable of specifically targeting the *Wolbachia* strains found in parasitic worms that infect humans.

Chapter 3 discusses the observation that *Wolbachia* endosymbionts of *Brugia pahangi* exhibit the Eagle effect, a paradoxical phenomenon in which higher concentrations of antibiotic prove to be less effective at reducing bacterial titer. While the Eagle effect is a known phenomenon seen in other bacterial and even some fungal systems, it had never before been reported in this *Wolbachia-Brugia* symbiosis. The causes of the Eagle effect are not known, but one theory to the underlying mechanism suggests that higher concentrations of antibiotics may induce a quiescent state within the bacteria, allowing the bacteria to elude the effects of the drug and persist in this state until the compound dissipates out of host cells and tissues [4-6].

These findings are of great importance in the effort to cure filarial diseases by way of targeting *Wolbachia* because it underscores the importance of finding the correct concentration to rid the parasites of their bacterial endosymbionts. If treating human patients with too high of a concentration can result in persistence of the bacteria, we may be creating

a worse situation for those afflicted with these diseases. A better understanding of the correct dosage for anti-*Wolbachia* compounds is crucial for the success of these efforts. In addition, more studies must be performed to fully understand if antibiotic treatment is inducing a dormant, “persister” state in *Wolbachia*. This may be the cause of the formation of *Wolbachia* bacteriocytes described in Chapter 4 and Chapter 5.

In addition to observing the Eagle effect on *Wolbachia* dispersed throughout the germline tissue of filarial nematodes, we wonder if the Eagle effect can be seen in the number of *Wolbachia* bacteriocytes described in Chapters 4 and 5. Perhaps there is an optimal concentration of antibiotics that will specifically target these bacteriocytes. Discovering the Eagle effect in *Wolbachia* has implications not only for the specific compounds that target *Wolbachia*, but also the specific concentrations of those compounds. It could prove important to test anti-bacteriocyte compounds at differing concentrations to see if there is an optimal concentration for reducing occurrence of bacteriocytes in filarial nematodes.

Chapter 4 describes the long-term effects of a short-course antibiotic treatment on a parasite-infected mammalian model. While a one-week treatment of rifampicin was enough to reduce *Wolbachia* numbers by 95% in the filarial worms, the bacteria rebounded to control levels after 36-weeks post-treatment. Due to time and cost, researchers do not extend drug-treatment studies in mammalian models past 17 weeks. This finding that recrudescence of *Wolbachia* occurs only eight months post-treatment poses an extreme problem for anti-*Wolbachia*-mediated efforts to treat filarial diseases. Even with the continual discovery of anti-*Wolbachia* compounds for the use of treating lymphatic filariasis and onchocerciasis, if these drugs are not tested for their long-term effects, any treatment may be ineffective in a human patient. Furthermore, the complete rebound of antibiotic-resistant bacteria in this study shows that short-course treatments may actually apply a selective pressure toward super-strains of *Wolbachia*. This could create *Wolbachia* strains that evade all known antibiotics, rendering anti-*Wolbachia* efforts useless. The cause of rebound must be addressed for fear that we find

ourselves in an arms race with *Wolbachia*, continually discovering potent drugs, then creating resistant bacteria to these drugs.

In the rifampicin experiment described in Chapter 4, I discovered a new morphology of clustering bacteria in the germline of the filarial nematode that succinctly fits the definition of bacteriocytes seen in other invertebrate species. These *Wolbachia*-based bacteriocytes persisted throughout each time point of the study (6-week, 17-week, and 36-week timepoints), and showed no difference in number, size, or bacterial density when compared to the vehicle controls. This led to the hypothesis that these antibiotic-resistant bacteriocytes may provide a protective niche and be the source of bacterial rebound seen eight months post-treatment. These findings highlight the importance of microscopic analysis, in conjunction with qPCR assessment, of total bacterial load. While qPCR is a relatively quick and easy method of identifying amounts of *Wolbachia*, the clustering morphology would not have been found without the important work of visualizing the cellular landscape of the parasite.

In Chapter 5, I set out to answer several pressing questions that presented themselves in Chapter 4: Are these clustering bacteria intracellular or extracellular? Are *Wolbachia* in these clusters actively replicating? Can we identify potent compounds that specifically target these clusters and effectively reduce their occurrence in the filarial nematode germline? Through confocal microscopy, we showed actin boundaries surround *Wolbachia* clusters, indicating they reside with the confines of a host cell plasma membrane. These results were confirmed through electron microscopy, in which a clear membrane can be seen surrounding dense groups of *Wolbachia*. In addition, the vast majority of *Wolbachia* clusters associate with a host nucleus that appears oblong and flattened, and occur at the surfaces of germline tissue, both characteristics quintessential to the sheath cells of nematode germline tissues. Due to these observations, we conclude that *Wolbachia* clusters are harbored in *Brugia pahangi* sheath cells.

While the observation of clustering *Wolbachia* in filarial nematode germline tissue is novel, clustered bacterial endosymbionts are a long-studied occurrence in many arthropod species. These are known as bacteriocytes, and they provide a protective niche for symbionts in which to live and/or proliferate in order to provide their arthropod host with essential amino acids or other nutrients. We performed an EdU assay to assess whether *Wolbachia* in these bacteriocytes is actively replicating. We found that the assay identified actively replicating *Wolbachia* in the hypodermal chords of the nematode, but EdU did not incorporate in *Wolbachia* found within bacteriocytes or other parts of the germline tissue. Either these *Wolbachia* populations are replicating at a rate slower than those in the hypodermal chords (we saw EdU incorporation after three days), or these bacteria are in a quiescent, non-replicating state. Further studies need to be performed to address the question of how *Wolbachia* can achieve high densities within these bacteriocytes.

One major question regarding *Wolbachia* bacteriocytes in filarial nematodes remains: If this is the source of bacterial rebound, how do the *Wolbachia* repopulate germline tissue? Do they maintain mechanisms by which they can break through the actin cytoskeleton of the sheath cells and invade oocyte tissue? *Wolbachia* is shown to have cell-to-cell transfer capabilities in both Drosophila [2] and the nematode host [4]. It is not a stretch to suggest they perform this mechanism in sheath cells as well. Despite much effort, I was not able to observe cell-to-cell transfer from the bacteriocyte. Perhaps it occurs on a timeframe that is not conducive with the three-day *in vitro* assays presented in this body of work.

Screening for compounds that specifically target *Wolbachia* bacteriocytes proved time-consuming and labor-intensive. In addition, sourcing live female *Brugia pahangi* poses challenges as resource centers are limited in the number of parasites they can provide each year. It would be beneficial to develop a faster, easier, and cheaper screen for anti-bacteriocyte drugs. *Wolbachia* found in *Drosophila melanogaster* brain tissue exhibit a clustering morphology similar to that seen in the germline tissue of filarial nematodes [5]. In addition, Radousky et al. discovered natural strains of *Wolbachia*-infected Drosophila species

that also display a clustering morphology of the bacteria in oocyte tissue [6]. It would be worthwhile to test Corallopyronin A and Fexinidazole on these clustering *Wolbachia* in *Drosophila* brain or oocyte tissues to see if these systems could be used as viable assays to discover other anti-bacteriocyte compounds.

Lastly, it will be crucial to test Corallopyronin A and Fexinidazole in a nematode-infected mammalian model to see the long-term effects of these compounds that directly decrease bacteriocyte number. If these sheath cell-based bacteria are in fact the source of *Wolbachia*, then we would expect to see maintained *Wolbachia* reduction in the filarial nematodes eight months post-antibiotic treatment. It would also be expected that micro- and macro-filarial counts would decrease. Perhaps even a combination of anti-*Wolbachia* and anti-bacteriocyte compounds would prove to have long-term synergistic effects capable of obliterating all *Wolbachia* levels in these human parasites.

REFERENCES

1. Brown AM, Wasala SK, Howe DK, Peetz AB, Zasada IA, Denver DR. *Genomic evidence for plant-parasitic nematodes as the earliest Wolbachia hosts*. Sci Rep, 2016. **6**:34955.

2. White PM, Pietri JE, Debec A, Russell S, Patel B, Sullivan W. *Mechanisms of Horizontal Cell-to-Cell Transfer of Wolbachia spp. in Drosophila melanogaster*. Appl Environ Microbiol, 2017. **83**(7): e03425-16.

3. Manoj RRS, Latrofa MS, Louni M, Laidoudi Y, Fenollar F, Otranto D, Mediannikov O. *In vitro maintenance of the endosymbiont Wolbachia of Dirofilaria immitis*. Parasitol Res, 2023. **122**(4): 939-943.

4. Bulman CA, Chappell L, Gunderson E, Vogel I, Beerntsen B, Slatko BE, Sullivan W, Sakanari JA. *The Eagle effect in the Wolbachia-worm symbiosis*. Parasit Vectors, 2021. **14**(1): 118.

5. Wu ML, Tan J, Dick T. Eagle effect in nonreplicating persister mycobacteria. Antimicrob Agents Chemother. 2015; 59:7786–7789. doi: 10.1128/AAC.01476-15.

6. Prasetyoputri A, Jarrad AM, Cooper MA, Blaskovich MAT. The Eagle effect and antibiotic-induced persistence: two sides of the same coin? Trends Microbiol. 2019; 27:339–354. doi: 10.1016/j.tim.2018.10.007.

7. Landmann F, Bain O, Martin C, Uni S, Taylor MJ, Sullivan W. *Both asymmetric mitotic segregation and cell-to-cell invasion are required for stable germline transmission of Wolbachia in filarial nematodes*. Biol Open, 2012. **1**(6): 536-547.

8. Casper-Lindley C, Kimura S, Saxton DS, Essaw Y, Simpson I, Tan V, Sullivan W. *Rapid fluorescence-based screening for Wolbachia endosymbionts in Drosophila germ line and somatic tissues*. Appl Environ Microbiol, 2011. **77**(14): 4788-4794.

9. Radousky YA, Hague MTJ, Fowler S, Paneru E, Codina A, Rugamas C, Hartzog G, Cooper BS, Sullivan W. *Distinct Wolbachia localization patterns in oocytes of diverse host species reveal multiple strategies of maternal transmission*. Genetics, 2023. **224**(1): iyad038.